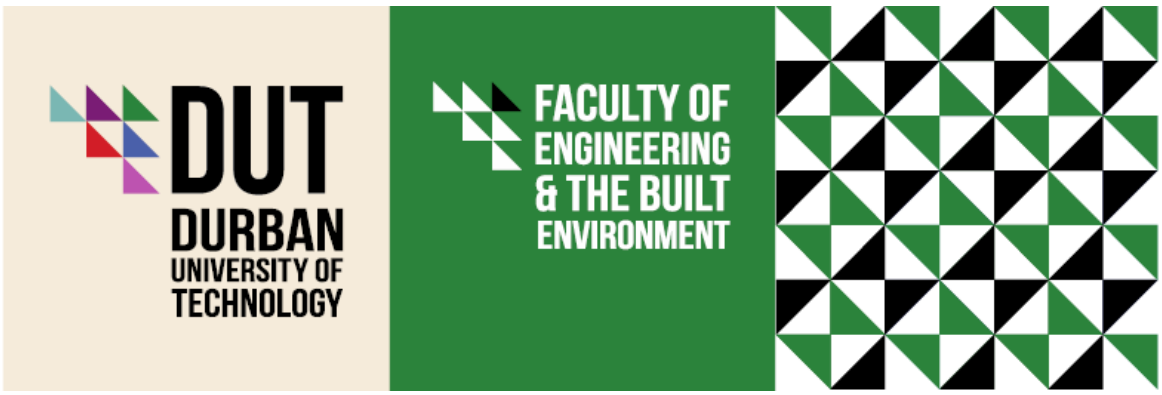

EXPERIMENTAL INVESTIGATION ON NATURAL CONVECTION OF HYBRID-WATER NANOFLUIDS IN CAVITY FLOW

By

TEMILOLUWA OLATUNJI SCOTT

STUDENT NUMBER: 22176532

Thesis submitted in fulfilment of the requirements for the Degree

of

MASTERS OF ENGINEERING: MECHANICAL ENGINEERING

Department of Mechanical Engineering

Faculty of Engineering and the Built Environment

Durban University of Technology

Supervisor

Dr Daniel Raphael Ejike Ewim

Co-supervisor

Professor Andrew C. Eloka- Eboka

SEPTEMBER 2022

DECLARATION

I, Temiloluwa Olatunji Scott, declare that this dissertation is my original work. It has not been presented and will not be presented to any other university for a similar or any other degree award.

……..	27 September 2022 …….
T.O Scott	Date
Student Number: 22176532	

Approved for submission by

……...	03 October 2022 ……
Dr DRE Ewim	Date
Supervisor	

……..	02 October 2022 ……
Professor A.C. Eloka-Eboka	Date
Co-Supervisor	

DEDICATION

To my family

ACKNOWLEDGEMENTS

I write this acknowledgment with great pleasure as I thank God Almighty for the strength, wisdom, knowledge, and understanding I expected to finish this study.

I would also like to acknowledge the following people for their help and support:

- My supervisor, Dr Daniel Ewim, for his patience, guidance and financial support throughout my research.
- My co-supervisor, Prof. Andrew Eloka-Eboka, for his invaluable inputs and guidance throughout the course of this study.
- Prof. Sharifpur, Dr Suseel, Mr Modaser, Mr Chris, and Mr Donald for their technical advice and support with the experimental setup and testing at the Nanofluids Research Laboratory, University of Pretoria.

I acknowledge Durban University of Technology for providing me with the financial support and opportunity to conduct this study. A special thank you goes out to my family for the many sacrifices they made for me on this journey. My beloved wife, Joy Scott, for her moral support, and my son Jason Scott for his understanding and for being a motivation. My parents Abayomi and Aina Scott, and siblings Abimbola, Moyosoreoluwa, and Similoluwa, for their continued support during the completion of my studies. I love you all.

I must also express my appreciation to everyone, friends, family, and colleagues alike, who, in one way or another supported me during the course of this study.

PUBLICATIONS

The following conference papers and journal articles were produced during this research with the candidate as first author and the supervisors as co-authors, respectively.

Journal Articles

(1) **Scott, T.O**., Ewim, D.R. and Eloka-Eboka, A.C., 2022. Hybrid nanofluids flow and heat transfer in cavities: a technological review. International Journal of Low-Carbon Technologies, 17, pp.1104-1123. (**Q1 Journal: Oxford University Press**)

(2) **Scott, T.O**., Ewim, D.R. and Eloka-Eboka, A.C., 2022. Experimental investigation of natural convection Al_2O_3-MWCNT/water hybrid nanofluids inside a square cavity. Experimental Heat Transfer, pp.1-19. (**Q1 Journal: Taylor & Francis**)

Conference Papers

(1) **Scott, T.O**., Ewim, D.R. and Eloka-Eboka, A.C., 2021. An Overview of Natural Convection of Hybrid-Water Nanofluids in Cavity Flows, *13th International Conference on Applied Energy*, Bangkok, Thailand, Nov. 29 – Dec. 2, 2021.

(2) **Scott, T.O**., Ewim, D.R. and Eloka-Eboka, A.C., 2022. Experimental Investigation on Natural Convection of Hybrid-Water Nanofluids in Cavity Flow [Poster]. *ASME International Mechanical Engineering Congress & Exposition.* Greater Columbus Convention Centre, Columbus, Ohio, Oct. 30 – Nov. 3, 2022.

(3) **Scott, T.O**., Ewim, D.R. and Eloka-Eboka, A.C., 2022. Experimental study on the influence of volume concentration on natural convection heat transfer with Al_2O_3-MWCNT/water hybrid nanofluids. *6th International Conference on Engineering for a Sustainable World*, Covenant University, Nigeria, Nov. 28 – 30, 2022.

ABSTRACT

The heating and cooling of fluid play a crucial role in many industries, such as transportation, electronics, and manufacturing; however, among other concerns like size, weight, and cost reduction of cooling and heating systems, heat transfer enhancement is a primary concern in many industrial applications. As a result, a large number of researchers have carried out numerous studies to find alternatives to enhance heat transfer. The research on nanofluids has proliferated in the past decade, and reports indicate that nanofluids can be used for heat transfer applications in engineering and in general and/or commercial industries. Nevertheless, a growing area of research in recent years has involved employing more than one type of nanoparticles in a base fluid, known as hybrid nanofluids. Studies showed that hybrid nanofluids exhibited improved rheological and thermal characteristics than single nanoparticle nanofluids. In this study, the natural convection of alumina – multiwalled carbon nanotube /water hybrid nanofluid formulated using a two-step technique at a percentage weight ratio of 10:90 Al_2O_3: MWNCT at various nanoparticles volume concentrations of 0.00, 0.05, 0.10, 0.15, and 0.20 vol% was studied inside a square cavity with two vertical walls which are isothermal, aimed at the Rayleigh number (*Ra*) range of 2.81×10^8 to 8.58×10^8. The average Nusselt number (Nu_{av}), heat transfer coefficient (h_{av}), heat transfer (Q_{av}), and Rayleigh number (*Ra*) were considered at varying temperature gradients of 20 °C – 50 °C. Al_2O_3-MWCNT/water hybrid nanofluid with 0.10 vol% volume concentration was discovered to have the maximum value for h_{av}, $Q_{av,}$ and Nu_{av}. However, it was also observed that a further increase in the hybrid nanoparticles' volume concentration led to their deterioration at various temperature gradients. The maximum enhancements of 43.98%, 49.27%, and 42.20% were noted for h_{av}, Q_{av}, and Nu_{av}, respectively, at ΔT = 50 °C, in comparison with the base fluid. Al_2O_3-MWCNT/water hybrid nanofluid application in a square cavity demonstrated enhanced free convection. Several results from this study indicate that hybrid nanofluids offer an advantage over mono-particle nanofluids and base fluids.

Keywords: heat transfer, volume concentration, hybrid nanofluids, natural convection, cavity flow, convective heat transfer.

NOMENCLATURE

Abbreviation	Meaning
Ag	Silver
Al	Aluminium
Al_2O_3	Alumina
Au	Gold
CMNC	Ceramic Matrix Nanocomposites
CNTs	Carbon Nanotubes
COOH	Carboxylic acid
C	Heat capacity ((kJ/kg.K)
Cr	Chromium
Cu	Copper
CuO	Copper Monoxide
D_B	Brownian diffusion
EG	Ethylene Glycol
Fe	Iron
Fe_2O_3	Iron (III) Oxide
Fe_3O_4	Ferrosoferric Oxide
Fn	Thermophysical ratio factor
h	Heat transfer coefficient (W/m^2 K)
HEG	Hydrogen exfoliated graphene
IEP	Iso-Electric Points
k_B	Boltzmann constant
Lpm	Litre per minute
MEMS	Micro Electro Mechanical Systems
MEPCM	Micro Encapsulated Phase Change Material
Mg	Magnesium

MgO	Magnesium Oxide
ml	Millilitre
MMNC	Metal Matrix Nanocomposites
MWCNT	Multi-Wall Carbon Nanotubes
n	Shape factor
ND	Nano Diamond
Ni	Nickel
NiO	Nickel Oxide
Nm	Nano metre
NP	Nanoparticles
Nu	Nusselt number
$\overline{Nu}$	Average Nusselt number
Pr	Prandtl number
PVP	Polyvinylpyrrolidone
PWE	Pulse Wire Evaporation
Ra	Rayleigh number
Re	Reynolds number
r_c	Average radius of nanoparticles clusters
SEM	Scanning Electron Microscope
SiC	Silicon carbide
SiO_2	Silicon dioxide
SLS	Sodium Lauryl Sulphate
Sn	Tin
T	Fluid temperature (℃)
TEM	Transmission Electron Microscopy
TiO_2	Titanium dioxide
wt	Mass fraction (%)

X	Percentage weight of nanoparticles' type (%)
ZnO	Zinc Oxide
ZrO_2	Zirconium dioxide

Symbols	**Descriptions**
β	Volumetric thermal expansion coefficient (1/K)
ν	Kinematic viscosity (m^2/s)
ζ	Zeta potential
φ	Nanoparticles volume concentration (%)
k	Thermal Conductivity ($W/m.K$)
ρ	Density (kg/m^3)
μ	Dynamic viscosity (Pa.s)

Subscripts	**Descriptions**
av	Average
bf	Base fluid
c	Cold
eff	Effective
h	Hot
hnf	Hybrid nanofluid
hnp	Hybrid nanoparticles
nf	Nanofluids
np	Nanoparticles
rel	Relative

TABLE OF CONTENTS

LIST OF FIGURES

LIST OF TABLES

CHAPTER ONE

INTRODUCTION

1.1. Background of Study

This research titled - *Experimental Investigation on Natural Convection of Hybrid-Water Nanofluids in Cavity Flow* - mainly focuses on studying cavity flow natural convection of various volume concentrations of hybrid-water nanofluids experimentally. Science and technology have advanced rapidly in recent years, and the past few years are a clear example of this continuous growth in diverse areas like manufacturing, power generation, and electronics, where heat transfer is vital. In the past, extensive research works have been carried out to enhance the heat transfer rate through various active or passive techniques; however, the low thermal conductivity of working fluids like water and ethylene glycol limits their heat transfer capability. Alternatively, improving the thermophysical properties of these working fluids can greatly enhance heat transfer and substantially reduce energy consumption and cost. Nanofluids are potential engineered colloids for the enhancement of heat transfer, which has paved the way for a thriving field of research in the studies of heat transfer. Nanofluids have been reported to enhance heat transfer compared to traditional fluids by numerous researchers. However, this study focuses on utilizing a more advanced type of fluid known as hybrid nanofluid, which has better properties of more than one nanoparticle to improve the abilities of heat transfer of the base fluids. More so, experimental evidence on the natural convection of hybrid nanofluids in diverse cavity geometries is sparse, and not much investigation has been carried out to investigate their efficiencies. In order to address these identified gaps, this study aimed to conduct an experimental research on the convective heat transfer behaviour of Al_2O_3-MWCNT/water nanofluids in a cavity with varying change in temperatures. In the study, Al_2O_3-MWCNT/water hybrid nanofluids at a percentage weight ratio of 10:90 (Al_2O_3-MWCNT) for φ of 0.05, 0.10, 0.15, and 0.20 vol% in a square cavity were examined for their performance in natural convection.

According to Zeitoun and Ali [1], fluid heating and cooling play vital roles in several industries, including power generation, production processes, transportation, and electronics. However, among other concerns like size, weight, and cost reduction of cooling and heating systems, heat transfer enhancement is a main concern and challenge in many industrial applications [2]. This has

led to several studies seeking means to enhance heat transfer in the past decades. In addition, heat transfer enhancement techniques are vital to energy saving [3].

One of the fundamental technical challenges that many industries like manufacturing, micro-electronics, and transportation face is the need to achieve cooling of components, systems and materials [4]. However, natural convection is known to have a low heat transfer coefficient which is primarily due to the low fluid velocity [5]. The process of heat transfer where the motion of fluid happens naturally and is not generated by external sources like pumps, fans, or any prime mover, is known as natural convection [6]. In natural convection, the film coefficient or effectiveness (h) is relatively lower compared to methods like forced convection used in thermal transportation [7]. It is, therefore, imperative to investigate in what way the natural convection film coefficient can be improved [5].

Ghodsinezhad, et al. [5] stated that in a system, there are two methods that could be used to improve the performance of heat transfer; the first is designing a new geometry, for instance, designing an optimised geometry; nonetheless, this is not applicable for systems that are miniaturised like the micro electro-mechanical systems (MEMS), while the second is to increase the capacity of heat transfer by means of novel heat transfer fluids. Liquids such as ethylene glycol (EG), oils, and water have a low thermal conductivity in comparison to most solids [7]; for instance, the thermal conductivities of copper oxide (CuO) and copper (Cu) respectively are 30 times and 700 times higher than that of water [8]. Therefore, nanoparticles can be introduced to improve the performance of heat transfer of the base fluids drastically [9]. When nanoparticles smaller than 100 nm are dispersed into the base fluids, they are called nanofluids [10]. Nanofluids have the ability to improve the heat transfer process since they have intricate properties such as improved viscosity, thermal conductivity, convective heat transfer coefficient, and thermal diffusivity [11].

1.1.1. Natural Convection in Cavity Flow

Several authors have studied heat convection in cavities that flow mainly due to buoyancy since the early part of the last century [12]. Natural convection is a type of convection heat transfer in which self-induced forces cause bulk motion. These forces occur due to temperature or concentration gradients [13] and can also be affected significantly by an increase in the working fluid's viscosity and density [14]. In engineering, it is a common practice to apply natural

convection in enclosures, cavities, or confined volumes [5]. Some examples of these applications are the cooling of electronic devices, heat exchangers, solar energy desalination and collectors, nuclear energy, electric ovens, geophysics, and some engineering processes like lubrication, solidification, and melting [15].

Many studies have been conducted in order to increase the rate of heat transfer in the past decades, like altering the geometry, boundary conditions, and boosting the heat transfer fluid's thermal conductivity to design effective heating systems [16]. Among these techniques, nanofluids which are dispersions of high thermal conductivity nanoparticles in a base fluid is an effective technique to improve the transfer of heat [10].

1.1.2. Nanofluid

Choi and Eastman [17] were the first to introduce nanofluids. Nanofluids are described as engineered colloidal suspension of nano-scaled particles of about 10 – 100 nm in a base fluid. These nano-scaled particles are commonly metallic oxides, some carbon-based elements, or metals [18]. Metallic oxides such as Fe_2O_3, Al_2O_3, Fe_3O_4, CuO, TiO_2, ZrO_2, and SiO_2; metals such as Au, Cu, Ni, and Ag; carbon materials like diamond, graphite, and carbon nanotubes are commonly used [19]. Several experiments proved that nanofluid's thermal conductivity is higher compared to the base coolant [20].

Consequently, nanofluids are utilised as working fluids to improve heat transfer performance [21]. There are generally two methods used to synthesise nanofluids: the one-step method (physical or chemical), which combines nanoparticles' production with nanofluids' synthesis. As a result, processes of nanoparticles like drying, storing, transporting, and dispersing are avoided, which in turn reduces the agglomeration of the nanoparticles, and increases the fluid's stability. On the other hand, the two-step method is the second method which involves two procedures. The first procedure is the synthesis of nanoparticles, followed by the subsequent procedure, which involves the dispersion of nanoparticles in the base fluid and dispersant in order to improve the nanofluid's stability [22, 23]. Even so, the two-step method is the most widely used approach, which is also the most economical method to produce large nanofluids [24].

Giwa, et al. [15] reported that Putra, et al. [25] were the first to examine the natural convection of Al_2O_3/water and CuO/water nanofluids inside a horizontal cylindrical vessel. The nanofluids used

in the study were selected based on the number of previous studies which showed a widespread knowledge of their thermal and flow properties. The results showed that heat transfer reduced with an increase in the volume concentration of the nanoparticles [25]. Aminossadati and Ghasemi [26] also observed the natural convection in a square cavity using four separate nanofluids, namely TiO_2/water, Al_2O_3/water, Cu/water, and Ag/water. Constant heat flux was applied at the cavity's bottom wall in order to heat it, while a cold temperature was maintained for the rest of the cavity walls. The researchers stated that Ag and Cu nanoparticles had a greater thermal conductivity which led to a further attenuation of the heat source temperature compared to Al_2O_3 and TiO_2. Also, at low Rayleigh numbers (*Ra*) and an increment in the nanofluids volume concentration, the heat source temperature decreased [26]. Recently, there have been new findings on the development of nanofluid, known as hybrid nanofluid [10].

1.1.3. Hybrid Nanofluid

Hybrid nanofluids refer to nanofluids prepared from a suspension of distinct nanoparticle types in a base fluid [9]. Hybrid materials can be divided into three categories depending on the metal matrix; (a) Metal matrix nanocomposites (MMNC), for example, Al_2O_3/Ni, Al_2O_3/Cu, MgO/Fe, ND/Ni, Al_2O_3/Fe-Cr, Mg/CNT, and Al/CNT (b) Ceramic matrix nanocomposites (CMNC), for example, Al_2O_3/CNT, Al_2O_3/TiO_2, SiO_2/Ni, Al_2O_3/SiC, CNT/Fe_3O_4, and Al_2O_3/SiO_2 [19] (c) Polymer nanomaterials, for example., polymer/CNT, thermoplastic/layered silicates polymer, polymer/hydroxides and polyester/TiO_2 [27]. Jamil and Ali [28] reported that Turcu, et al. [29] were possibly the first to prepare hybrid nanofluids using multiwall carbon nanotubes (MWCNTs) and polypyrrole-carbon nanotubes (CNTs) on magnetic ferrosoferric oxide (Fe_3O_4) hybrid NPs. There are, however, only a few experimental investigations on the convective heat transfer behaviour of hybrid nanofluids within certain cavities in literature, and these existing studies were noted to be carried out essentially through numerical techniques. Whereas experimentally conducted investigations were scarce [15].

Using a numerical technique, Chamkha, et al. [30] analysed the natural convection of Al_2O_3/Cu with water as the base fluid in a semi-circular cavity. They reported that the results obtained showed that the application of hybrid nanofluid resulted in a high value of *Ra* and thermal conductivity ratio, enhancing heat transfer. Rashad, et al. [31] also numerically investigated the convectional heat transfer of Cu- Al_2O_3/water hybrid nanofluids filled into a triangular cavity. The

cavity was subjected to a constant magnetic field and was heated by a constant heat flux element from underneath the cavity. It was reported that the hybrid nanofluid, containing equal amounts of Al_2O_3 and Cu nanoparticles dispersed in water base fluid, had no major effect on the mean Nusselt number (*Nu*) in comparison with the regular nanofluid.

In light of the above, a lack of experimental evidence on the natural convection of hybrid nanofluids in diverse cavity geometries is sparse, and not much investigation has been carried out to investigate their efficiencies. Therefore, in order to fill the gap identified in experimental heat transfer behaviour associated with natural convection, this study will focus on the experimental study of the convective heat transfer behaviour of Al_2O_3 - MWCNT/water hybrid nanofluids in a cavity with varying changes in temperatures.

1.2. Motivation of the Study

We live in the era of advanced technologies, and the past few years are a clear indication of phenomenal growth in a variety of areas like power generation, electronics, manufacturing, and so on., where heat transfer is essential [32]. The extensive usage of this equipment suggests that a slight increase in their effectiveness would substantially save capital costs and energy consumption [33]. In mechanical equipment, water and EG are mostly utilised [34], but studies have shown nanofluids provide enhanced thermal conductivity than base fluids [35].

In recent years, the research community has shown interest in developing fluids that have better properties of more than one nanoparticle to improve the abilities of heat transfer of the base fluids [36]. These fluids are called hybrid nanofluids and have become promising. Furthermore, based on published literature, the total amount of numerical investigation that has addressed the convective heat transfer of nanofluids has considerably outnumbered the number of experimental studies [37]. This study investigates cavity flow natural convection of hybrid-water nanofluids experimentally for these reasons.

1.3. Research Problem

In the early stages, the thermal conductivity properties of traditional heat transfer fluid were improved by using micro and millimetre-sized particles of metallic solids [38]. Still, the size of the particles presented numerous drawbacks like clogging in the flow channel, rise in pressure drop and particles settling [18].

Nanotechnology has become known to be an important part of technology and science, and its development has been massive [38]. The interest in nanofluid technology is established in several properties it possesses, for instance, viscosity, thermal conductivity, and several other physical properties. Thermal conductivity is one of the important properties of nanofluid as it plays a key role in the enhancement of heat transfer, thus making it highly valued in industrial applications [11]. Researchers are now focusing on a new, improved working fluid known as hybrid nanofluid with the aim to develop working fluids with high thermal performance. As a matter of fact, many researchers have made efforts toward these aims for several decades. However, there are very few experimental studies on hybrid nanofluid's convectional heat transfer in different cavity configurations in the open literature. Therefore, this research will contribute to the new knowledge that will guide future researchers in this field of study. It will lead to a better understanding of the impact of hybrid water nanofluids on cavity flow natural convection.

The overgrowing needs for high stability, thermal conductivity enhancement, and energy sector have raised the interest of researchers to develop fluids with better properties of more than one type of nanoparticle. In order to enhance the base fluid’s ability to transfer heat, hybrid nanofluids are seen to be promising [36]. However, experimental studies on hybrid nanofluid's convectional heat transfer in different cavity shapes are sparse in literature.

1.4. Aim and Objectives of the Study

The aim of this research is to experimentally investigate the natural convection of Al_2O_3–MWCNT (10:90)/water hybrid nanofluid in a square cavity flow.

The objectives of achieving the research aim are as follows:

i. to formulate and characterize different volume concentrations of Al_2O_3–MWCNT/water hybrid nanofluids that are of suitable stability for natural convection in a square cavity;
ii. to investigate the effect of the Al_2O_3–MWCNT/water hybrid nanofluid volume concentrations on the performance of h, Nu, and Q at several Ra;
iii. to observe the temperature distribution of Al_2O_3–MWCNT/water hybrid nanofluid at various volume concentrations in the cavity.

1.5. Scope of the Study

This study focused on the experimental study of natural convection of Al_2O_3–MWCNT/water hybrid nanofluids in cavity flow. First, it involved the preparation and characterization of different volume concentrations of Al_2O_3–MWCNT (10:90 percentage weight of nanoparticles)/water hybrid nanofluids with appropriate stability for natural convection in a square cavity. Then the investigation of the effect of the hybrid nanofluids volume concentrations on the heat transfer coefficient performance at various *Ra* values as well as the Nusselt number (*Nu)* and heat transfer (*Q*). Lastly, the temperature distribution of Al_2O_3–MWCNT/water hybrid nanofluids at various volume concentrations in the test cell was observed and analysed.

1.6. Thesis Overview

Chapter 1 covers the introduction of the study which consists of the background and purposes of the study, research problem, aim and objectives of the study, scope of the study, and the overview of the thesis. Chapter 2 comprises of a detailed review of literature on hybrid nanofluid characterization, the preparation, thermophysical properties, and stability analysis of hybrid nanofluids. It also discusses natural convection hybrid nanofluid's numerical and experimental studies. Chapter 3 presents the research methodology, including the description of the experimental setup, hybrid nanofluid formulation details, and the validity of the experimental setup. Chapter 4 covers the hybrid nanofluid formulation results and the findings of the experimental measurement of the hybrid nanofluid heat transfer coefficient, Nusselt number, and heat transfer at different volume concentrations. Finally, Chapter 5 presents the study’s conclusion and recommendations for future work.

CHAPTER 2

LITERATURE REVIEW

2.1. Introduction

This chapter centres on the review of literature on various hybrid nanofluid formulation techniques, stability evaluations, and a detailed review of the hybrid nanofluid's thermophysical properties, which play an essential role in the hybrid nanofluids' heat transfer. Lastly, experimental and numerical studies on natural convection heat transfer hybrid nanofluid will be reviewed.

2.2. Hybrid Nanofluids

Nanofluids are engineered colloidal suspensions of nano-scaled particles of about 10 – 100 nm in a base fluid [18]. To researchers, they are of great value due to their high transfer rates, which have also increased their uses in the industry significantly [39]. Recently, there has been a new development or class of nanofluid called hybrid nanofluids [10], which is used further to improve the heat transfer characteristics [39]. Hybrid nanofluid is formulated by suspending distinct nanoparticles type in a base fluid [40]. These base fluids are usually water, ethylene glycol, engine oil, polymetric solutions, and other primary fluids [19, 39].

2.2.1. Preparation of Hybrid Nanofluids

Hybrid nanofluid stability depends on the method of preparation [41]. However, for researchers preparing stable hybrid nanofluid is a technical difficulty due to the cohesive forces and strong van der Waal amongst the nanoparticles, which causes aggregation. This accumulation or aggregation in the hybrid nanofluids, therefore, causes it to lose its ability to transfer heat by reducing the Brownian motion of particles [32]. Therefore, it is crucial to prepare hybrid nanofluids using the right approach. Generally, there are two methods to synthesise hybrid nanofluids: the one-step method (physical or chemical) and the two-step method [22]. The one-step, also known as the single-step method, is appropriate for the smaller-scale production of hybrid nanofluids. In contrast, the two-step method is economical for the mass production of hybrid nanofluids [42].

2.2.1.1. Single -step method

The single-step method is a combination of the formulation of nanoparticles and nanofluids [23]. According to literature, methods like wet chemical synthesis [41], chemical vapour deposition [40,

43], a wet grinding method [44, 45], chemical reduction, hot-wire technique, and mechanical ball milling [40, 46] were used for the production of hybrid nanofluids. Sidik, et al. [47] indicated that the pulse wire evaporation (PWE) method, which is a single-step method, is the most prominent method for producing hybrid nanofluids. They reported that some researchers utilised this method to prepare Ag/MWCNT. MWCNT was purified using a chemical process. Sulfuric acid and nitric acid were utilised to enhance the exterior activity of the MWCNT due to their hydrophobic nature. At the same time, silver nanofluid was obtained using the PWE method at a pulse voltage of 300 V using a 90 mm wired diameter. Jena, et al. [48] experimented in four cases that were aimed at producing homogenous Cu-Al_2O_3 composites from chemically prepared Cu-Al_2O_3 mixture by hydrogen reduction. Hybrid nanofluids synthesised using a single-step method usually have high quality and are physically stable relative to the thermal characteristics and physical specifications [49]. However, the major drawback of this technique is that they are only compatible with low vapour pressure base fluids [23].

2.2.1.2. Two-step method

As its name implies, this method involves two procedures or techniques. Firstly, the nanoparticles are prepared individually by different mechanical, physical, or chemical techniques such as sol-gel grinding or milling are commercially available and then suspended in suitable base fluids through magnetic stirring, high-speed mixing, homogenizing, and ultra-sonication [49]. This technique is currently the most commonly used to prepare hybrid nanofluids [23, 50] and is economical for the mass production of hybrid nanofluids [42]. However, researchers reported that the high surface energy of nanoparticles led to aggregation and eventually sedimentation of nanoparticles when using this method, reducing the stability of the hybrid nanofluid [50]. As a result, dispersants or surfactants are usually added in synthesizing to improve the stability of the hybrid nanofluids [23]. Figure 2.1 illustrates the two-step method of preparing a hybrid nanofluid.

Bahrami, et al. [51] utilised this method in preparing Fe/CuO nanofluid with EG and water as base fluids, and the solutions were exposed to an ultrasonic processor. Soltani and Akbari [52] used a two-step method to synthesise MgO-MWCNT nanofluid with EG as the base fluid. First, a magnetic stirrer was used for 2 h and later exposed to an ultrasonic process for 7 h. Suresh, et al. [53] produced Al_2O_3–Cu nanofluids using a two-step method. They dispersed the nanoparticles in DI water with sodium lauryl sulphate (SLS) as a dispersant by means of an ultrasonic vibrator for

6 h. Chen, et al. [54] also utilised this technique in preparing MWCNT/Fe_2O_3 nanofluids, with water as the base fluid, and sodium dodecylbenzene sulfonate was added as a surfactant to stabilize the solution.

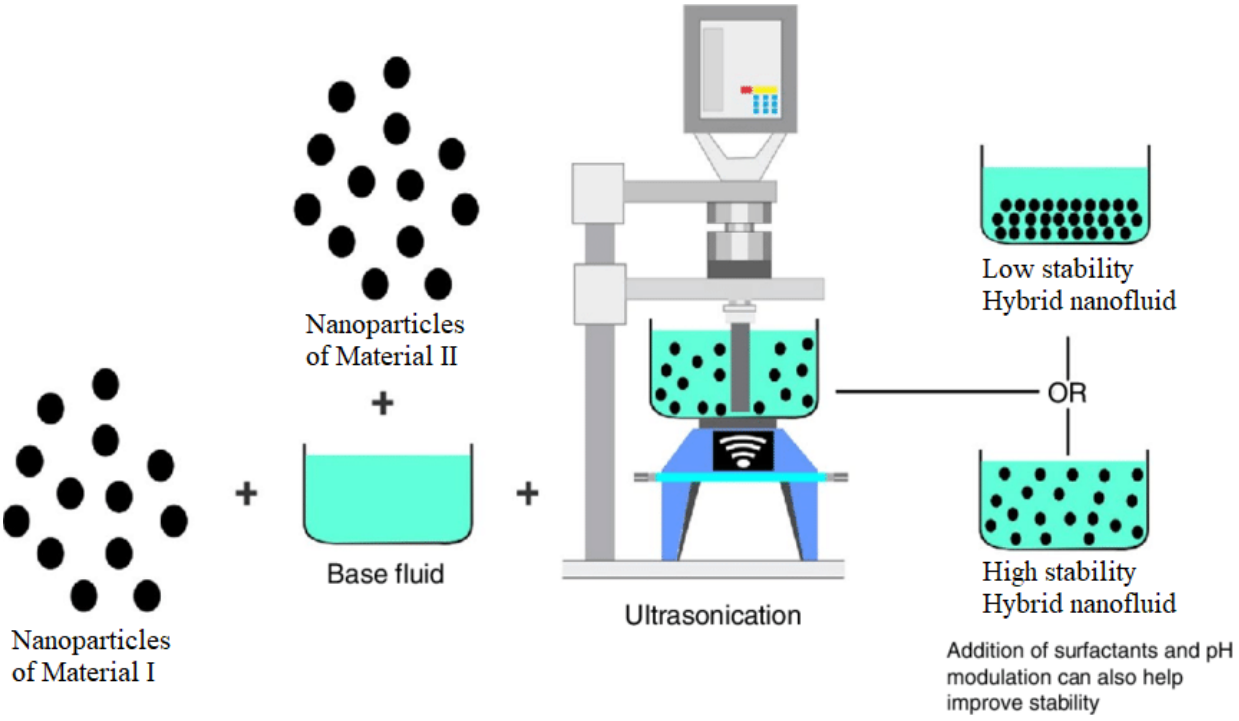

Figure 2.1: Two-step method of preparing hybrid nanofluid [18]

2.2.1.3. Addition of surfactants

Surfactants are also known as dispersants or stabilizers and are utilised in the two-step preparation method [55]. Research revealed that achieving a long-term, well-suspended hybrid nanofluid remains one of the biggest challenges [56]. However, with the addition of surfactants, hybrid nanofluid can be stabilized. The surface tension is influenced because the surface tension of the base fluid is lowered, which increases the immersion of the particles [57, 58]. Thermal conductivity, density, specific heat capacity, and viscosity are thermophysical properties of hybrid nanofluids that depend on the stability of hybrid nanofluids [55]. According to Chakraborty and Panigrahi [59], surfactants are classified mainly into four types cationic, anionic, non-ionic, and amphoteric. However, the most significant ones are (a) cationic-: cetyl trimethyl ammonium

bromide (CTAB) and Dodecyl trimethyl ammonium bromide (DTAB); (b) anionic-: sodium dodecyl sulphate (SDS) and sodium dodecylbenzene sulphonate (SDBS); (c) non-ionic-: polyvinyl pyrrolidone (PVP), gum arabic and oleic acid [58].

Iyahraja and Rajadurai [60] added PVP and SDS as dispersants to the silver–water nanofluids they prepared. It was observed that SDS stabilized the nanofluid better than PVP. However, the addition of PVP demonstrated higher thermal conductivity compared to that of SDS. Khairul, et al. [56] studied the effect of anionic surfactants SDS on two nanofluids, Al_2O_3 and CuO, at various nanoparticle concentrations. Their results revealed that the stability of nanofluid strongly relates to viscosity and thermal conductivity. This is because, in the study, the nanofluid's stability was observed to improve but with a decrease in viscosity and an increase in thermal conductivity. It is apparent that the amount and nature of surfactant added to any nanofluid would affect the heat transfer and physical properties of the hybrid nanofluid [55, 58]. Megatif, et al. [61] formulated a CNT/TiO_2-water hybrid nanofluid with an addition of about 1.5 wt% SDBS surfactant. It was reported that the fluid was stable. Therefore, selecting the right kind of surfactant and the suitable amount of surfactant is essential to provide a good coating on the nanoparticles' surface, influencing electrostatic repulsion and compensating for the Van der Waal forces of attraction [55, 58]. Table 2.1 summarizes the hybrid nanoparticles, base fluids, preparation methods and surfactants used by other researchers.

2.3. Stability Analysis of Hybrid Nanofluids

Hybrid nanofluid stability is a critical parameter for the proper functioning of thermal systems [32]. In other words, it is one of the crucial factors that affect hybrid nanofluids' performance. Instability occurs due to the tendency of mutual attraction between nanoparticles caused by the nanoparticle's high surface energy [23, 42]. A hybrid nanofluid can eventually lose its ability to transfer heat if it becomes coagulated. Therefore stability evaluation and investigation are essential [42]. Several methods have been developed to analyse hybrid nanofluid's stability, for example, spectral analysis method, centrifugation method, zeta potential analysis, sedimentation method, transmission electron microscopy (TEM), scanning electron microscope (SEM), and light scattering methods [32, 47]. The stability analysis method for hybrid nanofluids will be discussed.

Table 2.1: Synthesis methods of hybrid nanofluids

Nanoparticles	Base fluid	Preparation method	Surfactant	Ref
Al_2O_3/MWCNT	Water	Two-step method	Sodium dodecyl sulphate (SDS)	[15]
MWCNT/Fe_3O_4	Distilled water	Two-step method	NanoSperse AQ	[33]
ZnO/TiO_2	EG	Two-step method	--	[35]
Ag/MWCNT	Distilled water	Two-step method	Cetyl trimethyl ammonium bromide	[36]
Cu/Cu_2O	DI water	Two-step method	--	[45]
Al_2O_3/Cu	Deionized (DI) water	Two-step method	Sodium lauryl sulphate	[53]
CNT/TiO_2	Distilled water	Two-step method	Sodium dodecylbenzene sulphonate	[61]
Ag/MWCNT	Water	One-step method	--	[62]
MWCNT/MgO	Water-EG	Two-step method	--	[63]
SiO_2/MWCNT	EG	Two-step method	--	[64]
Ag/SiO_2	Oil	One-step method	--	[65]

2.3.1. Zeta Potential Analysis

Zeta potential is a physical property that is exhibited by any particle in the suspension or surface of a material [66]. According to Kong, et al. [23], the liquid layer surrounding the particles comprises of two different regions; the first is an inner region, also known as the stern layer. The other is an outer or diffuse region. In the inner region, ions are firmly bound due to a thin layer of positive charge which structures around the negatively charged particle and is lightly connected to the outer region with a broader layer of mostly opposite charge. However, inside the outer layer, there is a notional boundary where the particles and ions form a stable entity. At this boundary, the potential is known as zeta potential [23, 40]. It shows the potential difference between the

charged hybrid nanoparticles and base fluid [42]. Figure 2.2 illustrates the schematic representation of zeta potential.

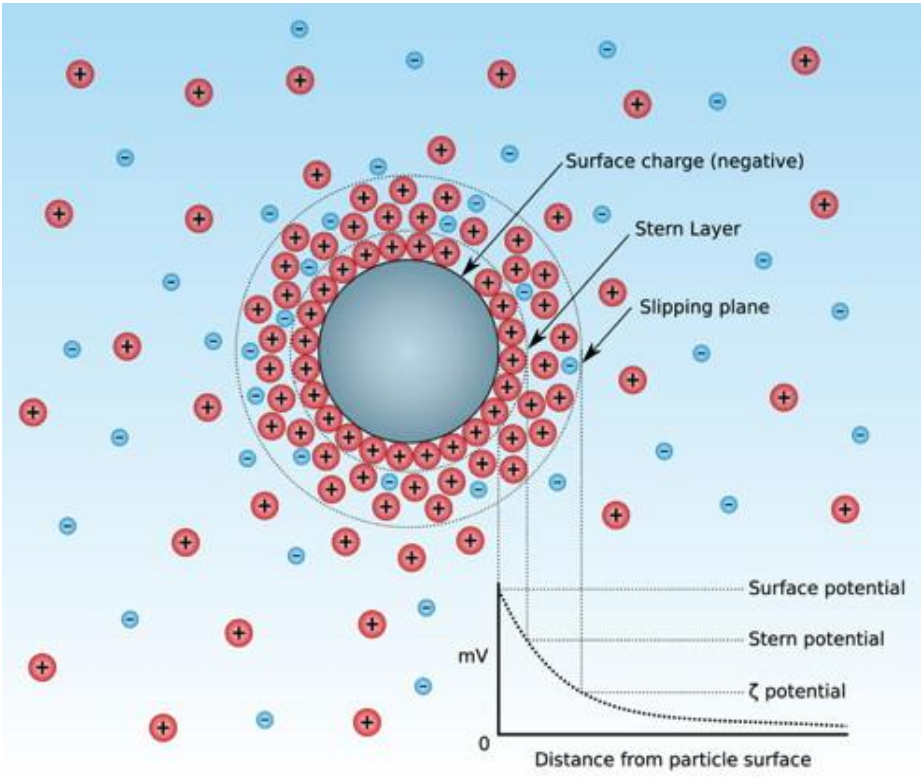

Figure 2.2: Schematic representation of zeta potential [67]

The primary importance of the zeta potential value is to analyse the stability of the dispersed nanoparticles. When colloids have a high zeta potential be it positive or negative, it is said to be electrically stabilized; however, when colloids have a low zeta potential value, they tend to coagulate [40]. As shown in Table 2.2, hybrid nanofluids with zeta potential below 15 mV are unstable, and values from 30 mV to 60 mV indicate they are moderately stable. Hybrid nanofluids with zeta potential above 60 mV demonstrate exceptional stability with minor settling. Another importance of zeta potential analysis is that it reduces the time needed to produce trial formulations and helps in predicting long-term stability [66]. According to literature, researchers used Zeta potential analysis since it is one of the most effective methods to quantify the dispersion stability of hybrid nanofluids [68].

Table 2.2: Relationship between zeta potential and the stability of hybrid nanofluids

Zeta potential (mV)	Stability of hybrid nanofluids
0	Very little or no stability
15	Little stability with settling
30	Moderate stability with sedimentation
45	Good stability with possible settling
60	Excellent stability with minor settling

pH is one of the most critical factors that affect its zeta potential [66]. When the results of pH values are distant from the isoelectric points (IEP) of the formulated hybrid nanofluids, results showed that the formulated hybrid nanoparticles were dispersed well and stable for a few hours due to their high repulsive forces on the nanoparticles [40]. Figure 2.3 shows a qualitative description of the zeta potential versus pH behaviour. Although the IEP of the sample shown is around pH 5.5, the plot can help predict that at pH <4, hybrid nanofluids should be stable since there is a presence of sufficient positive charge and more significant than pH 7.5 since sufficient negative charge is present [66]. At pH between 4 and 7.5, there are some issues with dispersion stability since the zeta potential values are between +30 and -30 mV [66]. Numerous pH values for alumina nanofluid were examined, and changes were noted in agglomeration by altering the pH value [69].

2.3.2. UV–vis Spectrophotometer

Ultraviolet-visible spectrophotometer, commonly known as UV-vis spectrophotometer, was introduced in 2003 by Jiang et al. as a new method for stability measurement [70]. Its application is another effective method for stability evaluation [42]. The dispersion dynamics can be monitored, and the colloidal stability of dispersed particles can be quantitatively characterized using UV-visible spectroscopy [40].

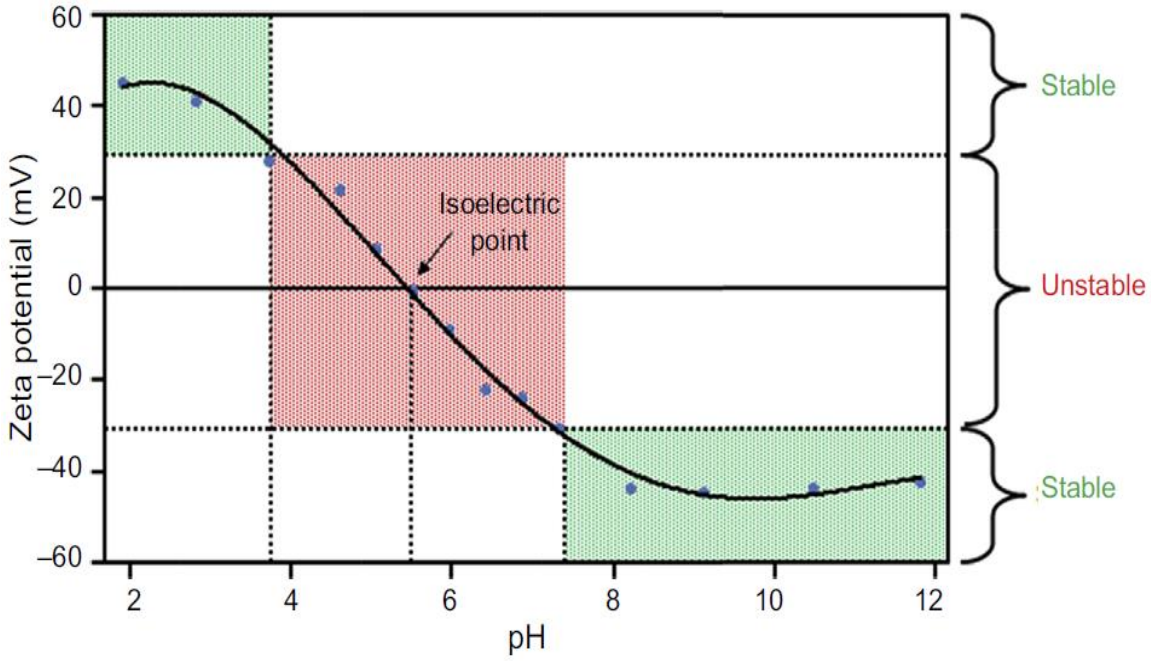

Figure 2.3: Typical plot of zeta potential versus pH [71]

Ghadimi, et al. [70] studied the stability of aqueous titania nanofluid of 0.1wt. % utilizing UV-vis Spectrophotometer at the elapsed time intervals of one day, two days, one week, and one month after preparation. Based on the results, they reported that a UV-vis spectrophotometer is suitable for detecting nanofluid's stability for two days after preparation. Gupta, et al. [72] studied metal/COOH-MWCNT hybrid nanofluid's stability. They measured the absorbance by extracting 0.1 ml of each hybrid nanofluid and then mixing it with double distilled water. Afterward, it was sonicated for a period of 5 minutes. The researchers stated that at 800 nm, the absorbance measured was simply due to the presence of MWCNT. Cabaleiro, et al. [73] also evaluated the stability of ZnO/ethane-1,2-diol nanofluids in the wavelength range of 201 to 800 nm, while for ZnO/ethane-1,2-diol + water nanofluids, a wavelength of 310 nm was selected. They reported that the rate of deposition estimated from the absorbance decreases by 10% for ZnO/ethane-1,2-diol nanofluids and 11% for ZnO/ethane-1,2-diol + water nanofluids during the 70 h check.

2.3.3. Sedimentation and Centrifugation Method

Sedimentation is the most reliable and straightforward stability evaluation method [40]. Sedimentation is when nanoparticles dispersed in a base fluid tend to settle and ultimately come to rest against an external force [23]. Although using this technique, the variation of nanoparticle

concentration with residue time is achieved. Hybrid nanofluids are deemed stable when the nanoparticle concentration is kept constant [40]. In this method, a camera is also used to capture photographs of the sediments in hybrid nanofluid stores in visible containers or test tubes. However, months are usually needed to observe the presence of sediments with naked eyes [40, 74]. Figure 2.4 schematically illustrates the sedimentation-based stability evaluation method. When comparing the sedimentation method with other methods, the disadvantage of this approach is the observation time because it needs a longer period to analyse the stability of the formulated hybrid nanofluids [40].

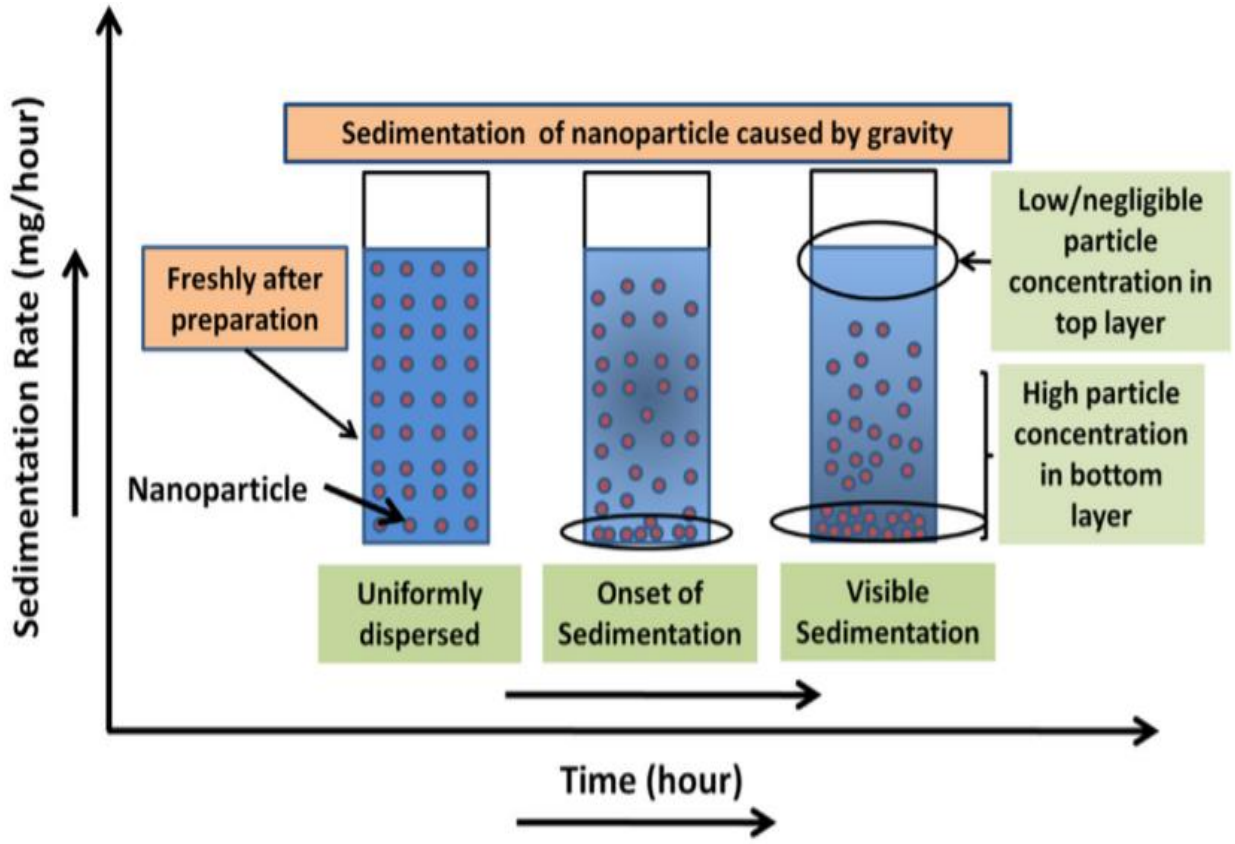

Figure 2.4: Schematic representation of sedimentation-based stability evaluation method [59]

Like the sedimentation method, the centrifugation method is another method for the stability evaluation of hybrid nanofluid. The difference is that centrifugal force is exerted to separate sediments and supernatant instead of depending on gravity's force, which is time-consuming [74]. Singh and Raykar [75] applied microwave synthesis to prepare stable Ag-ethanol nanofluids with

PVP. In their experiment, they studied the stability of the nanofluid at room temperature using the centrifugation method at 3000rpm for more than 10 h. They reported that there was no sign of sedimentation within the time frame compared to the sedimentation method which was observed to be stable for more than one month.

2.3.4. Electron Microscopy Analysis

Electron microscopy analyses are used to examine the stability of hybrid nanofluids by analysing the aggregation and distribution of nanoparticles [23]. Several researchers have used TEM and SEM to characterize nanoparticles' distribution, shape, and size in a nanofluid [58]. In TEM, electrons shoot through the sample and measure how the electron beam changes as it is scattered in the sample [58]. It also offers high-resolution images that can reach roughly 0.1 nm in the case of lattice images [23]. In contrast, SEM images the sample surface by scanning it with electron beams in a raster scan pattern [58]. In addition, it studies the morphology of the nanostructured materials, changes in structure and nanoparticles shape [40].

TEM is utilised to directly examine the aggregation of nanoparticles within the hybrid nanofluids [23]. An increase in the size of the nanoparticles or the formation of irregular particle clusters indicates agglomeration, which is an unstable hybrid nanofluid [58]. Sun, et al. [76] examined the stability of Ag/MWCNT nanoparticles at different ratios using SEM. Figure 2.5 (a) and (c) show the SEM images of Ag and MWCNT nanoparticles, respectively. According to the images, Ag nanoparticles are nearly spherical, and the gaps between each particle group are more prominent and unevenly distributed. In contrast, MWCNT nanoparticles are tubular, with significant gaps between tubes, and unevenly distributed. Figure 2.5 (b) is the SEM image of the hybrid nanoparticle, which depicts that Ag nanoparticles are embedded in the tubular MWCNT nanoparticles since Ag nanoparticles consistently filled the gaps of the MWCNT; therefore, the dispersion stability was enhanced, and they reported that no apparent agglomeration was observed [76].

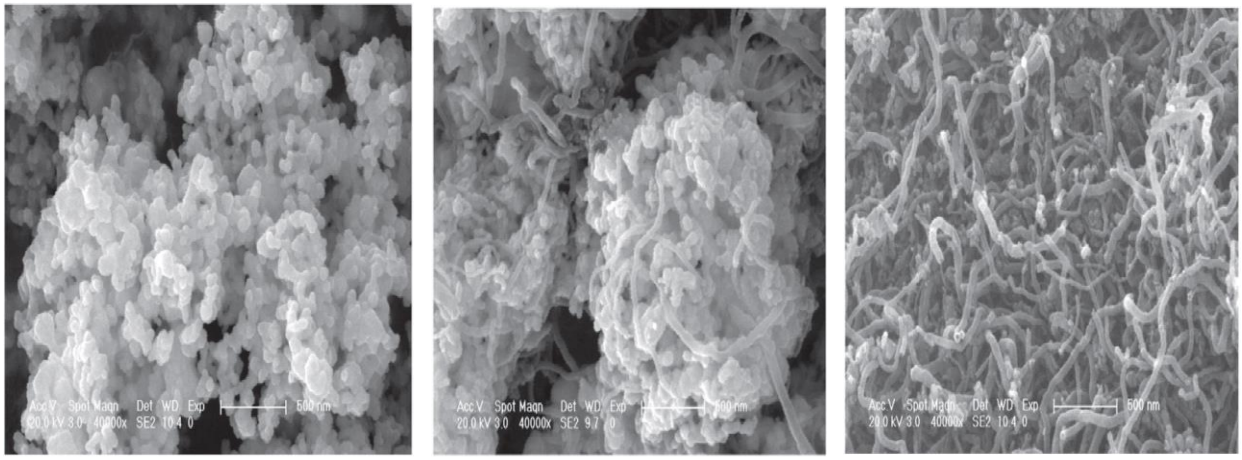

(a) 10: 0 (b) 5:5 (c) 0:10

Figure 2.5: SEM image of Ag-MWCNT hybrid nanoparticles with different matching ratios [76]

2.4. Thermophysical Properties of Hybrid Nanofluids

Generally, hybrid materials have different chemical and physical properties that form one homogeneous phase. Therefore, in synthesizing hybrid nanofluids, the main aim is to enhance the properties of single materials where they have great exponents of rheological or thermal properties that are superior to those of conventional nanofluids separately [77].

The effect of thermophysical properties on natural convection was clarified by Ho, et al. [78]. They disclosed that the possibility of natural convection enhancement depends solely on the thermophysical properties ratio factor, as shown in Eq (2.1). It is noted that if Fn is greater than 1, then it is probable to use the nanofluid for enhancement of heat transfer, but if Fn is lesser or equal to 1, then it is not probable. Therefore, a typical exponent value (n) was taken to be 1/3 for the ranges of the Rayleigh number they considered in their study.

$$F_n = \left(\frac{\beta_{nf}}{\beta_{bf}}\right)^n \left(\frac{C_{nf}}{C_{bf}}\right)^n \left(\frac{k_{nf}}{k_{bf}}\right)^{1-n} \left(\frac{\upsilon_{nf}}{\upsilon_{bf}}\right)^{-n} \tag{2.1}$$

Dynamic viscosity, thermal conductivity, thermal expansion coefficient, density, specific heat capacity, and thermal diffusivity are some of the thermophysical properties of fluids. However,

among these properties, thermal conductivity, dynamic viscosity, and specific heat capacity play vital roles in heat transfer characteristics [79].

2.4.1. Thermal Conductivity

This is a fundamental thermophysical property. A thermal system will have high efficiency as a result of high thermal conductivity [80]. Many types of fluids like ethylene glycol and water are used as heat carriers in various heat transfer applications like heat exchangers in power plants, cooling systems in buildings, vehicles air conditioning systems, and cooling systems of almost every processing plant [46, 81]. However, these engineered devices have a significant drawback in heat exchange because the fluids have a lower thermal conductivity [7, 46].

To overcome this situation, researchers used nanofluids. In addition, researchers used nanoparticles of high thermal conductivity materials, such as metals, metal oxides, and carbon-derived materials to improve the thermal conductivity of oil, water, and ethylene glycol [18, 46]. The thermal conductivities of heat transfer fluids, metals, metal oxides, and carbon materials are compared in Figure 2.6.

According to Sajid and Ali [80], the steady-state parallel plate method, transient hot-wire method, and thermal constants analyser are suitable for determining the thermal conductivity of hybrid nanofluids. The steady-state parallel technique comprises of two circular copper plates positioned parallel to each other, and a test sample is positioned between them. Heat is then transferred between the test sample placed in the middle of the plates, and the thermal conductivity is determined using the equation of one-dimensional heat conduction.

In the transient hot-wire technique, a pulse of heat is applied to the needle. Then, the temperature response is measured on the adjacent needle throughout the use of heat pulse, with the response in temperature depending on the material's thermal properties. Finally, the thermal analyser operates based on the transient hot-wire technique [80, 82, 83]. In this method, the temperature is raised by a hot disc sensor and measured by a resistive thermometer with respect to time. Figure 2.7 illustrates the thermal conductivity measurement from the KD2-pro thermal property analyser used by several researchers.

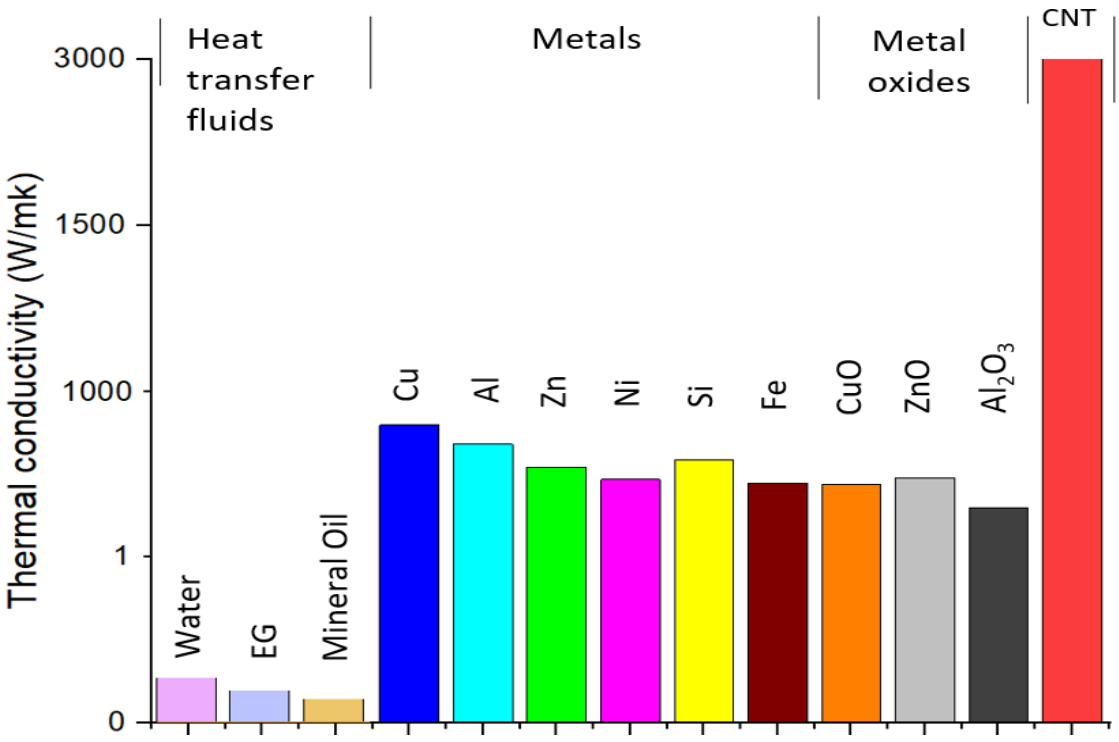

Figure 2.6: Thermal conductivity comparison of common liquids, and solids [81]

Huminic, et al. [84] analysed the thermal conductivity of Fe/Si- water hybrid nanofluids with mass concentrations of 0.25%, 0.5%, and 1.0% within the temperature range of 20 °C – 50 °C using the KD2- pro thermal properties analyser.

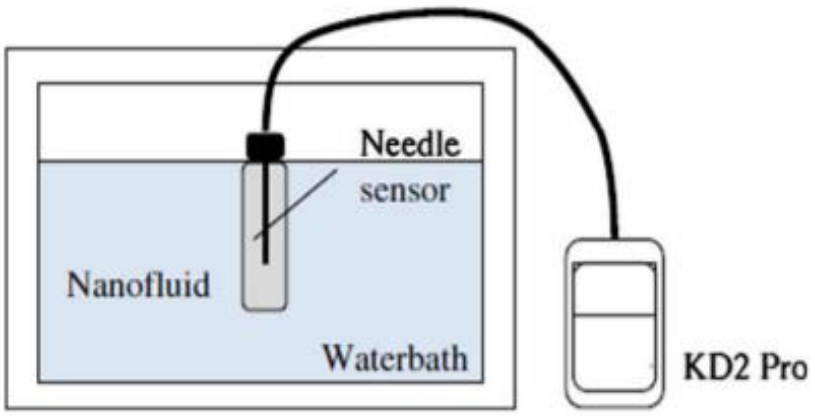

Figure 2.7: Thermal conductivity measurement using KD2-pro [80]

They observed that an increase in mass concentration enhances the nanofluid thermal conductivity due to the formation of chains of nanoparticles and the high thermal conductivities of the solid nanoparticles in the base fluid. In addition, they reported that the thermal conductivity also increases with a rise in temperature, which may possibly be attributed to the thermal energy increase of the dispersed Fe and Si nanoparticles.

Shahsavar, et al. [85] examined the temperature and concentration effect on ferrofluid and CNT thermal conductivity. They also reported that a rise in the temperature and volume concentration led to an enhanced thermal conductivity of the hybrid nanofluids. According to the findings, a maximum enhancement in thermal conductivity of about 44.6% was obtained for a maximum concentration of CNTs (1.35%) + Fe3O4 (0,9%) at 55 °C. Table 2.3Table 2.3 summarizes some research and findings on measuring thermal conductivities.

2.4.5.1.Parameters that affect the thermal conductivity of nanofluids

Several parameters can affect the thermal conductivity of nanofluids directly or indirectly, such as the size, shape, properties of the nanoparticles, stability in the fluid, base fluid, concentration, temperature, preparation method, sonication time, surfactant, pH, and so on [83, 86]. For example, Figure 2.8 presents various properties that impact the thermal conductivity of nanofluids. Researchers have tested different types of nanoparticles. According to some reports, the thermal conductivity of nanoparticles has little effect on the heat transfer rate of nanofluids. In contrast, others claim that nanoparticles with high thermal conductivity can speed up the heat transfer process. For example, Gonçalves, et al. [83] explained that Wang compared the thermal conductivity of copper and aluminium oxide nanofluids. The results showed that the thermal conductivity of copper nanofluid was higher, resulting from the high thermal conductivity of copper. However, another study by Yoo showed that TiO_2 nanofluid had a more substantial improvement in thermal conductivity than Al_2O_3 nanofluid, even though TiO_2 nanoparticles had lower thermal conductivity values.

Table 2.3: Summary of some research and findings on measuring thermal conductivities

Nanoparticles	Base fluid	Major findings	Authors
Al_2O_3/Cu	Distilled water	They found that at 2% volume concentration, the hybrid nanofluid showed a maximum enhancement of 12.11% in thermal conductivity, whereas a single nanofluid of Al_2O_3 showed a maximum enhancement of 7.56%.	[34]
Al_2O_3/MWCNT	Distilled water	It was observed that the hybrid nanofluid's thermal conductivity was higher than that of a single nanofluid of Al_2O_3-water. It was also noted that the shape of nanoparticles has a negligible effect on thermal conductivity since they realized a slight increase in thermal conductivity of hybrid nanofluids with spherical particles with respect to cylindrical shape particles.	[43]
CNT/TiO_2	Distilled water	They compared CNT nanofluid to CNT/TiO_2 hybrid nanofluid and discovered that the hybrid nanofluid has about 2.5% higher thermal conductivity due to the nanoparticles clustering effect.	[61]
Ag/MWCNT	Distilled water	It was observed that thermal conductivity was 20% more than distilled water.	[87]
Al/Zn	EG	They reported that the thermal conductivity was enhanced by 16% for smaller nanoparticles of 0.10 vol% compared to EG.	[88]
Hydrogen exfoliated graphene (HEG)/MWCNT	DI water	The thermal conductivity increased by about 9% and 20% at volume fractions of 0.005% and 0.05%, respectively.	[89]

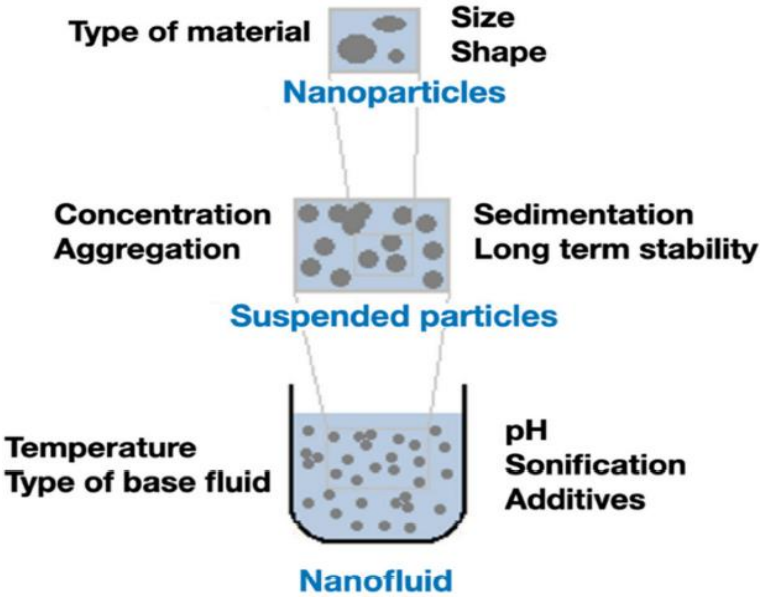

Figure 2.8: Different properties that affect the thermal conductivity of nanofluids [83]

The influence of the size of nanoparticles is still controversial in the scientific community [83, 90]. However, Ahmadi, et al. [86] stated that a nanoparticle's size could affect the nanofluid's thermal conductivity since, like temperature, the size of the particles influences the likelihood of collision between particles. In addition, a reduction in nanoparticle size increases the Brownian motion, thickens the interfacial layering, and increases the effective surface area [90]. Therefore, it is an influential factor in nanofluid's thermal conductivity [91]. Ahmadi, et al. [86] reported that Esfe and other researchers investigated the effect of particle size (20, 40, 50, and 60 nm) on MgO/water nanofluid thermal conductivity and found that the decrease in size of nanoparticles enhances thermal conductivity. Furthermore, a study by Anoop and co confirmed that smaller particles led to an enhanced thermal conductivity [83].

The shape of nanoparticles is another factor affecting nanofluid's thermal conductivity [86]. Various shapes like a rod, cylindrical, spherical, nearly rectangular, banana-shaped, blade, brick and platelet have been tested theoretically and experimentally. Observed results generally indicate that a more significant aspect ratio (AR) of particles enhances thermal conductivity since thermal penetration increases and the detrimental effects of interfacial thermal resistance on heat transfer are mitigated [83]. On the other hand, the thermal conductivity enhances when the particles have

a small sphericity factor [92]. An investigation of enhanced thermal conductivity of TiO_2/water nanofluid was carried out. It was observed that thermal conductivity increased when using rod-shaped nanoparticles compared to spherical nanoparticles [93]. Another study investigated thermal conductivity using MWCNT of different lengths. Results confirmed that enhanced thermal conductivity was noted with the longest nanotubes [94].

Investigations have shown that base fluid with more excellent thermal conductivity corresponds to nanofluids with smaller increases in thermal conductivity. Gonçalves, et al. [83] explained that there is evidence that EG-based nanofluids offer higher thermal conductivity compared to water-based nanofluids, using Al_2O_3, MWCNTs, and CuO nanoparticles, respectively. Wang, et al. [91] measured the effective thermal conductivities of Al_2O_3 and CuO nanoparticles dispersed in engine oil, EG, water, and vacuum pump fluid. Results showed that EG and engine oil were the highest in terms of thermal conductivity, while vacuum pump fluid was the lowest.

Concentration is another parameter that affects the thermal conductivity of nanofluids. An increase in the concentration of nanoparticles enhances the thermal conductivity as a result of the larger interfacial area between the nanoparticles and base fluid [95]. Nabil, et al. [77] reported an investigation that compared the volume concentration effect on thermal conductivity between Silica and MWCNTs. Although the concentration increment of both nanomaterials improved the thermal conductivity, it was found that silica nanofluids demonstrated a minimum increment compared to MWCNT water-based nanofluids. Gonçalves, et al. [83] further noted that on the contrary, some researchers reported that high concentration values decreased the thermal conductivity, and it must be as a result of stability since it performs a significant role in defining an ideal concentration.

Temperature is another significant parameter [46]. A study was recently done by Wole-Osho, et al. [96]. It was about nanoparticle temperature's effect on hybrid nanofluid's thermal conductivity. They experimented using alumina and ZnO, and it was observed that an increase in temperature enhances the thermal conductivity of the hybrid nanofluid. They further concluded that the enhancement rate with temperature is relatively constant for all mixture ratios considered at all volume concentrations. In theory, the reduction of the particle's surface energy and Brownian motion enhancement are the causes of the increase in thermal conductivity as the temperature increases [83].

There are numerous models for predicting the nanofluid's thermal conductivity, based mainly on an average of the nanoparticles' properties and the base fluid, which measures the fraction between both [97].

$$K_{nf\,Maxwell} = K_{bf}\left(\frac{K_{np} + 2K_{bf} + 2\varphi\left(K_{np} - K_{bf}\right)}{K_{np} + 2K_{bf} + 2\varphi\left(K_{np} - K_{bf}\right)}\right) \tag{2.2}$$

The Maxwell model, Eq (2.2), was one of the first models with good approximation and simplicity valid for volume fraction <1%. It included the thermal conductivities of the base fluid and nanoparticles [83, 98]. Some other models, for example, included parameters like the particle shape, temperature, and viscosity of the base fluid, geometry and diameter of the nanoparticles, *Ra* and Prandtl numbers, depending on the application, as shown in Table 2.4.

2.4.2. Viscosity

After thermal conductivity, dynamic viscosity is the second most essential thermophysical property of hybrid nanofluids. It is defined as a fluid's internal resistance against the current convection [8]. Several researchers used Brookfield cone and plate viscometer to measure fluids' viscosity [77]. The addition of nanoparticles and increment in nanoparticles volume concentration increases the hybrid nanofluid viscosity due to the agglomeration of nanoparticles in suspension at higher concentrations. In short, several factors like temperature, particle size, and volume fraction play a vital role in the colloidal suspension viscosity [99, 100].

An investigation on dynamic viscosity was done by Esfe, et al. [101] on Ag-MgO water-based hybrid nanofluid. They reported that the viscosity increased with an increase in nanoparticle concentration. Suresh, et al. [34] experimentally investigated the effect of concentration on the viscosity of alumina-copper water-based hybrid nanofluids and reported a maximum of 115% increment in viscosity at 2% volume concentration in comparison to the base fluid.

Table 2.4: Thermal conductivity empirical models

Model	Parameters Included	Ref
$K_{nf\ H\&C} = K_{bf}\left(\frac{K_{nf}+(n-1)K_{bf}-\varphi(n-1)(K_{bf}-K_{np})}{K_{np}+(n-1)K_{bf}+\varphi(K_{bf}-K_{np})}\right)$	Thermal conductivities of BF and NPs, particle shape, and composition.	[83]
$K_{nf\ Xue} = K_{bf}\left(\frac{1-\varphi+2\varphi\frac{K_{np}}{K_{np}-K_{bf}}\ln\left(\frac{K_{np}+K_{bf}}{2K_{bf}}\right)}{1-\varphi+2\varphi\frac{K_{bf}}{K_{np}-K_{bf}}\ln\left(\frac{K_{np}+K_{bf}}{2K_{bf}}\right)}\right)$	Logarithmic progressions of the thermal conductivities of BF and NPs, particle shape, and composition.	[83]
$K_{nf\ Maiga\&Nyugen} = K_{bf}\left(1+2.72\varphi+4.97\varphi^2\right)$	Thermal conductivities of BF.	[102]
$K_{nf\ Xuan} = K_{nf\ Maxwell} + \frac{1}{2}\rho_{np}c_{np}\varphi\sqrt{2D_B}$ **where** $D_B = \frac{k_B T}{6\pi\mu_{bf} r_c}$	The temperature and viscosity of the BF, average radius and viscosity of the clusters, and Brownian motion.	[103]

Abbasi, et al. [104] examined the viscosity of MWCNT/TiO_2 (34%), which contains more MWCNT than MWCNT/TiO_2 (61%). The results showed that the hybrid nanofluid with more MWCNT possesses a higher viscosity. Even with their high viscosity, it was reported that a vast majority of nanofluids and hybrid nanofluids exhibits better heat transfer performances than conventional liquids used as base fluids [99]. Asadi, et al. [105] reported that Yu and co studied the effect of various temperatures (283, 281, 279, 277, and 275 K) and volume fractions of 0.0047–0.2381vol% on MWCNT water-based nanofluid. Results showed that viscosity reduced with an increase in the temperature, although the relative viscosity increased slightly at medium shear stress when the temperature increased.

Researchers have used existing classic models and correlations, such as Einstein [106], who in 1906 developed the first nanofluid viscosity correlation based on the assumptions that the viscous fluid particles are spherical at a volume concentration lower than 5%, followed by Brinkman [99] who introduced his in 1952 as an extension of Einstein's correlation and his viscosity correlation is apparently more reliable [106]. The correlations of Einstein and Brinkman are presented in Eqs (2.3) and (2.4), respectively.

$$\mu_{nf} = \mu_{bf}\left(1 + 2.5\varphi\right) \tag{2.3}$$

$$\mu_{nf} = \mu_{bf}\left(\frac{1}{(1-\varphi)^2}\right) \tag{2.4}$$

Table 2.5 shows some other correlations used by researchers to predict nanofluid viscosity.

Table 2.5: Some correlations to predict the viscosity of nanofluids

Correlation	Assumptions/ Observations	Ref
$\mu_{nf\ Pak\&Cho} = \mu_{bf}\left(1 + 39.11\varphi + 533.9\varphi^2\right)$	Developed based on particle volume fraction and room temperature as a reference.	[99]
$\mu_{nf\ Batchelor} = \mu_{bf}\left(1 + 2.5\varphi + 6.2\varphi^2\right)$	For spherical shape NPs, impact on Brownian motion on NPs.	[106]
$\mu_{nf\ Wang} = \mu_{bf}\left(1 + 7.3\varphi + 123\varphi^2\right)$	It was derived for Alumina–EG–water system. They observed that an increment in particle concentration led to an increase in viscosity.	[106]
$\mu_{nf\ Suganthi} = \mu_{bf}\left(1 + 5.9765\varphi - 5T^{-0.1802}\varphi^{0.5455}\right)$	Specifically derived for ZnO–EG–water system and based on temperature and nanoparticle concentration.	[107]

Despite this, most correlations proposed to predict the viscosity of hybrid nanofluids are based on laboratory and experimental data. These hybrid nanofluids are not suitable for other types of hybrid nanofluids [99]. According to literature, experimental measurements showed a deviation, especially at high volume concentrations amongst the value calculated utilizing the experimental measurements and theoretical model. Therefore, experimentally measuring the nanofluid's viscosity may guarantee a precise conclusion in nanofluids' natural convection heat transfer analysis [8].

2.4.3. Specific Heat Capacity

As mentioned previously, specific heat capacity plays a vital role in the heat transfer characteristics of hybrid nanofluids [79], yet little interest has been paid to the study of heat capacity [108]. Since 2008, there has been an increasing interest in determining the effective specific heat capacity of nanofluids, with only 5% of publications in the literature focused on this aspect [108]. Nanofluid's specific heat capacity exclusively depends on the size of the colloidal suspension dispersed. In other words, nanoparticles with smaller sizes have higher specific heat compared to particles of bigger sizes. This is because the surface atom of the smaller-sized particles is more compared to the bigger-sized particles, hence they possess more specific heat. Therefore, it follows that observing a higher heat capacity with smaller particles is consistent with assessing surface atomic properties [46].

Tiwari, et al. [108] experimentally compared the specific heat capacity of three different metal oxides, i.e., CuO, MgO, and SnO_2, with MWCNT/ water-based hybrid nanofluids. The results showed that the specific heat of hybrid nanofluids at a particular particle concentration increases with increasing temperature. Also, at a particular temperature and particle size, the heat capacity value decreases as the volumetric concentration increases, as presented in Figure 2.9 (a) - (c). The results have also stated that the specific heat of hybrid nanofluid enhances while density decreases and vice versa.

(a)

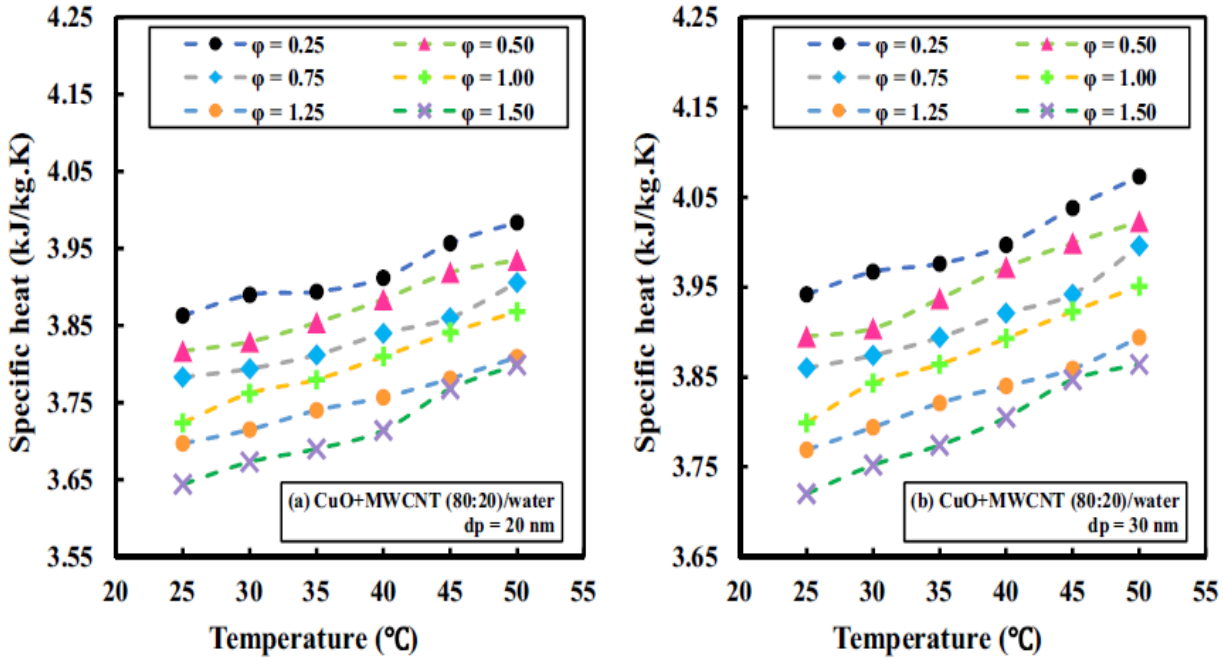
φ = 0.25
φ = 0.50
φ = 0.75
φ = 1.00
φ = 1.25
φ = 1.50
(a) CuO+MWCNT (80:20)/water
dp = 20 nm
(b) CuO+MWCNT (80:20)/water
dp = 30 nm
Specific heat (kJ/kg.K)
Temperature (℃)

(b)

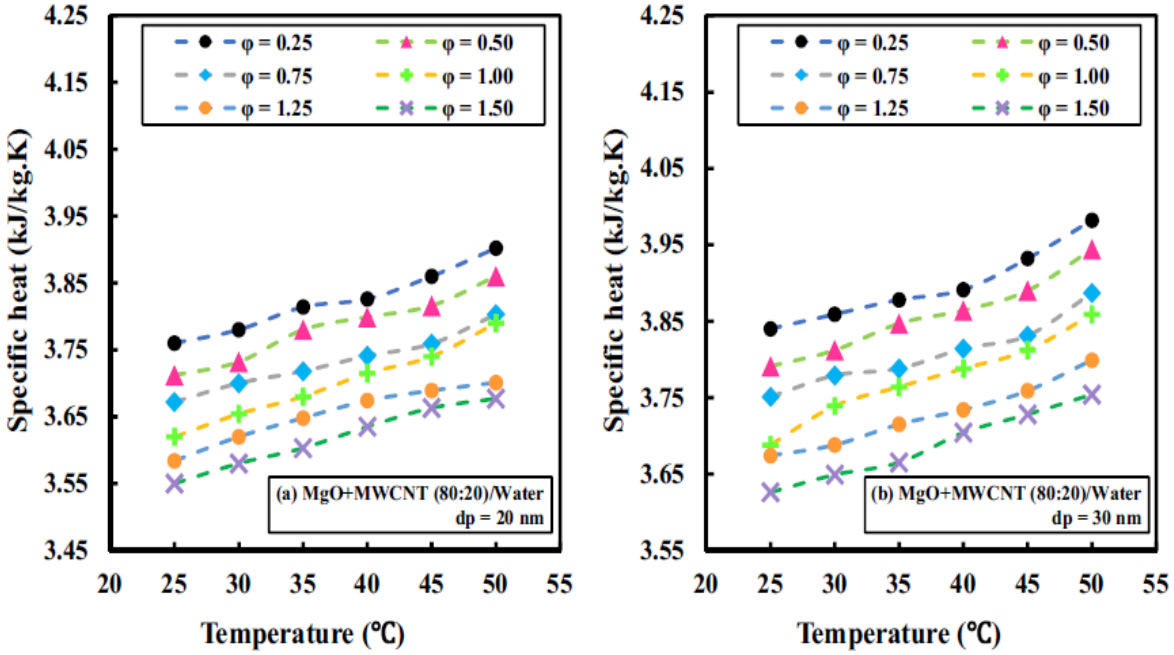
φ = 0.25
φ = 0.50
φ = 0.75
φ = 1.00
φ = 1.25
φ = 1.50
(a) MgO+MWCNT (80:20)/Water
dp = 20 nm
(b) MgO+MWCNT (80:20)/Water
dp = 30 nm
Specific heat (kJ/kg.K)
Temperature (℃)

(c)

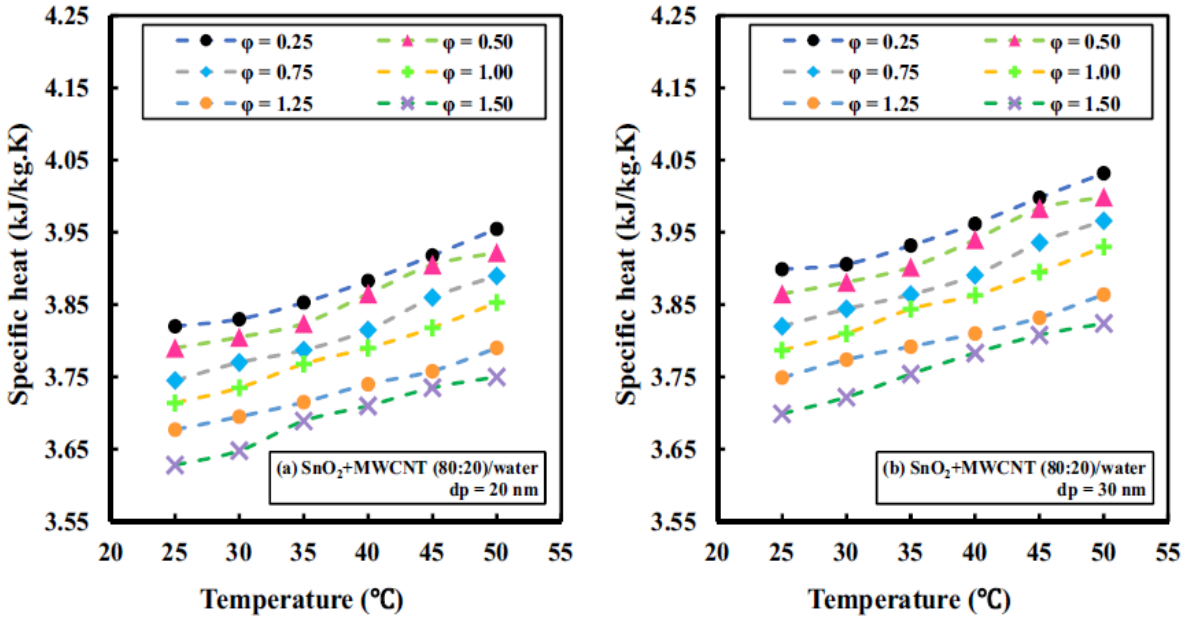

Figure 2.9: Specific heat capacity measurement of (a) CuO- MWCNT (80:20) (b) MgO-MWCNT 80:20) (c) SnO_2- MWCNT (80:20) water-based hybrid nanofluid at nanoparticle diameter of 20 nm and 30 nm [108]

Several researchers have developed and proposed equations to calculate the specific heat capacity of nanofluids. Pak and Cho made use of Equ (2.5) to estimate the heat capacity. They reported that it decreased with increased nanofluid volumetric concentration [8]. Çolak, et al. [109] used Pak and Cho model to compare the experimental measurement of heat capacity, and the results showed that the correlation could predict experimental results within the range of ±1%. Additionally, they found similar results to previous research that the specific heat capacity increased as temperature increased and decreased as volume concentration increased.

$$C_{p_{nf}} = \varphi C_{p_{np}} + (1-\varphi) C_{p_{bf}} \tag{2.5}$$

Gonçalves, et al. [83] stated that Equ (2.6) is also commonly used. Gupta, et al. [46] also presented Equ (2.7) to calculate the heat capacity of hybrid nanofluids, similar to Equ (2.6) but considering the second nanoparticle.

$$C_{p\,nf} = \frac{\rho_{np}\varphi C_{p\,np} + (1-\varphi)\rho_{bf} C_{p\,bf}}{\rho_{nf}} \tag{2.6}$$

$$C_{p\,hnf} = \frac{\rho_{np1}\varphi C_{p\,np1} + \rho_{np2}\varphi C_{p\,np2} + (1-\varphi_{np1}-\varphi_{np2})\rho_{bf} C_{p\,bf}}{\rho_{hnf}} \tag{2.7}$$

In addition, Vajjha and Das [110] analysed the specific heat capacity of Al_2O_3, ZnO, and SiO_2 nanofluids and established that Eq (2.6) was more consistent with the experimental findings. Hence it was used in their study.

2.4.4. Other Thermophysical Properties of Hybrid Nanofluids

The effective thermophysical properties, for example, thermal expansion coefficient and density, are less significant than the likes of specific heat capacity, thermal conductivity, and dynamic viscosity of nanofluids in the natural convection of nanofluids [8].

The density of hybrid nanofluids can be expressed by the law of mixture:

$$\rho_{hnf} = \varphi_{np1}\rho_{np1} + \varphi_{np2}\rho_{np2} + (1-\varphi_{np1}-\varphi_{np2})\rho_{bf} \tag{2.8}$$

Where ρ_{hnf} is the density of the hybrid nanofluid, ρ_{bf} is the density of the base fluid, ρ_{np} is the density of the nanoparticles, and finally φ_{np} is the volume concentration of the nanoparticles. The equation depicts the hybrid nanofluid effective density as a function of nanoparticles volume concentration, nanoparticles and base fluid density. Compared to thermal conductivity and viscosity, experimental data regarding the density of the hybrid nanofluid are limited in the literature [111]. Ho, et al. [112] experimentally studied the density of a water-based hybrid suspension of alumina nanoparticles and micro-encapsulated phase change material (MEPCM) particles. They used the mixture density theory formula at a temperature of 30 ℃. A good agreement was noted between the observed mixture density and experimental values, as shown in Figure 2.10.

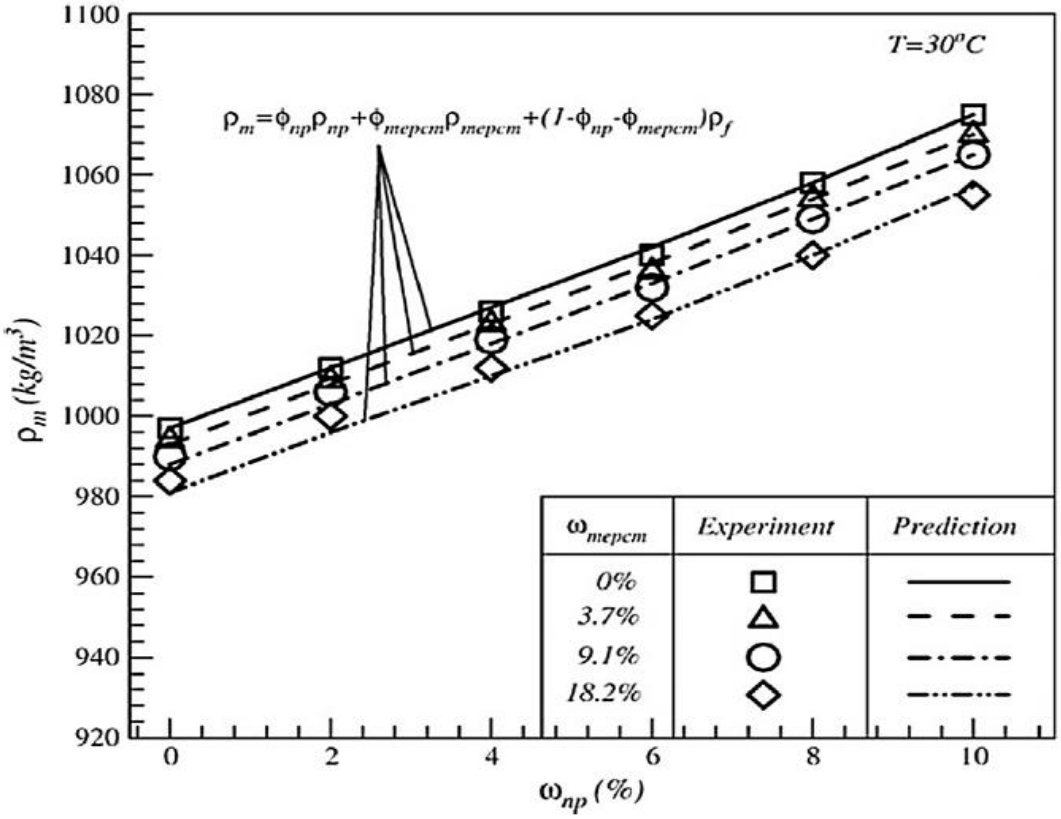

Figure 2.10: Density measurement of Al_2O_3 nanoparticles and MEPCM particles hybrid water-based suspensions [112]

Askari, et al. [113] also measured the density of hybrid nanofluids Fe_3O_4 and graphene/kerosene at room temperature. They reported that the addition of nanoparticles to the base fluid resulted in an increase in density; however, the increase in density is negligible. They noted that the experimental data agree with the theoretical models.

Nanofluid's thermal expansion coefficient is estimated by utilizing the mixing solid-liquid theory [98, 114], as shown in Equ (2.9) and Equ (2.10) , which are commonly adopted in the literature [78].

$$\beta_{nf} = \varphi_{nf}\beta_{np} + (1-\varphi_{nf})\beta_{bf} \tag{2.9}$$

$$\beta_{nf}\rho_{nf} = \varphi_{nf}\rho_{np}\beta_{np} + (1-\varphi_{nf})\rho_{bf}\beta_{bf} \tag{2.10}$$

Ho, et al. [78] numerically evaluated nanofluid's effective volumetric thermal expansion coefficient containing various volume fractions of Al_2O_3 nanoparticles. They noted that the effective thermal expansion coefficient reduced drastically as the Al_2O_3 nanoparticles were dispersed in water. They also reported that Equ (2.9) overestimated the effective thermal expansion coefficient of the nanofluid, but Equ (2.10) predictions were closer to the values they achieved in their study. Nayak, et al. [115] used various nanofluids, such as Al_2O_3, CuO, SiO_2, and TiO_2 were measured for their volumetric thermal expansion coefficient in order to evaluate their potential use in heat removal systems that use natural convection as a heat removal method. They reported that CuO nanofluid showed the highest thermal expansion coefficient, while TiO_2 nanofluid showed the lowest among the nanofluids tested. Nevertheless, in conclusion, all the nanofluids had a significant thermal expansion coefficient increase compared to water at low temperatures than at higher temperatures.

2.5. Heat Transfer of Hybrid Nanofluids

James Maxwell, a Scottish scientist, was the first to introduce the idea of suspension of solid particles into convectional fluids such as water, oils, and EG to enhance heat transfer in the nineteenth century [116]. However, the rapid settling of a millimetre- or micrometre-sized particles in liquid or solids suspension has been the main impediment to developing suspensions for industrial applications [117]. The rapid settling causes an increase in the viscosity of the fluids and an increase in pressure drop [116].

Choi and Eastman [17] then introduced nanofluid. They suspended copper nanophase materials with a diameter of less than 100 nm in water to enhance the thermal conductivity of water. The result of their theoretical study on the thermal conductivity of nanofluid showed that the nanofluid could drastically reduce the heat exchanger pumping power. Typical materials include metals such as Cu, Au, Ag, and Ni; metal oxides such as Al_2O_3, CuO, Fe_2O_3, Fe_3O_4, SiO_2, TiO_2, and ZrO_2; and carbon materials such as carbon nanotubes, graphite, and diamond [19]. These nanoparticles named at the outset have been commonly used due to the findings on their thermophysical properties, i.e., high thermal conductivity, etc. Other factors such as cost, toxicity, chemical stability availability, compatibility with base fluid, and thermophysical properties of the nanomaterials are to be considered when selecting nanoparticles for heat transfer application [81].

Wu, et al. [118] investigated the heat transfer coefficient of water-based alumina nanofluid in the turbulent and laminar regimes and proposed Equ (2.11) and (2.12) below for the respective regimes. They noted that at the same Reynolds number (*Re*), an augmentation in nanoparticles volume fraction enhanced *h*.

$$\frac{h_{nf}}{h_{bf}} = \left(\frac{\rho_{nf}}{\rho_{bf}}\right)^{0.85} \left(\frac{k_{nf}}{k_{bf}}\right)^{0.6} \left(\frac{\mu_{nf}}{\mu_{bf}}\right)^{0.45} \left(\frac{C_{p\,nf}}{C_{p\,bf}}\right)^{0.4} \tag{2.11}$$

$$\frac{h_{nf}}{h_{bf}} = \left(\frac{\rho_{nf}}{\rho_{bf}}\right)^{0.775} \left(\frac{k_{nf}}{k_{bf}}\right)^{0.6} \left(\frac{\mu_{nf}}{\mu_{bf}}\right)^{0.375} \left(\frac{C_{p\,nf}}{C_{p\,bf}}\right)^{0.4} \tag{2.12}$$

In terms of increasing heat transfer, nanofluid increases heat transfer based on the type of base fluid, temperature, nanoparticle concentrations, nanoparticle properties, and other factors that affect nanofluid properties, such as nanoparticle agglomeration and surfactants [118]. A concept known as the hybridization of nanoparticles is employed to make nanofluids more thermally efficient [119]. Hybrid nanofluid refers to nanofluids prepared from a suspension of distinct nanoparticle types in a single base fluid [46]. They are a new class of fluid used in applications of heat transfer, which contain nanoparticles as small as 100 nm in size [111].

Suresh, et al. [34] investigated the heat transfer characteristics of Al_2O_3–Cu/water hybrid nanofluid. Results showed that the natural convection heat transfer coefficient increased with *Re*, and the *Nu* of hybrid nanofluid was enhanced by 13.56% in comparison to the base fluid. Sundar, et al. [33] measured the convective heat transfer coefficient of MWCNT–Fe_3O_4/water hybrid nanofluids. The researchers reported a 31.1% increase in *Nu*, despite a 1.18-times increase in pumping power for particle loads of 0.3% at 22,000 *Re* compared to water. Their findings claimed that composite-based hybrid nanofluids have higher thermal performance than single-particle nanofluids like Al_2O_3, TiO_2, and Fe_3O_4.

2.5.1. Natural Convection

There are three categories of heat transfer in hybrid nanofluids, namely natural convection, mixed convection, and forced convection. Natural convection produces less noise, consumes less energy,

and requires less maintenance compared to forced convection [116]. Natural convection is a kind of heat transfer mode where the fluid motion occurs naturally and is not caused by external sources like pumps, fans, or any prime mover [6]; density variations are the only cause of this phenomenon. Industries like transportation, micro-electronics, and manufacturing face technical thermal challenges, but cooling is one of the indispensable challenges typically due to natural convection's low *h* [4, 5]. The heat transfer coefficient of natural convection is relatively lower compared to other methods used in thermal transportation. It is, therefore, imperative to investigate in what way the natural convection film coefficient can be improved [120].

Putra, et al. [25] studied the natural convection of nanofluids in a cavity, using CuO and Al_2O_3 water-based nanofluids filled into a cylindrical vessel. The nanofluids used in the study were selected based on the number of previous studies which showed a widespread knowledge of their thermal and flow properties. The number of studies on synthesizing and thermophysical properties of hybrid nanofluids has increased in recent years. However, minimal analyses have been done on the free convection of hybrid nanofluids in cavity flow. According to several pieces of literature, researchers have experimented on various cavities like triangular, semi-circular, cylindrical, square, and unconventional shapes. These studies were noted to have been carried out with numerical techniques, whereas the studies conducted experimentally have not been ventured into and are unavailable [15].

Ghalambaz, et al. [121] numerically investigated the natural convection of Ag-MgO/water hybrid nanofluids inside a square cavity, demonstrated in Figure 2.11. They noted that the inclusion of hybrid nanoparticles in the base fluid sometimes does not improve the rate of heat transfer in a square cavity. Meaning that other factors, such as *Ra*, can change the effects of the hybrid nanoparticles since the result of the study showed that the heat transfer rate increased with the addition of hybrid nanoparticles at a low *Ra*. Chamkha, et al. [30] analysed the natural convection in a semi-circular cavity filled with Al_2O_3/Cu-water nanofluid using a numerical technique. They studied the effects of nanoparticles volume fraction, *Ra*, and thermal conductivity ratio on the flow patterns and heat transfer. It was noted that the addition of a low volume fraction of hybrid nanoparticles inside the cavity led to the improvement of the heat transfer.

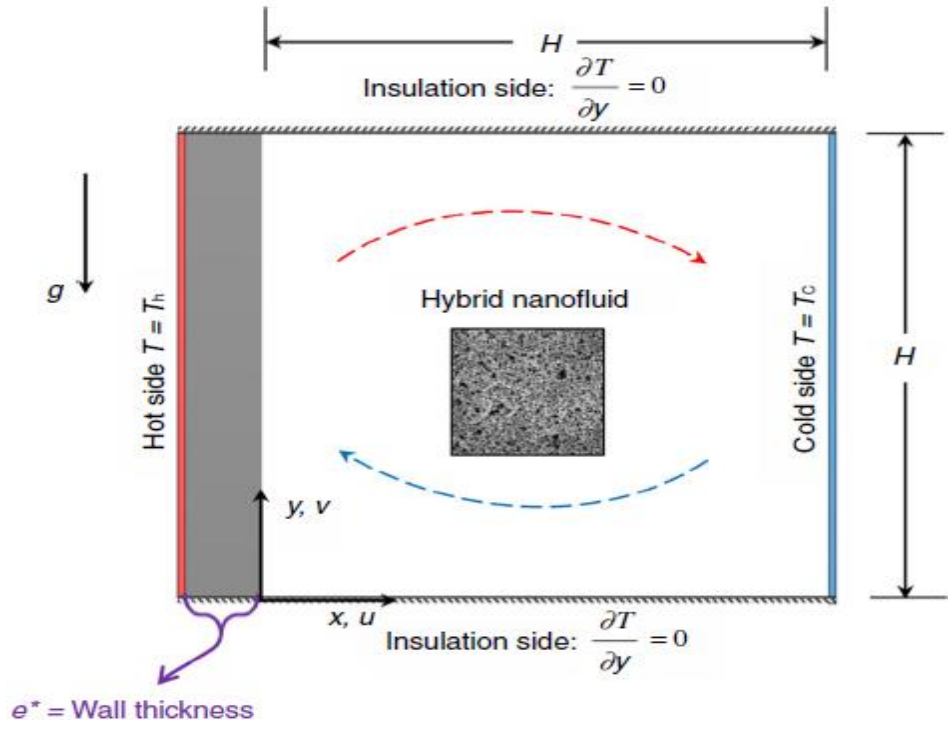

Figure 2.11: Schematic view of the physical model and coordinate system [121]

Selimefendigil and Chamkha [122] numerically investigated the convective heat transfer of Al_2O_3/Cu-water hybrid nanofluid in a triangular annular cavity with an opening in the inclined side of the outer triangle and the inner and outer surfaces of the triangular cavities isothermally. Their study considered the influence of the *Ra* number between 10^4 – 5 x 10^5, between 0 and 0.02 solid volume fraction of the nanoparticles, and the opening ratio between 0 and 0.625 on the fluid flow and heat transfer. They reported that the effects of the opening ratio on the heat transfer enhancement are more effective for higher *Ra*. Also, *Nu* enhanced with *Ra* and the opening ratio. Maskeen, et al. [27] studied numerically convective heat transfer performance of Al_2O_3/Cu−water hybrid nanofluid over a stretching cylinder, shown in Figure 2.12. The researchers examined the performance of heat transfer by comparing hybrid nanofluids and single material nanofluids with water as the base fluid for both nanofluids. It was reported that convective heat transfer was the lowest in the case of Cu/water nanofluid and was improved by adding hybrid material.

Rashad, et al. [31] numerically examined the natural convection heat transfer of Cu-Al_2O_3/water hybrid nanofluids filled in a triangular cavity. The cavity was subjected to a constant magnetic field and was heated by a constant heat flux element from underneath the cavity. The researchers reported that the hybrid nanofluid, containing equal amounts of Al_2O_3 and Cu nanoparticles dispersed in water base fluid, had no major effect on the mean Nusselt number (*Nu*) in comparison with the regular nanofluid.

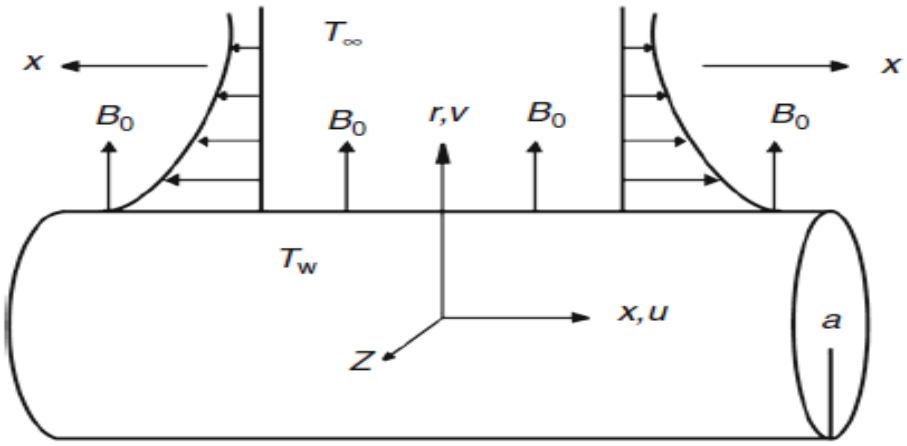

Figure 2.12: Schematic overview of the geometry and coordinate system [27]

Ashorynejad and Shahriari [123] numerically investigated natural convection heat transfer of Al_2O_3-Cu/water hybrid nanofluid within an open wavy cavity. The top and bottom walls were insulated against heat and mass, the right wall was opened, and the left wavy wall of the cavity was heated sinusoidally. Their study investigated the effect of nanoparticle volume fractions, *Ra*, Hartmann number, and phase deviation. The results showed a reduction in *Nu* as the Hartmann number increased. However, it increases with the increment of nanoparticle volume fraction and *Ra*.

A recent study by Asmadi, et al. [124] numerically analysed natural convection heat transfer inside a U-shaped cavity filled with Cu–Al_2O_3/water hybrid nanofluid on the effects of constant, linear, quadratic, and sinusoidal with different amplitudes and periods. They considered *Ra* ranging from 10^4 – 10^6 and nanoparticle volume fractions between 0 and 0.1 on the fluid flow for each thermal profile. It was reported that the constant heating profile gave the best heat dissipation performance,

while the sinusoidal thermal profile performed the worst. Almeshaal, et al. [125] studied a three-dimensional numerical simulation of natural convection inside a T-shaped cavity filled with CNT–Al_2O_3/water hybrid nanofluid. They used a hybrid nanofluid with 25:75 wt% of CNT and Al_2O_3 nanoparticles. It was observed that the heat transfer enhanced with an increase in size, volumetric percentage of nanoparticles, fraction of CNT composites, and *Ra*.

The numerical investigation results on natural convection in enclosures have been inconsistent, resulting in more experimental work. However, very few experimental investigations have been published in the literature [8], especially on hybrid nanofluids since it is a new class of nanofluids compared to mono nanofluids. Hu, et al. [126] experimentally investigated the natural convection heat transfer of Al_2O_3 -water nanofluid in a square cavity. They studied the effect of different nanoparticle volume fractions of 0.25%, 0.50%, and 0.77%, and various *Ra* ranging from 30×10^6 – 70.52×10^6. According to the study, heat transfer is more sensitive to thermal conductivity than viscosity at low nanoparticle fractions, and at high nanoparticle fractions, it is more sensitive to viscosity than thermal conductivity. Figure 2.13 illustrate the average *Nu* of the nanofluid at different *Ra*. It shows that the heat transfer characteristic is enhanced at the lowest nanoparticle mass fraction of 1%. At 2% nanoparticles mass fraction, the *Nu* is closer to that of the base fluid. However, an increase in the mass fraction of nanoparticles at 3% weakens heat transfer enhancement. A good agreement between the experimental and numerical results was found.

An experimental study on natural convection heat transfer of SiO_2 water-based nanofluid inside a rectangular enclosure at different concentrations and inclination angles was carried out by Torki and Etesami [16]. The researchers reported that heat transfer did not change significantly at low concentrations. However, the heat transfer coefficient decreased with the volume fraction of nanoparticles greater than 0.5% due to the increased viscosity of the nanofluid. In relation to the effect of inclination angles, they found that increasing tilt angle had a negative impact on heat transfer. However, it did not affect *Nu* in nanofluids with high concentrations. In addition to this, it was confirmed that the film coefficient or effectiveness decreases with an increasing inclination angle of the cavity. Furthermore, they exclaimed that contrary to what the numerical results implied, there is no increase in convection heat transfer as the concentration of nanofluid increases.

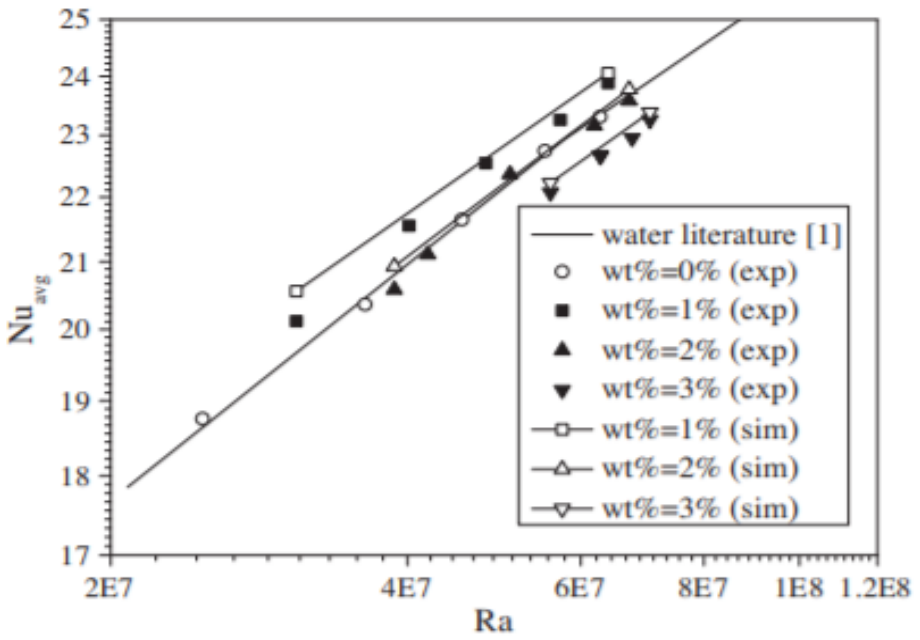

Figure 2.13: Average Nu of nanofluid at different Ra [126]

Sharifpur, et al. [127] studied the natural convection heat transfer of TiO_2 – water with volume fractions varied from 0.05 - 0.80 vol% in a square cavity. It was reported that the addition of TiO_2 nanoparticles enhanced the heat transfer. They also stated that an optimum volume concentration of 0.05% was found for a maximum heat transfer enhancement of 8.2% in their study. Choudhary and Subudhi [128] investigated the performance of convective heat transfer of Al_2O_3 nanofluid experimentally with DI water as the base fluid filled in a rectangular cavity with an AR of 0.3 - 2.5. The volume concentration of the nanofluid studied was 0.01% and 0.10%, while the range of *Ra* was from 10^7 - 10^{12}. They reported that the volume concentration and aspect ratio influenced the natural convection performance. They also noted that higher volume concentrations resulted in lower heat transfer, while lower volume concentrations produced higher heat transfer. A 29.5% maximum heat transfer enhancement was observed at 0.01 vol% and an aspect ratio of 0.5.

Garbadeen, et al. [129] experimentally studied the convective heat transfer performance of MWCNT/water nanofluids filled in a square cavity. The volume concentration ranged from 0 – 1%. Their results showed a maximum enhancement of 45%, which occurred at approximately 0.10% volume concentration.

Dey and Sahu [130] experimentally studied ZnO and Al_2O_3 nanofluids' natural convection heat transfer behaviour in a cavity using various working fluids. They used air, tap water, and distilled water. They calculated the heat transfer coefficient and *Nu* based on the measured temperatures using Eqs (2.13) - (2.14). In their findings, the researchers confirmed that air had a very low *h* due to its low thermal conductivity. In contrast, distilled water had the highest heat transfer coefficient since tap water contains impurities, while distilled water is free of them.

$$h = \frac{Q}{A\left(T_h - T_c\right)} \tag{2.13}$$

$$Nu = \frac{hL}{k} \tag{2.14}$$

Ho, et al. [78] analysed the natural convection heat transfer of Al_2O_3 water-based nanofluid at various volumetric fractions ranging from 0.1% to 4% in a vertical square cavity. They considered *Ra* values ranging from 6.21×10^5 - 2.56×10^5. Findings revealed that heat transfer was reduced in nanofluids containing a volume concentration of 2% or more. However, this was not the case for nanofluid of 0.10% vol as they recorded 18% heat transfer enhancement compared to the base fluid. Ilyas, et al. [14] examined the convective heat transfer behaviour of MWCNT-thermal oil nanofluid in a vertical rectangular enclosure with an aspect ratio of 4. As the previous researchers indicated, they also noted a major reduction in the film coefficient of nanofluids with higher concentrations. In addition, they stated the importance of thermal conductivity as an essential property in heat transfer, although other thermophysical properties influence heat transfer performance.

Kiran and Babu [131] experimentally examined the natural convection heat transfer behaviour of TiO_2-transformer oil nanofluid at various volume concentrations of 0, 0.05, 0.1, 0.15, and 0.20 vol% in a vertical cylinder. The researchers reported that at a volume concentration of 0.15%, the thermal performance enhanced, but an increase in the volume concentration of nanoparticles led to a deterioration. Furthermore, they stated that a volume concentration of 0.15% was found for a maximum heat transfer enhancement of 16.8% in their study as the heat transfer coefficient increased from 356.172 W/m^2k to 670.465 W/m^2k.

Giwa, et al. [15], through an experiment, examined the natural convection of Al_2O_3−MWCNT/deionized water hybrid nanofluids at various hybrid nanoparticles percentage weights at 0.10 vol% in a square cavity. The study considered a range of *Ra* 1.65×10^8 - 3.80×10^8. It was reported that the hybrid nanofluid with a percentage weight of 60% Al_2O_3 and 40% MWCNT nanoparticles had the most outstanding value for *Ra*, Q_{av}, Nu_{av}, and h_{av} at various temperatures gradient. In their conclusion, the addition of hybrid nanofluids in the cavity enhanced the performance of natural convection. According to the researchers, the *Ra* of the natural convection of water and hybrid nanofluids in the cavity was determined using Eq (2.15).

$$Ra = \frac{g\beta(T_h - T_c)\rho^2 C L^3}{\mu k} \tag{2.15}$$

The authors also validated the obtained experimental result of water using the models proposed by Berkovsky and Polevikov [132] in Eq (2.16), Cioni, et al. [133] in Eq (2.17), and Leong, et al. [134] in Eq (2.18).

$$Nu = 0.18 \times \left(\frac{\mathrm{Pr}}{(0.2 + \mathrm{Pr})} Ra \right)^{0.29}$$
$$(\mathrm{Pr} \le 10^5;\ Ra \le 10^{10}) \tag{2.16}$$

where

$$\mathrm{Pr} = \frac{\mu C}{k}$$

$$Nu = 0.145 \times Ra^{0.292}$$
$$\left(3.7 \times 10^8 \le Ra \le 7 \times 10^9\right) \tag{2.17}$$

$$Nu = 0.08461 \times Ra^{0.3125} \quad \left(10^4 < Ra < 10^8\right) \tag{2.18}$$

A recent study on the thermo-convection behaviour of MgO-ZnO/ DI water hybrid nanofluid with a volume concentration of 0.05 vol% and 0.10 vol% at various percentage weight ratios in a square cavity was carried out by Nwaokocha, et al. [135]. They studied several parameters such as Q_{av},

Ra, Nu_{av}, and h_{av} at different temperature gradients from 20 ℃ to 50 ℃. The researchers observed that the percentage weight ratios and temperature gradients influence the performance of heat transfer of the hybrid nanofluids. It was reported that the volume concentration of 0.05% at a percentage weight ratio of 40:60 was found to have a maximum heat transfer enhancement of 72.2% in comparison to the base fluid.

Choudhary and Subudhi [128] studied the convective heat transfer performance of Al_2O_3 /DI water nanofluid with volume concentrations of 0.01 and 0.10 vol% filled in a rectangular cavity with an aspect ratio varying from 0.3 to 2.5. They noted that the performance depended on *Ra*, ϕ, and aspect ratio with the maximum enhancement of 29.5% for 0.01 vol% at $Ra = 7.89 \times 10^8$ and $AR = 0.5$. Giwa, et al. [15] experimentally studied the natural convection of Al_2O_3−MWCNT/ DI water hybrid nanofluids at several hybrid nanoparticles percentage weights at 0.10 vol% in a square cavity. The study considered a range of Ra $1.65 \times 10^8 - 3.80 \times 10^8$. They stated that the hybrid nanofluid with a volume concentration of 60% of Al_2O_3 and 40% of MWCNT nanoparticles had the most outstanding value for *Ra*, Q_{av}, $Nu_{av,}$ and h_{av} at various temperatures gradient. In their conclusion, the addition of hybrid water nanofluids in the cavity enhanced the natural convection performance.

2.6. Conclusion

The two-step preparation technique is the most commonly used method to formulate hybrid nanofluids, according to literature. However, the preparation method used in synthesizing hybrid nanofluid affects its stability. If the nanofluid is unstable, it loses its potential to transfer heat by diminishing the Brownian motion of particles. So it is therefore essential to prepare hybrid nanofluids using the right approach. Furthermore, it is necessary to characterize hybrid nanofluids throughout the study of heat transfer of hybrid nanofluids. Typically, the characterization of a hybrid nanofluid reveals details like the stability, shape, and size of the nanoparticles in the base fluid. TEM, SEM, zeta potential analysis, and sedimentation methods are commonly used to characterize.

There are many thermophysical properties of fluids, but thermal conductivity, viscosity, and specific heat capacity are the main properties. Since there is no general formula for hybrid nanofluids' viscosity and thermal conductivity, it is essential to select any theoretical model carefully. This is due to the natural convection of hybrid nanofluids' contractionary results when

making use of various models. More importantly, researchers should measure the thermal conductivity and viscosity of hybrid nanofluids experimentally, as the results would be used in the study of heat transfer.

The number of studies on synthesizing and thermophysical properties of hybrid nanofluids has increased in recent years. However, minimal analyses have been done on the free convection of hybrid nanofluids in cavity flow. Numerical analyses of convective heat transfer of hybrid nanofluids have produced contradictory results, and experimental studies of the natural convection in hybrid nanofluids have also been insufficient. Only some researchers have investigated the influence of hybrid nanofluid volume concentration on enhancing natural convection in a hybrid nanofluid at several *Ra* in a cavity flow. In addition, the discrepancies in numerical and experimental results clearly illustrate the need for more hybrid nanofluid experimental investigations in natural convection cavity flow, which is currently limited. Therefore, this present research intends to address these challenges.

CHAPTER 3

EXPERIMENTAL PROCEDURE

3.1. Introduction

This chapter briefly introduces the safety measures taken in this study, hybrid nanofluid materials, and the equipment used to characterize Al_2O_3–MWCNT (10:90)/DI water hybrid nanofluid. The experimental setup used to carry out the experiments on natural convection of Al_2O_3–MWCNT/ DI water hybrid nanofluids comprised of a square cavity with two isothermal vertical walls, while the rest of the cavity walls were insulated. First, the materials, experimental setup components, and instrumentation utilised are briefly examined. Next, the experimental results of the setup was validated and examined with the aid of existing correlations. Lastly, the analysis of the experimental measurement uncertainty is presented.

3.2. Materials

In this study, the hybrid nanoparticles of alumina and multi-walled carbon nanotube were used. The alumina nanoparticles (99.5% purity and 5nm in diameter) were acquired from Nanostructured and Amorphous Materials Inc., Houston, Texas, USA, while the MWCNT nanoparticles (99.5% purity with outer diameters and lengths of < 7 nm, and 10 – 30 μm, respectively) was sourced from MKnano Company, Ontario, Canada. The surfactant, Sodium dodecyl sulphate (SDS) of ≥ 98.5% purity used in this study was supplied by Sigma-Aldrich, Germany. Table 3.1 presents the thermophysical properties of Al_2O_3 nanoparticles, MWCNT nanoparticles and water. In addition, DI water purchased from Merck (Pty) Ltd was added to achieve the desired volume concentration of the hybrid nanofluids.

Table 3.1: Thermophysical properties of the studied materials

Properties	**DI Water**	**Al_2O_3**	**MWCNT**
Thermal conductivity (W/mK)	0.613	40	2000
Density (kg/m^3)	997	3970	2100
Specific heat capacity (J/kgK)	4179	765	710
Particle size (nm)	-	5	< 7

3.3. Equipment

In order to measure the dimensions within and around the enclosure, a vernier calliper and meter rule was used. The hybrid nanoparticles were weighed using a digital balance (Radwag AS220.R2; 10 mg –220 g and accuracy ± 0.01 g) after the weights of the principal nanoparticles were ascertained with Eq (3.1). The fraction of dispersion is expressed in Eq (3.2).

$$\varphi = \left[\frac{X_{Al_2O_3}\left(\frac{M}{\rho}\right)_{Al_2O_3} + X_{MWCNT}\left(\frac{M}{\rho}\right)_{MWCNT}}{X_{Al_2O_3}\left(\frac{M}{\rho}\right)_{Al_2O_3} + X_{MWCNT}\left(\frac{M}{\rho}\right)_{MWCNT} + \left(\frac{M}{\rho}\right)_{bf}} \right] \tag{3.1}$$

The mixture of hybrid nanoparticles, SDS at 0.8 dispersion fraction, and 1.4*L* of DI water was stirred for 30 minutes utilizing a magnetic stirrer (Lasec hotplate stirrer H4000-HSB, 500 W, 50 Hz) to attain even suspensions prior to ultrasonication.

$$Dispersion\ fraction = \frac{weight\ of\ surfactant}{weight\ of\ hybrid\ nanoparticles} \tag{3.2}$$

In order to break down the accumulation of the hybrid nanoparticles, an ultrasonic agitation probe (Qsonica Q-700; 20 kHz and 700 W with five seconds pulse on and two seconds pulse off with an intensity of 98%) was utilised, and the breaking down of nanoparticles aggregation was done for a period of 1 hour.

While sonication was in progress, the hybrid nanofluid's temperature rose; thus, the samples temperature was monitored through a programmable constant temperature bath (LAUDA ECO RE-1225 Silver). In order to formulate the various volume concentrations of the hybrid nanofluid, Eqs (3.1) – (3.2) were used, and a detailed table showing the measurements is presented in Appendix A.

The hybrid nanofluid viscosity was evaluated utilizing an SV-10 sinewave Vibro-viscometer (A&D in Japan). In addition, the morphology of the hybrid nanoparticles was examined using TEM.

3.4. Safety of the Experimental Investigation

There is insufficient information to predict all the situations that are likely to lead to exposure to nanomaterials. However, some factors could lead to potential exposure, such as working with nanomaterials in liquid media without adequate protection, increasing the risk of skin exposure, or increasing the likelihood of inhalation [136]. Therefore, the following measures were taken to avoid inhalation, dermal contact, or ingestion of nanoparticles during the study [137, 138].

- Washed hands frequently to minimise potential nanoparticle exposure through ingestion and dermal contact. Washed hands before eating or drinking after working in the lab.
- Hybrid nanofluids were stored in a well-sealed container that could be opened with minimal agitation of the contents.
- The student used a sealed, double-contained container when transporting hybrid nanofluids inside the laboratory.
- Containers were labelled correctly, indicating the nanoparticles/nanofluids they contained.
- Use of personal protective equipment like gloves, lab coat or protective clothing, safety goggles, long pants, closed-toe shoes, respiratory protection, and face shields, as appropriate, to prevent skin and eye contact with nanoparticles or hybrid nanofluids.
- The student collected spill cleanup materials in a tightly closed container.

3.5. Experimental Setup

The streamlined schematic diagram of the experimental setup used to test the natural convection of hybrid nanofluids is illustrated in Figure 3.1.

A square cavity (length 96 mm × breadth 96 mm × height 105 mm) filled with the prepared hybrid nanofluids was utilised to investigate the convection heat transfer performance. In this case, a square cavity was chosen since it has a broader range of applications than most other kinds of cavities. They are primarily applicable in solar systems and applications, double-glazed windows, and electronic devices. In this study, thermal insulation was applied to the top and bottom walls of the cavity, while the opposite vertical walls were differentially heated.

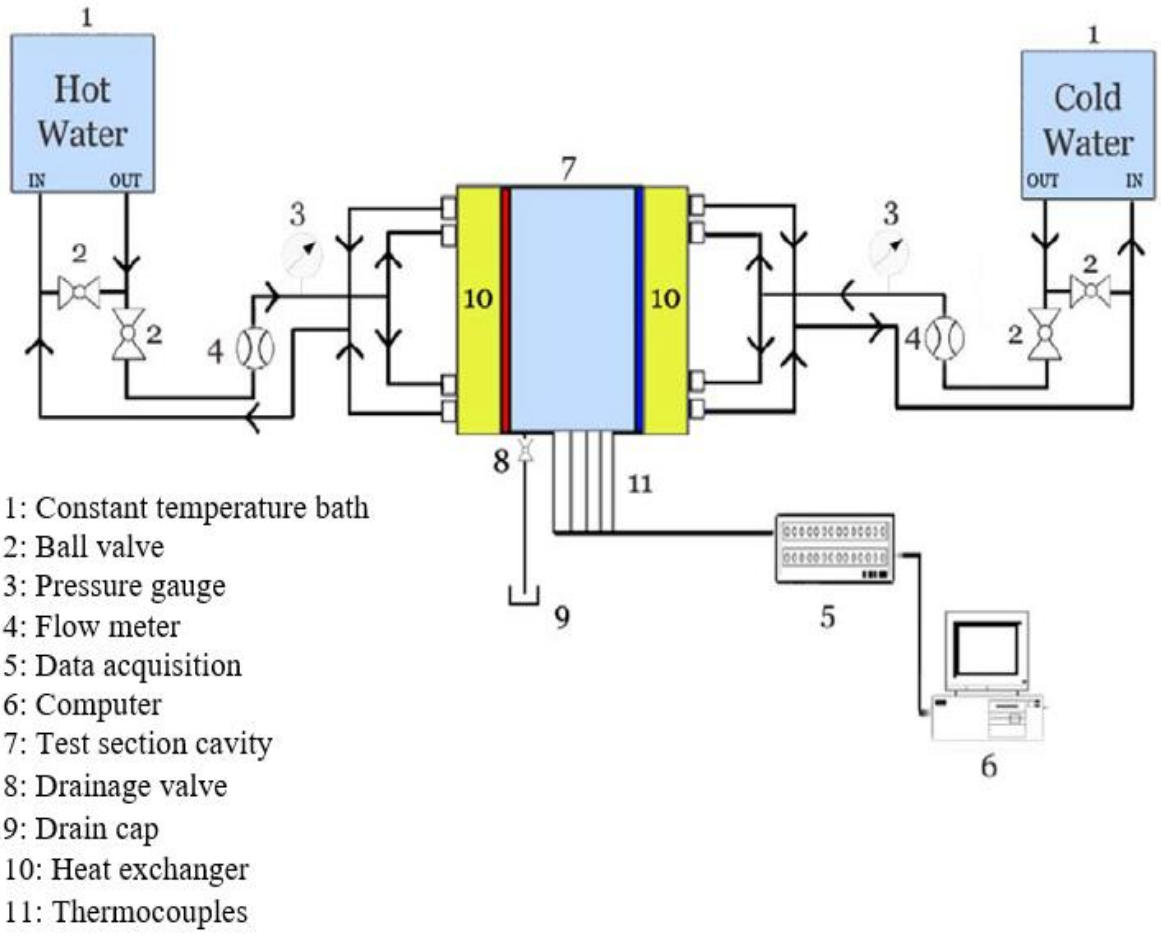

Figure 3.1: Schematic diagram of the experimental setup

Figure 3.2 illustrates the schematic overview of the studied geometry of the present study. The cavity and the pipe connections were well-insulated (20 mm with a thermal conductivity coefficient of 0.033 W/mK) to minimise the heat loss into the surrounding area. The T-type thermocouples (TT-T-30SLE(ROHS)) purchased from Omega Engineering Inc., USA, were installed at different spots outside and within the square cavity to measure different temperatures across the cavity as the experiment progressed. For accurate surface temperature readings, the thermocouples were submerged about 2 mm deep inside the walls with the aid of silicon and thermal glue to make sure accurate readings were achieved. Five thermocouples were mounted vertically at the midpoint between the cold and hot walls, while seven thermocouples were attached horizontally at the centreline between the cold the hot walls.

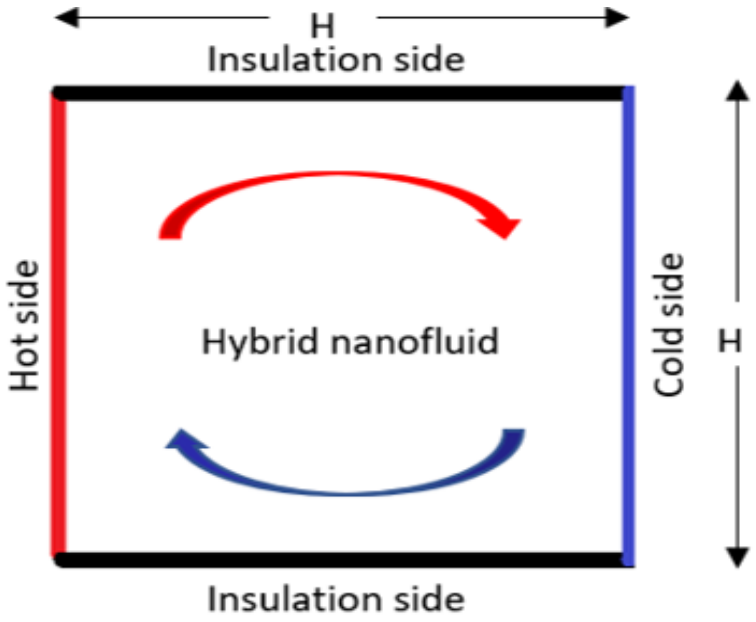

Figure 3.2: Schematic overview of the studied geometry

The schematic diagram of the thermocouple's position and the configuration are shown in Figure 3.3, and Figure 3.4, respectively.

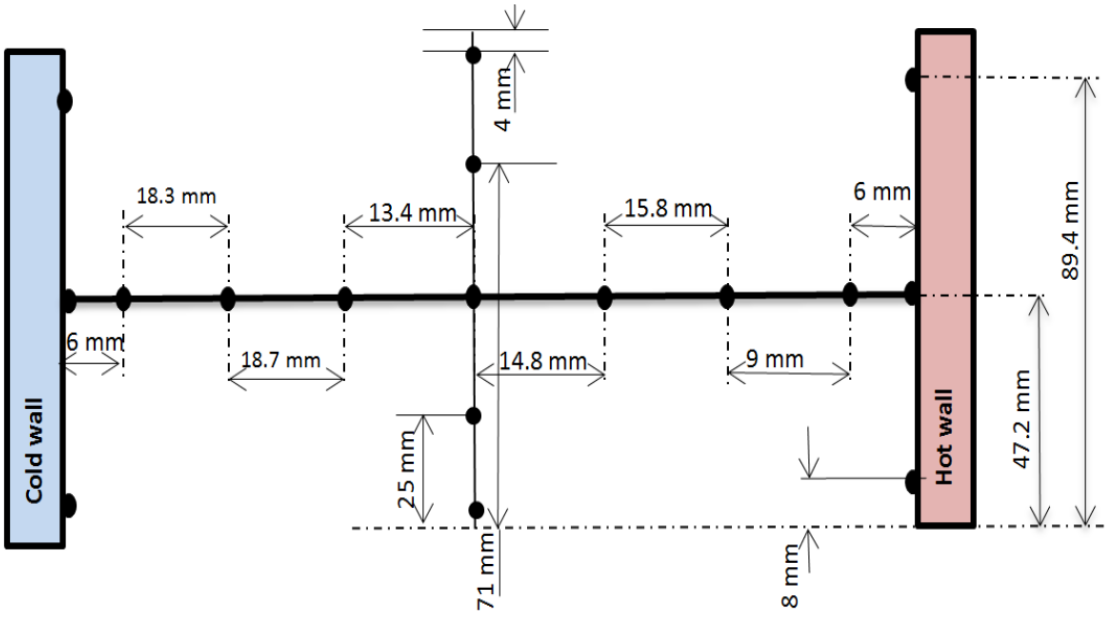

Figure 3.3: Schematic of the thermocouples in the experimental setup

Before this study began, the thermocouples were calibrated with temperatures ranging from 15 $°C$ and 65 $°C$. As a result of the difference in temperature between the insulated thermocouples and the environment, 3% of the heat was lost outside the cavity.

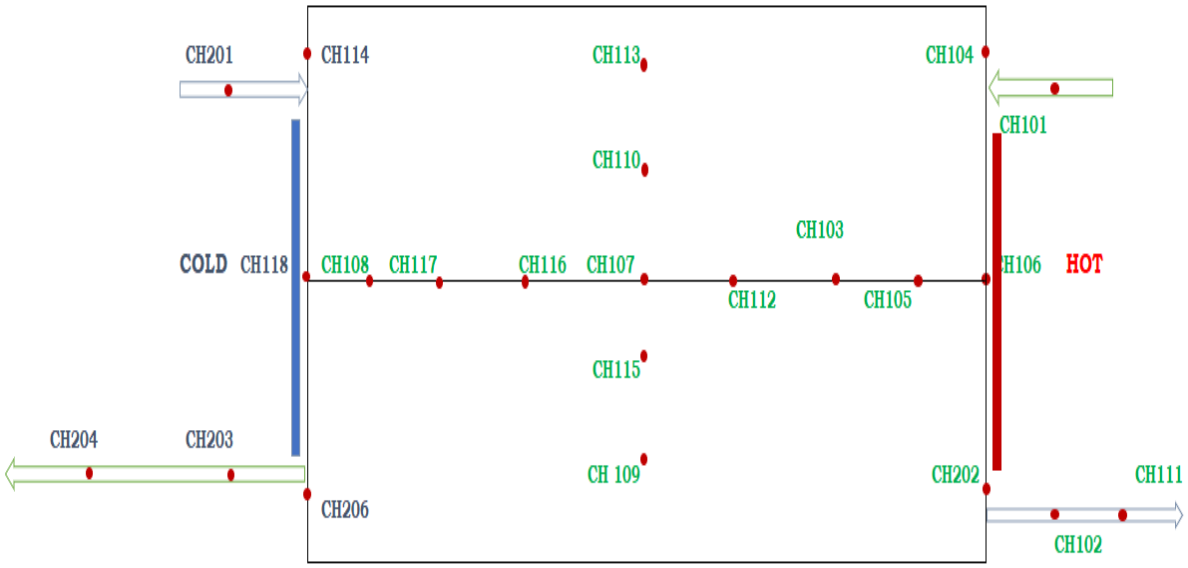

Figure 3.4: The thermocouples configuration in the cavity

In order to keep temperatures at the two heated walls of the cavity constant, isothermal shell and counter-flow tube heat exchangers were used. Additionally, the shell and tube sides of the heat exchanger both had the same hydraulic diameter, as shown in Figure 3.5, to facilitate uniform mass and temperature distribution.

Programmable water baths (PR20R-30 Polyscience; −30 to 200 °C; accuracy = 0.005 °C) were utilised as water at various constant temperatures of 6 $°C$ –56 $°C$ was circulated through the heat exchangers. The flow rate varying from 0.00717 to 0.0208 L/s at the desired range of constant temperature for the study was maintained in the thermal bath.

Figure 3.5: Heat exchangers with a similar hydraulic diameter in the shell and tube side

The flow meters (Burkert Type 8081; ±0.01% accuracy (full scale) + 2% (measured value)) were installed at the heat exchanger inlet points to measure the water flow rates flowing between the heat exchangers and the water baths. During the experiment, the obtained data of temperatures and flow rates were logged into a computer using a data logger (National Instrument; type SCXI-1303; 32 channels). The experimental setup for this study is illustrated in Figure 3.6.

Figure 3.6: The experimental setup for this study

Samples of various volume concentrations of hybrid nanofluids and DI water were poured inside the square cavity. Per sample, three runs of tests were done at various temperature differences of 20, 30, 40, and 50 $°C$ between the cold and hot vertical surfaces of the heated cavity. Thermal equilibrium in the cavity was maintained for each given temperature difference.

The transferred heat to the square cavity from the hot vertical wall and the heat taken out from the cold wall of the square cavity were expressed using Eq (3.3).

$$Q = \dot{m} C_p \Delta T = \dot{m} C_p \left(T_h - T_c \right) \tag{3.3}$$

The temperature change between the entry (inlet) and exit (outlet) of the heat exchangers is denoted by ΔT.

3.6. Experimental Method

The hybrid nanofluid was prepared at a percentage weight ratio of 10:90 (Al_2O_3:MWCNT) for φ of 0.05, 0.10, 0.15, and 0.20 vol% in the square cavity. The mixture of hybrid nanoparticles, SDS at 0.8 dispersion fraction, and 1.4L of DI water was stirred for 30 minutes using a magnetic stirrer to achieve uniform suspensions. Following this procedure, the solution was poured into a beaker and gently placed in a cold water bath at a uniform temperature to achieve good suspension of the hybrid nanoparticles in DI water through homogenization. A small sample volume was then taken to measure its viscosity experimentally and then stored in a container for visual observation.

Approximately 2 h after the experiments began, by observing the thermocouple station readings, a steady-state condition was confirmed, which revealed not more than a 0.10% difference in the cavity.

Each volume concentration was tested three times. First, a thousand data points were acquired using the data logger at a frequency of 2 Hz; afterward, the desired *Ra* was achieved by setting various ranges of temperatures. The quantity of heat transferred from the hot to the cold vertical wall of the cavity was controlled by regulating the water flow rate within the heat exchangers. As a result, the volume flow rate must be changed to maintain a change in temperature of less than 1.5 $°C$ between the outlet and inlet of the heat exchangers in order to avoid violating the assumption that the temperature of the walls is constant.

3.7. Experimental Data Reduction

Several crucial parameters, such as *Ra*, Nu_{av}, h_{av}, and Q_{av} examined in this paper were estimated utilizing the thermophysical properties, temperatures, and flow rates of the hybrid nanofluids and base fluid. Eq (3.4) and Eqs (3.5) - (3.7) are empirical and theoretical mixture correlations [139] used to estimate specific heat, thermal expansion coefficient, and density of hybrid nanofluid, respectively.

$$\frac{k_{hnf}}{k_{bf}} = \frac{\left(\begin{array}{l}\left(k_{Al_2O_3}X_{Al_2O_3} + k_{MWCNT}X_{MWCNT}\right) + 2k_{bf} + \\ 2\left(\varphi_{Al_2O_3}k_{Al_2O_3}X_{Al_2O_3} + \varphi_{MWCNT}k_{MWCNT}X_{MWCNT}\right) \\ -2\varphi_{hnp}k_{bf}\end{array}\right)}{\left(\begin{array}{l}\left(k_{Al_2O_3}X_{Al_2O_3} + k_{MWCNT}X_{MWCNT}\right) + 2k_{bf} - \\ \left(\varphi_{Al_2O_3}k_{Al_2O_3}X_{Al_2O_3} + \varphi_{MWCNT}k_{MWCNT}X_{MWCNT}\right) \\ +\varphi_{hnp}k_{bf}\end{array}\right)} \tag{3.4}$$

Where X is the percentage weight of nanoparticles.

$$\rho_{hnf} = \varphi_{Al_2O_3}\rho_{Al_2O_3} + \varphi_{MWCNT}\rho_{MWCNT} + \left(1-\varphi_{hnf}\right)\rho_{bf} \tag{3.5}$$

$$\left(\rho\beta\right)_{hnf} = \varphi_{Al_2O_3}\left(\rho\beta\right)_{Al_2O_3} + \varphi_{MWCNT}\left(\rho\beta\right)_{MWCNT} + \left(1-\varphi_{hnf}\right)\left(\rho\beta\right)_{bf} \tag{3.6}$$

$$\left(\rho C_p\right)_{hnf} = \varphi_{Al_2O_3}\left(\rho C_p\right)_{Al_2O_3} + \varphi_{MWCNT}\left(\rho C_p\right)_{MWCNT} + \left(1-\varphi_{hnf}\right)\left(\rho C_p\right)_{bf} \tag{3.7}$$

Using Eq (3.8), the heat transfer inside the square cavity subjected to the heating of its vertical walls was evaluated.

$$Q = \dot{m}C_p\Delta T \tag{3.8}$$

The heat transfer coefficient, Rayleigh, and Nusselt numbers of the free convection of water and hybrid nanofluid in the square cavity were estimated using Eqs (3.9) - (3.11). Through advection, radiation, and conduction, the transferred heat between the cold and hot walls occurs. However,

due to the slight change in temperature between the cold and hot walls, a fraction of the heat transfer as a result of conduction and radiation is insignificant.

$$h = \frac{Q}{A(T_h - T_c)} \tag{3.9}$$

$$Ra = \frac{g\beta(T_h - T_c)\rho^2 C_p {L_c}^3}{\mu k} \tag{3.10}$$

$$Nu = \frac{h L_c}{k_{eff}} \tag{3.11}$$

Where k is the effective thermal conductivity, h is the heat transfer coefficient, and L_c is the characteristics length, which is the distance between the square cavity's hot and cold walls. All the fluid's properties were estimated at an average temperature of the cold and hot walls, as shown in Eq (3.12).

$$T_{av} = \frac{T_h - T_c}{2} \tag{3.12}$$

3.8. Experimental Validation

In order for the experimental results of the setup to be validated, the *Nu* of the square cavity filled with water was investigated as a function of *Ra* obtained using empirical models in the literature, which was aided by fixing various temperatures at the heat exchangers. It is essential that the water flow rate from the isothermal baths be adjusted in such a way that the changes in temperature in between the heat exchangers inlet and outlet are not beyond 1 ℃.

The proposed models of Berkovsky and Polevikov [132], Cioni, et al. [133], and Leong, et al. [134] to predict *Nu* of water inside a cavity are presented as Eqs (3.13) [132], (3.14) [133], and (3.15) [134].

$$Nu = 0.18 \times \left(\frac{\mathrm{Pr}}{\left(0.2 + \mathrm{Pr}\right)} Ra \right)^{0.29}$$

$$\left(\mathrm{Pr} \le 10^5;\ Ra \le 10^{10}\right) \tag{3.13}$$

where

$$\mathrm{Pr} = \frac{\mu C}{k}$$

$$Nu = 0.145 \times Ra^{0.292}$$

$$\left(3.7 \times 10^8 \le Ra \le 7 \times 10^9\right) \tag{3.14}$$

$$Nu = 0.08461 \times Ra^{0.3125} \quad \left(10^4 < Ra < 10^8\right) \tag{3.15}$$

3.9. Uncertainty Analysis

The uncertainty analysis of the Al_2O_3–MWCNT water hybrid nanofluid's natural convection performance in the cavity was conducted to show the reliability and estimate the error associated with the experimental data. Kline [140] and Moffat [141] methods, commonly reported amongst researchers, were utilised to evaluate the uncertainty of the obtained data. The primary sources of errors and inaccuracies were the measurements of temperatures and flow rates taken and were analysed using Eqs. (3.16)- (3.18).

$$\delta Q = \left(\left(\frac{\partial Q}{\partial \dot{m}} \delta \dot{m} \right)^2 + \left(\frac{\partial Q}{\partial C_{p-bf}} \delta C_{p-bf} \right)^2 + \left(\frac{\partial Q}{\partial T_H} \delta T_H \right)^2 + \left(\frac{\partial Q}{\partial T_C} \delta T_C \right)^2 \right)^{\frac{1}{2}} \tag{3.16}$$

$$\delta Nu = \left(\left(\frac{\partial Nu}{\partial h} \delta h \right)^2 + \left(\frac{\partial Nu}{\partial L_c} \delta L_c \right)^2 + \left(\frac{\partial Nu}{\partial k_{eff}} \delta k_{eff} \right)^2 \right)^{\frac{1}{2}} \tag{3.17}$$

$$\delta h = \left(\left(\frac{\partial h}{\partial Q} \delta Q \right)^2 + \left(\frac{\partial h}{\partial A} \delta A \right)^2 + \left(\frac{\partial h}{\partial T_H} \delta T_H \right)^2 + \left(\frac{\partial h}{\partial T_C} \delta T_C \right)^2 \right)^{\frac{1}{2}} \tag{3.18}$$

3.10. Conclusion

The safety measures taken during the investigation to avoid inhalation, dermal contact, or ingestion of nanoparticles were discussed in this chapter because nanoparticles have been tested for potential adverse effects on the health of humans for almost two decades. Nevertheless, the knowledge of the toxicology of nanomaterials is still incomplete [142]. More so, there is presently no medical monitoring known to be relevant specifically for nanomaterials [137].

The description of the equipment used in this study to characterize the hybrid nanofluid was provided. A square cavity with AR= 1 was used as the experimental apparatus. The cavity has two walls that are vertical and act like shell and tube counterflow heat exchangers. Two constant temperature thermal baths were used to control the temperature of the cavity's cold and hot walls. The validation of the experimental results and data reduction were also reviewed. Lastly, in this chapter, the uncertainty analysis for the convective heat transfer experiments was described.

CHAPTER 4

RESULTS: HYBRID NANOFLUID AND NATURAL CONVECTION

4.1. Introduction

Advanced technologies are constrained by thermal management, especially in confined volumes, such as MEMS and electronic cooling. Although it is possible to improve thermal management by using natural convection, the problem is that it has a low heat transfer coefficient. However, with the use of an innovative colloidal engineered kind of fluid, known as hybrid nanofluids, it is possible to improve the convective heat transfer coefficient of traditional fluids filled in cavities.

In this chapter, Al_2O_3–MWCNT/DI water hybrid nanofluids preparation is first studied in detail. Information about its morphology was offered by TEM images. Viscosity stability tests and visual observations were done for stability evaluation. Then the natural convection of the dispersed two-step Al_2O_3–MWCNT/water hybrid nanofluid was studied experimentally.

A square cavity comprising of two opposite vertical walls, with the remaining walls well insulated, was utilised to study the natural convection in hybrid nanofluids. Two constant temperature baths were used to control or regulate the cavity's constant wall temperature in order for the temperature changes to provide the desired *Ra* of 2.81×10^8 to 8.58×10^8. Al_2O_3–MWCNT/water hybrid nanofluids volume concentrations of 0.00, 0.05, 0.10, 0.15, and 0.20% were formulated to study the influence of nanoparticles volume concentrations on hybrid nanofluids convective heat transfer coefficient. The temperature distribution of the hybrid nanofluids is presented at various *Ra* and volume concentrations. Finally, in order to demonstrate the reliability of the experimental data, an uncertainty analysis was conducted.

4.2. Hybrid Nanofluid Characterization and Stability

4.2.1. Transmission Electron Microscopy

The size of the particles and Al_2O_3–MWCNT/water hybrid nanofluids for 10:90 weight at 0.10 vol% morphology was monitored using transmission electron microscopy (TEM). The nanoparticles' aggregation within the hybrid nanofluids was examined directly using TEM. The spherical-shaped Al_2O_3 and cylindrical-shaped MWCNT were found to be suspended uniformly

in the base fluid as shown in Figure 4.1, and these shapes agreed with those of previous studies [5, 15, 142]. The TEM image for the hybrid nanofluids is presented in Figure 4.1. At the 200 nm nanoscale, it was spotted by TEM that the Al_2O_3 nanoparticles had an approximate size of 14 nm, whereas MWCNT nanoparticles had outside diameters of an approximate size of 11 nm.

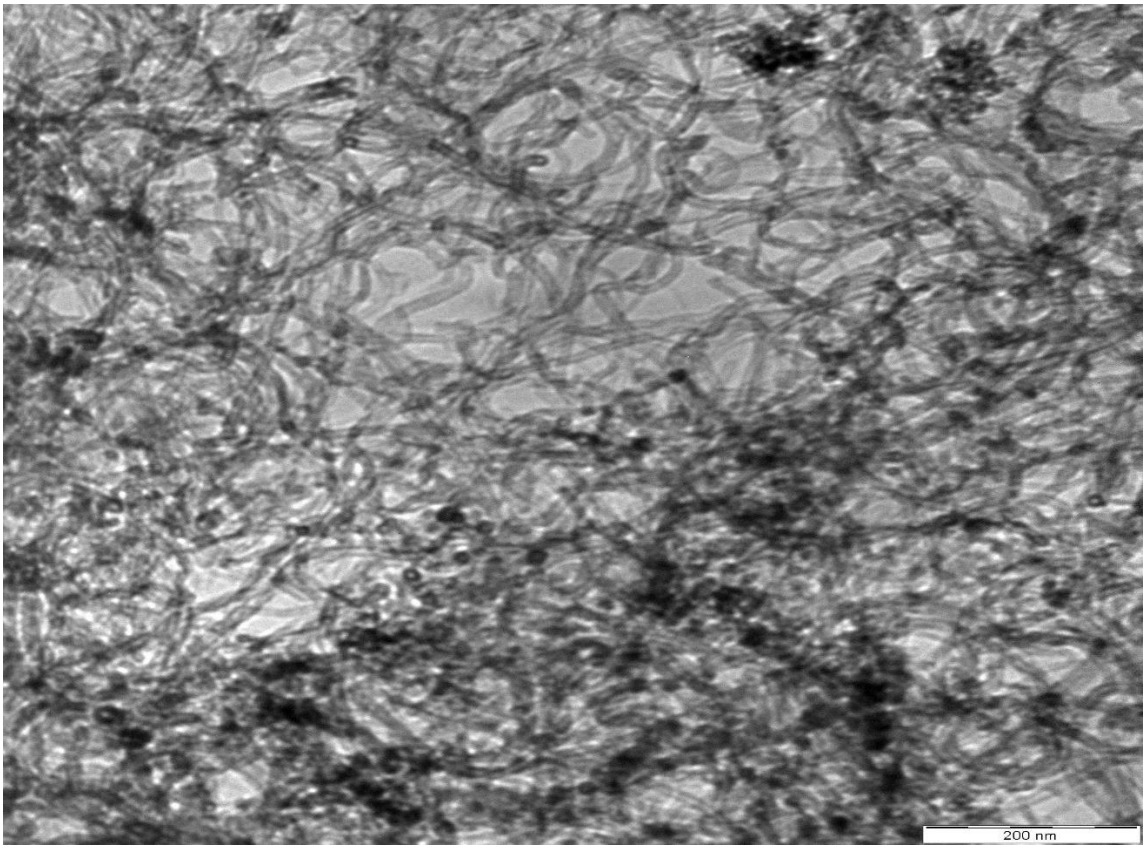

Figure 4.1: A TEM image of Al_2O_3-MWCNT (10:90)/water hybrid nanofluid at 0.10 vol%

4.2.2. Viscosity Stability

After the hybrid nanofluids were prepared, a small sample volume of Al_2O_3-MWCNT/water hybrid nanofluids (0.10 vol%) was taken to measure its viscosity experimentally at a constant temperature of 20 °C. Figure 4.2 illustrates the viscosity of the hybrid nanofluid with respect to time. It was noted that the viscosity of the hybrid nanofluid with a volume concentration of 0.10 vol% was 1.22 mPa.s at 20 °C and remained constant. The viscosity stability test indicated that the

stability of the formulated hybrid nanofluid is good and remained stable for up to 24 h. Even though the hybrid nanofluid prepared was stable for up to 24 h, the convective heat transfer tests were completed within 7 h from the time it was formulated.

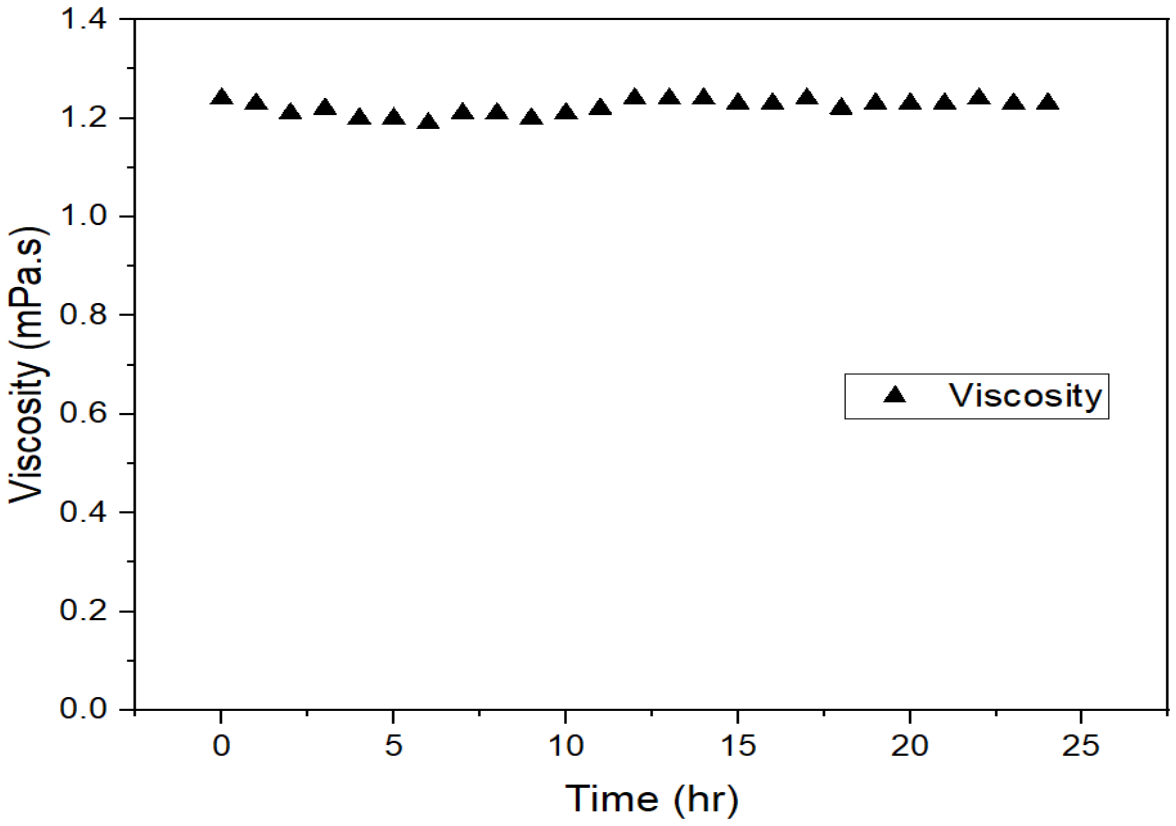

Figure 4.2: Viscosity stability test of Al_2O_3-MWCNT/water hybrid nanofluid at 0.10 vol%

4.2.3. Visual Observation

The visual method was employed to examine the hybrid nanofluid samples' stability. Small samples of Al_2O_3 - MWCNT (10:90)/DI water hybrid nanofluid at different φ ranging from 0.05 – 0.20 vol% were in visible plastic containers. The samples were studied using the visual technique for two months.

Figure 4.3 (a) shows the picture of the hybrid nanofluid samples after preparation. According to Figure 4.3 (b), the visual technique demonstrated no signs of sedimentation of the hybrid nanofluids after two months.

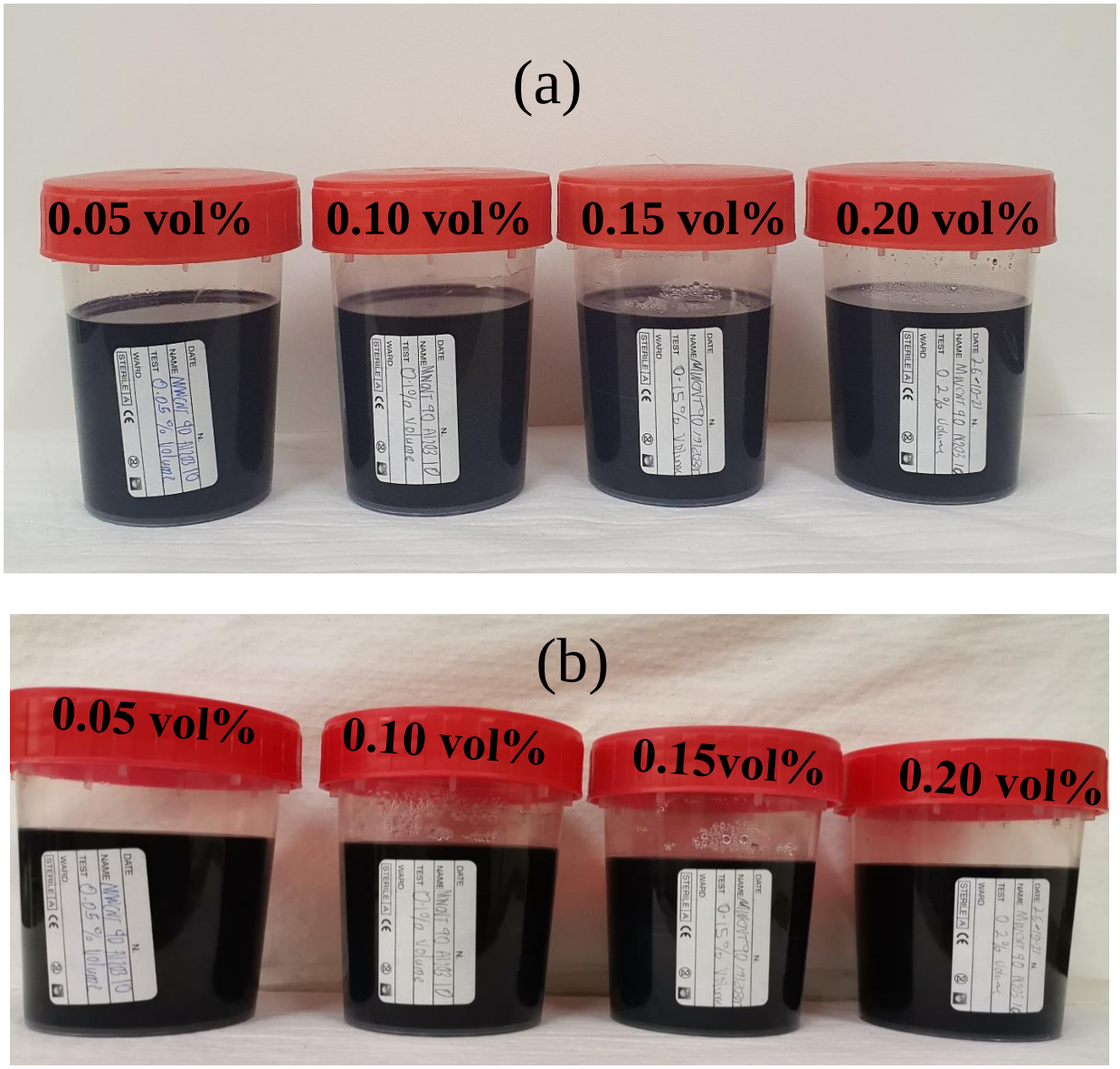

Figure 4.3: Visual stability of the hybrid nanofluids samples (a) after preparation (b) 60 days later

The fluids were visually stable over 60 days of observation since no sedimentation took place, and the colours and composition appeared constant over the said period.

4.3. The Viscosity of Hybrid Nanofluid

The measured viscosity of DI water was compared with Eq (4.1) obtained from the literature as a function of temperature [143], shown in Figure 4.4.

$$\mu = \frac{1}{557.82468 + 19.408782T + 0.1360459T^2 - 3.1160832\times10^{-4}T^3} \quad (4.1)$$

$$(0\,^oC \le T \le 150\,^oC)$$

Both data agreed with one another with a percentage error of 0.415% with an average deviation of 1.556%, which shows that the results are reliable.

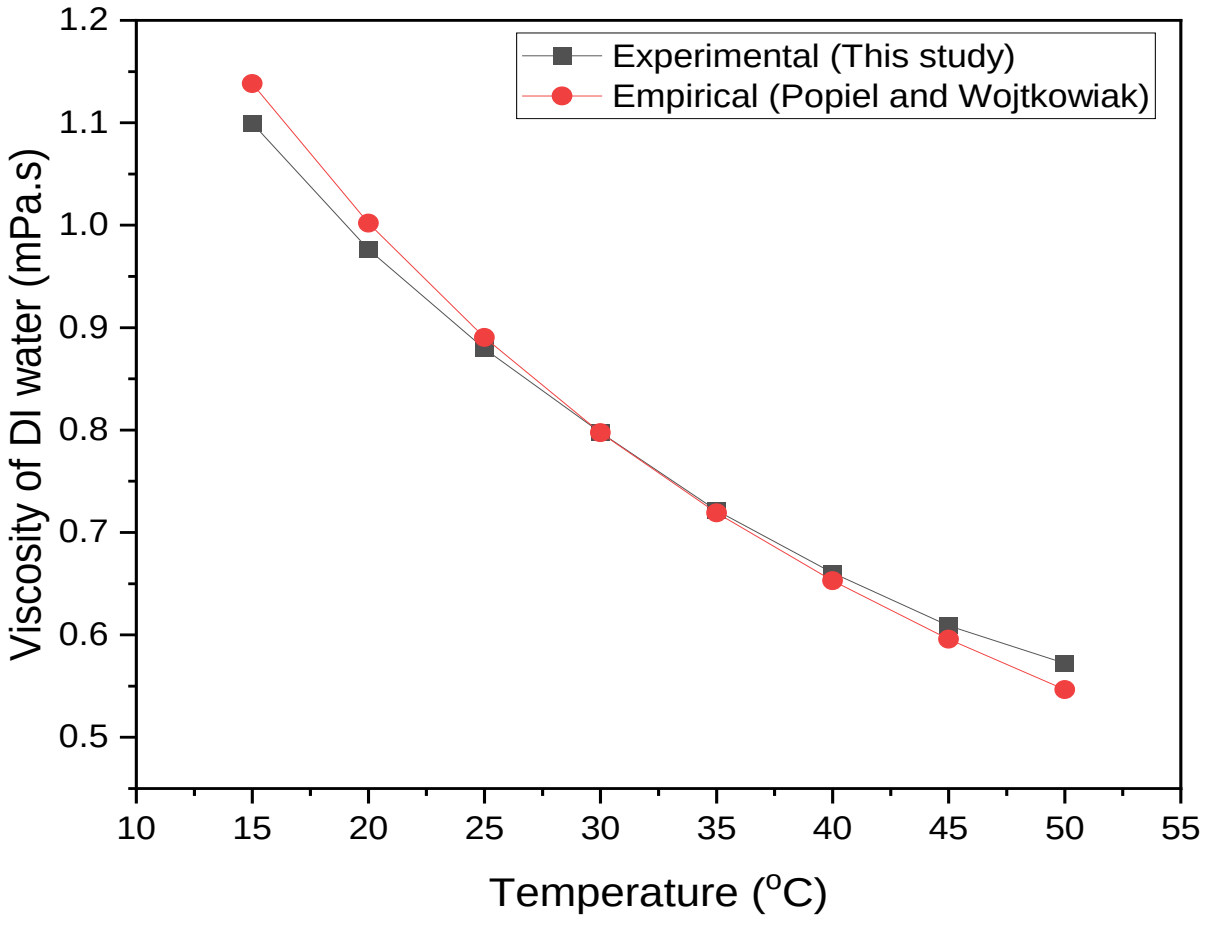

Figure 4.4: Comparison of measured and empirical viscosity values of DI water

According to literature, as nanoparticles are dispersed in a fluid, the viscosity increases [144]. Therefore, an analysis of viscous forces is conducted to determine their effect on natural convection. Figure 4.5 illustrates the relative viscosity of Al_2O_3 - MWCNT (10:90)/water nanofluids samples as a function of volumetric nanoparticle concentration and temperature using Eq (4.2).

$$\mu_{rel} = 1.09055 - 1.66 \times 10^{-3} T + 1.0855\varphi$$
$$(15\,^{o}C \le T \le 60\,^{o}C;\ 0.025 vol\% \le \varphi \le 0.2 vol\%) \tag{4.2}$$

The relative viscosity of DI water was noted to rise as the Al_2O_3 and MWCNT hybrid nanoparticles were suspended in the base fluid due to a higher density of the hybrid nanoparticles compared to the base fluid. Therefore, increasing the hybrid nanofluid volume concentration from 0.05 to 0.20 vol% improved DI water viscosity. More so, the rise in volumetric nanoparticle concentration increased the hybrid nanofluid's relative viscosity as a result of the agglomeration of nanoparticles in suspension at higher concentrations.

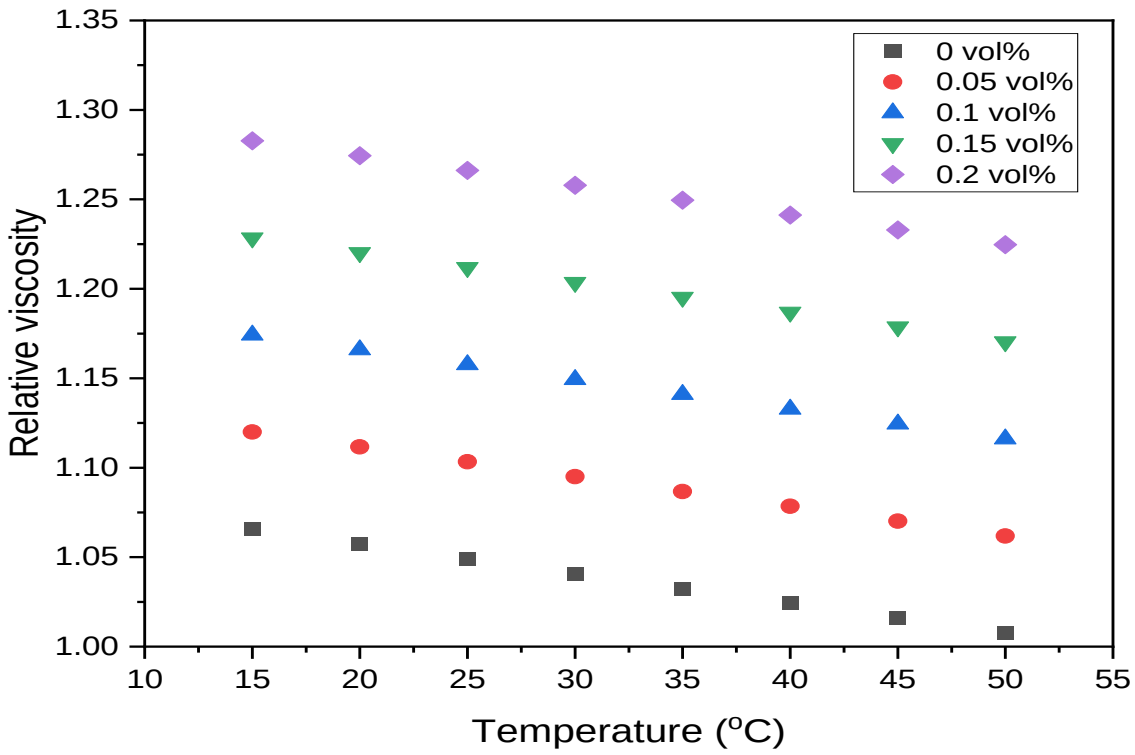

Figure 4.5: Relative viscosity of Al_2O_3-MWCNT (10:90)/water nanofluids samples

A temperature rise was found to attenuate the viscosity of DI water and Al_2O_3 - MWCNT (10:90) hybrid nanofluids. This is because the effect of temperature on viscosities is connected to the declination of the interparticle and intermolecular adhesion forces. The molecules' kinetic energy increases as the temperature of nanofluids increases, and the length of time they remain in contact with their nearest particles decreases. Therefore, an increase in temperature leads to a decrease in the average intermolecular forces and viscosity reduction. The combined effect of the volume concentration and temperature for Al_2O_3 - MWCNT (10:90) hybrid nanofluids was noticed to enhance the relative viscosity of DI water by 5.093% to 21.547%. In relation to the base fluid, a maximum increase of 21.547% was attained for Al_2O_3 - MWCNT (10:90)/water hybrid nanofluid at 0.20 vol% and 50 °C. Observations on the relationship between viscosity and temperature are in agreement with literature [15, 52, 85, 93, 100, 142, 145, 146].

4.4. Cavity Validation

In order to validate the experimental results of the setup, the Nu_{av} data of DI water achieved in this experiment were evaluated with the Nusselt number data estimated from the existing empirical model, which was proposed by Berkovsky and Polevikov [132] and Cioni, et al. [133]. The validation of the cavity using DI water as the base fluid is illustrated in Figure 4.6. The graph depicts that at *Ra*, ranging from 3.336×10^8 to 8.579×10^8, the Nu_{av} of DI water was 63.411 to 104.949. There was a noticeable difference between experimental and model data. The analysis revealed that this study's experimental data were significantly greater than the models predicted, which illustrates that the models underestimated the experimental data. Furthermore, the lack of ability of these models to predict experimental Nu_{av} data for the DI water-based fluid is consistent and agrees with previous research findings [15].

4.5. The Effect of Hybrid Nanofluid Volume Concentrations on *h*

According to literature, the hybrid nanoparticle volume concentration is a significant factor affecting the heat transfer coefficient of hybrid nanofluids [147]. However, researchers have reported contradictory findings regarding the influence and impact of hybrid nanofluid volume concentration on nanofluids' *h* in natural convection. Therefore, the experimental investigation of the natural convection of Al_2O_3 - MWCNT (10:90) hybrid nanofluids for volume concentrations of 0.00, 0.05, 0.10, 0.15, and 0.20 vol% and *Ra* ranging from 2.81×10^8 to 8.58×10^8 were performed in a differentially heated cavity at various ΔT (20. 30, 40 and 50 ℃).

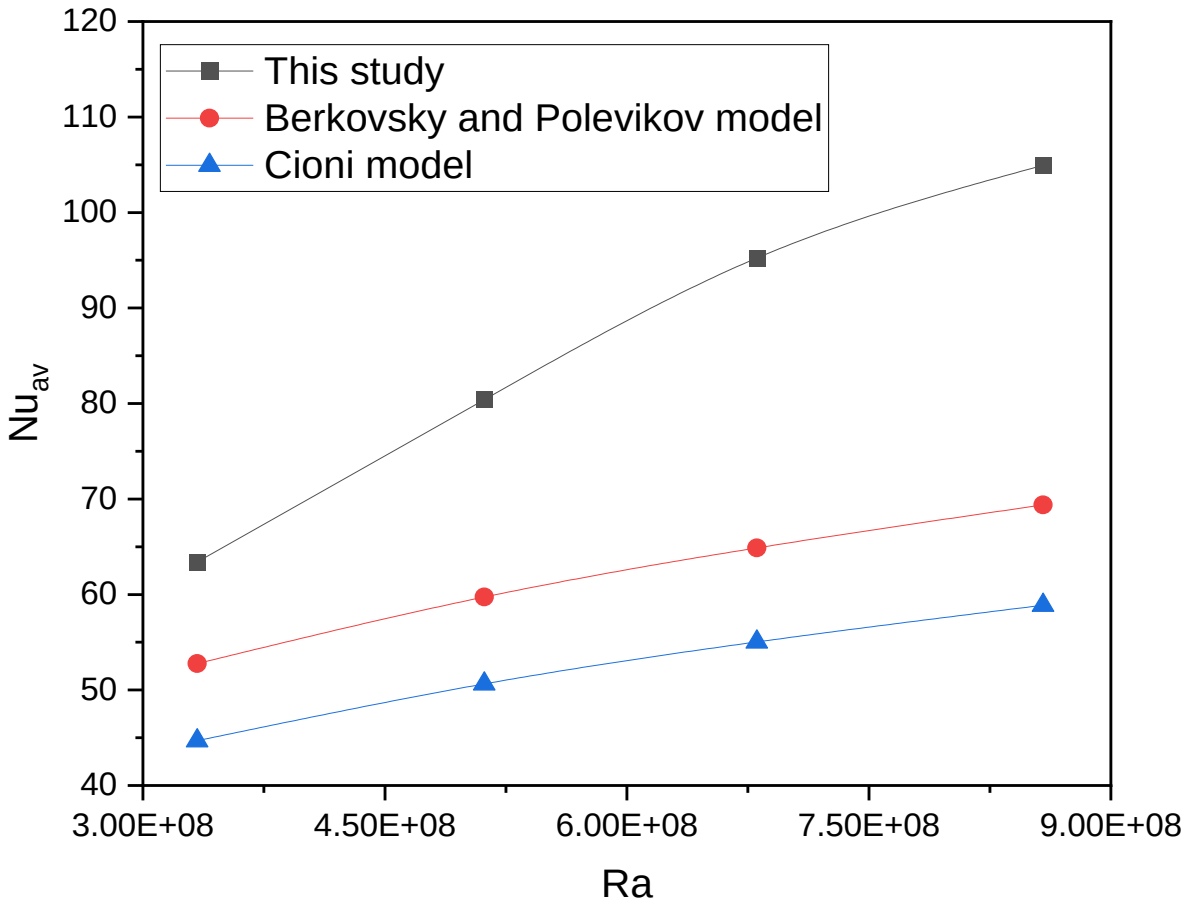

Figure 4.6: Cavity validation of DI water

The dependence of h_{av} on the volume concentration of Al_2O_3-MWCNT (10:90) hybrid nanoparticles at different temperature changes is presented in Figure 4.7. The suspension of alumina and MWCNT nanoparticles into DI water enhanced the natural convection heat transfer coefficient of DI water for some of the Al_2O_3-MWCNT (10:90) hybrid nanofluid samples. The peak h_{av} of 932.63 W/m^{2}K was observed with 0.10 vol% at ΔT of 50 ℃. The graph also shows that as the volume fraction increases from 0.00 to 0.20 vol%, h_{av} was enhanced. However, h_{av} deteriorated beyond 0.20 vol% according to the trendline.

The use of Al_2O_3-MWCNT (10:90) hybrid nanofluids in the cavity led to augmentations of h_{av} by 27.703% (0.05 vol%), 43.98% (0.10 vol%), 42.74% (0.15 vol%), and 22.58% (0.20 vol%) at ΔT of 50 ℃ compared to h_{av} of DI water. This could be related to the thermophysical properties such

as viscosity, which was enhanced at this concentration, leading to an attenuation of convective heat transfer inside the cavity and eventually resulting in a low heat transfer coefficient.

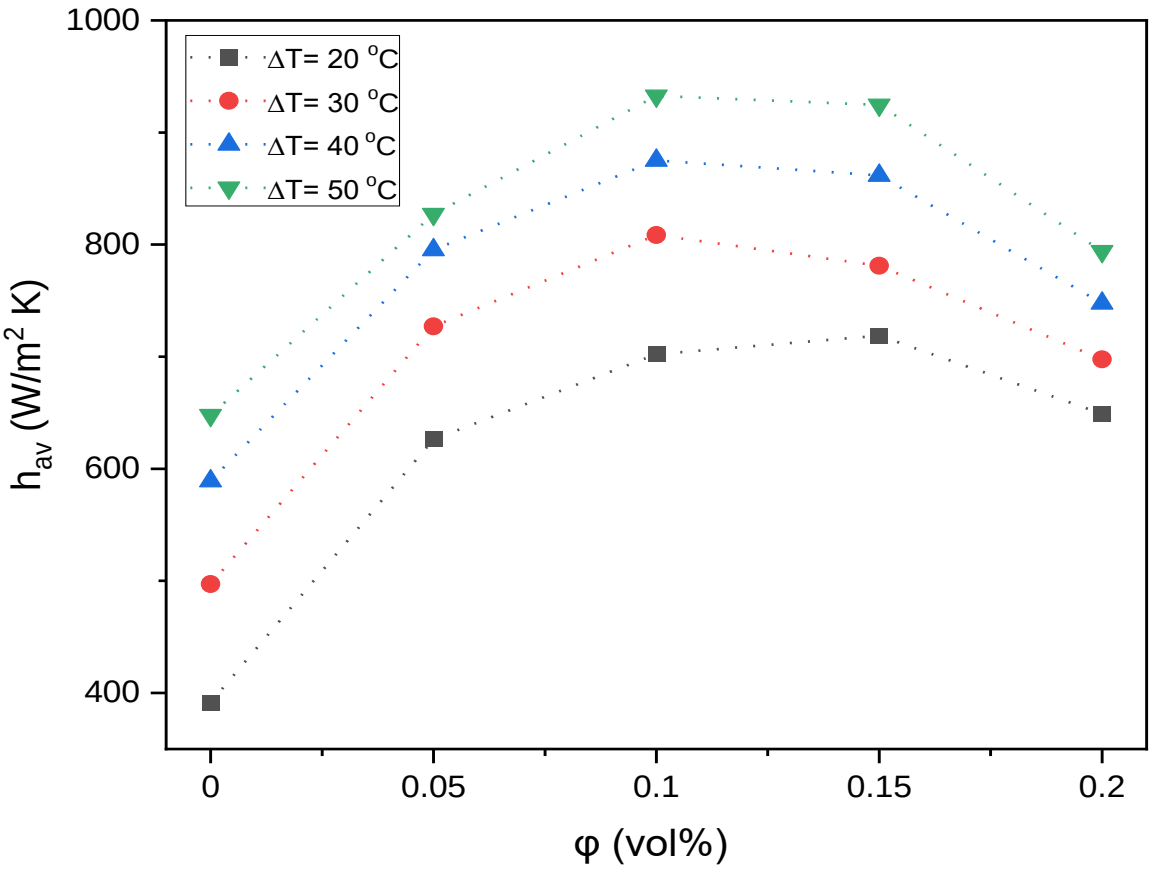

Figure 4.7: The effect of φ of Al_2O_3 - MWCNT (10:90) /water hybrid nanofluid on the natural convection heat transfer coefficient

In Figure 4.7, it was also observed that a rise in ΔT led to an increase in h_{av} for all the tested samples. For instance, a maximum augment of 32.8% between ΔT of 20 ℃ and 50 ℃ at 0.10 vol% was recorded. The observations regarding the relationship between heat transfer coefficient and volume concentration at varying ΔT were found to be consistent with the literature [15, 135].

4.6. The Effect of Hybrid Nanofluid Volume Concentrations on *Ra* and *Nu*

In order to facilitate comparisons with prior natural convection studies of hybrid nanofluids, the natural convection heat transfer variables of nanofluids are showcased non-dimensionally as *Ra*

and *Nu*. The effect of the hybrid nanofluid concentrations of 0.00 to 0.20 vol% and *Ra* ranging from 2.629 x 10^8 to 8.086 x 10^8 on Nu_{av} was studied and plotted in Figure 4.8.

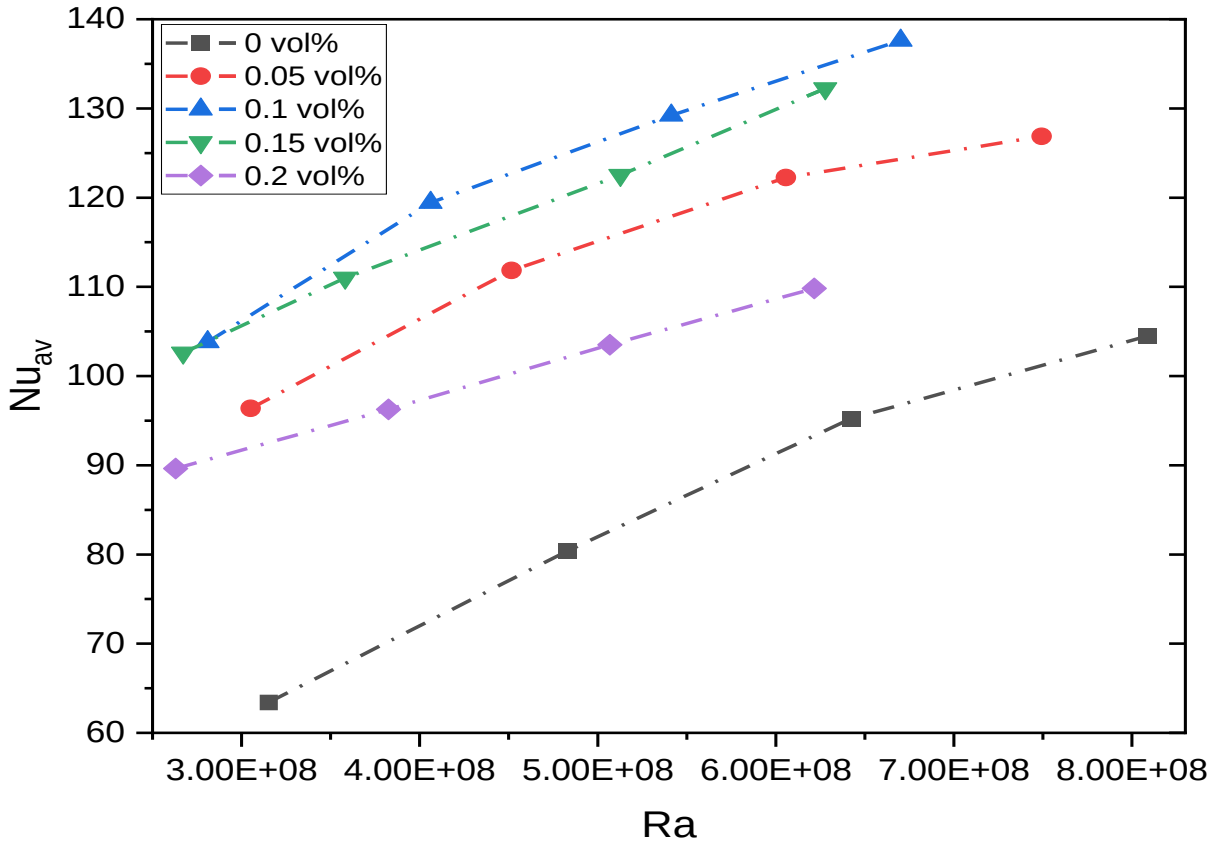

Figure 4.8: The effect of Ra and φ of Al_2O_3-MWCNT (10:90) hybrid nanofluids on Nu_{av}

Nu_{av} increased as *Ra* and ΔT increased for both Al_2O_3 - MWCNT (10:90) hybrid nanofluids samples and base fluid at different φ as illustrated in Figure 4.8 and Figure 4.9. However, at the same *Ra*, increasing the φ of hybrid nanofluids from 0.05 to 0.20 vol% resulted in a 10.85% reduction of Nu_{av}. Even though the increase in φ augmented the thermal conductivity and viscosity of the hybrid nanofluids, as shown in Figure 4.5 and Figure 4.10, respectively, *Ra* diminished.

Furthermore, the hybrid nanoparticle volume concentration also affects *Ra* in a way that, when the heated and cooled walls are heated to the same temperature, *Ra* falls with an increasing concentration of hybrid nanofluids. This is illustrated in Figure 4.11. For instance, when the

volume fraction increased from 0.00 to 0.20 vol% at ΔT of 50℃, the *Ra* value decreased by 23.12%.

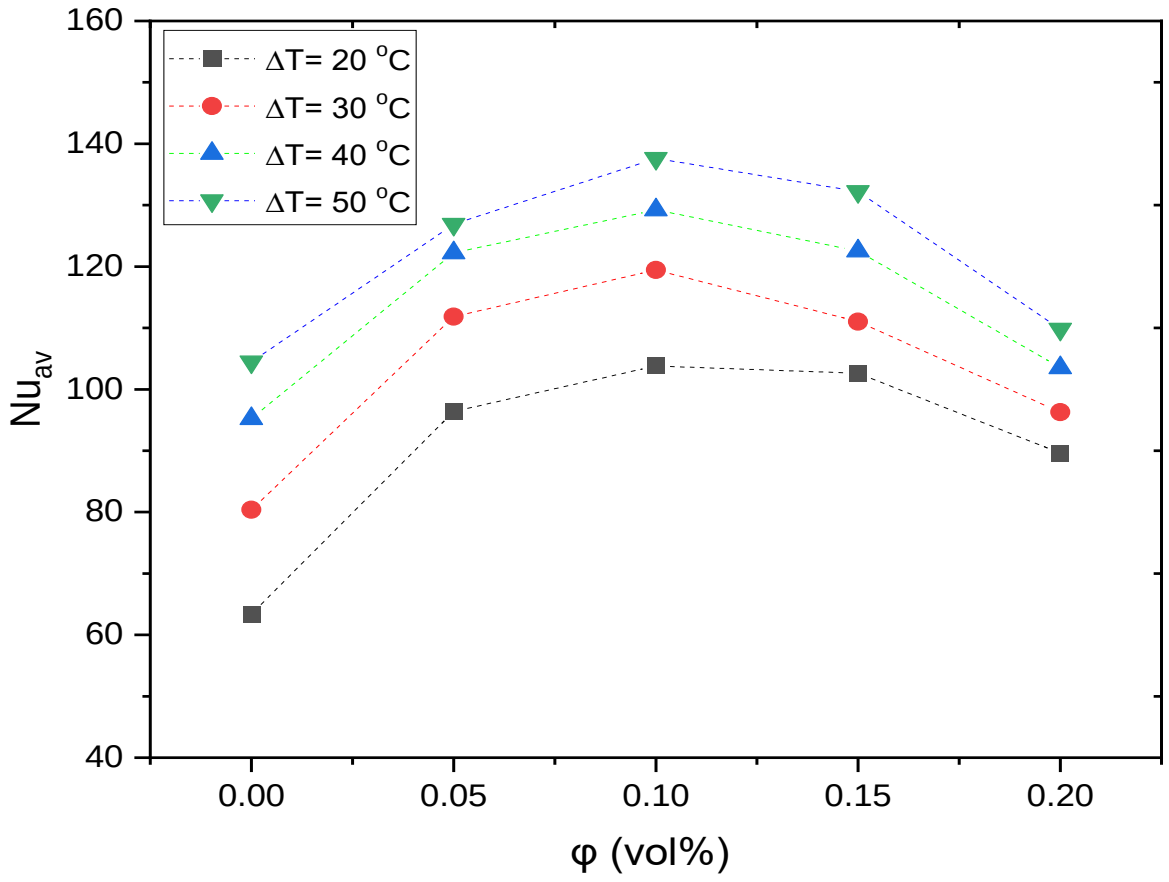

Figure 4.9: The effect of φ and ΔT of Al_2O_3 - MWCNT (10:90) hybrid nanofluids on Nu_{av}

According to Eq (4.3), it is clear that *Ra* reduces when both the thermal conductivity and viscosity of the hybrid nanofluid increases compared to the rest of the thermophysical properties. All observations were found to be consistent with literature [8, 148].

$$Ra_{hnf} = \frac{g\beta_{hnf}\left(T_h - T_c\right)\rho_{hnf}{}^2 C_{p_{hnf}} L_c{}^3}{\mu_{hnf}\, k_{hnf}} \tag{4.3}$$

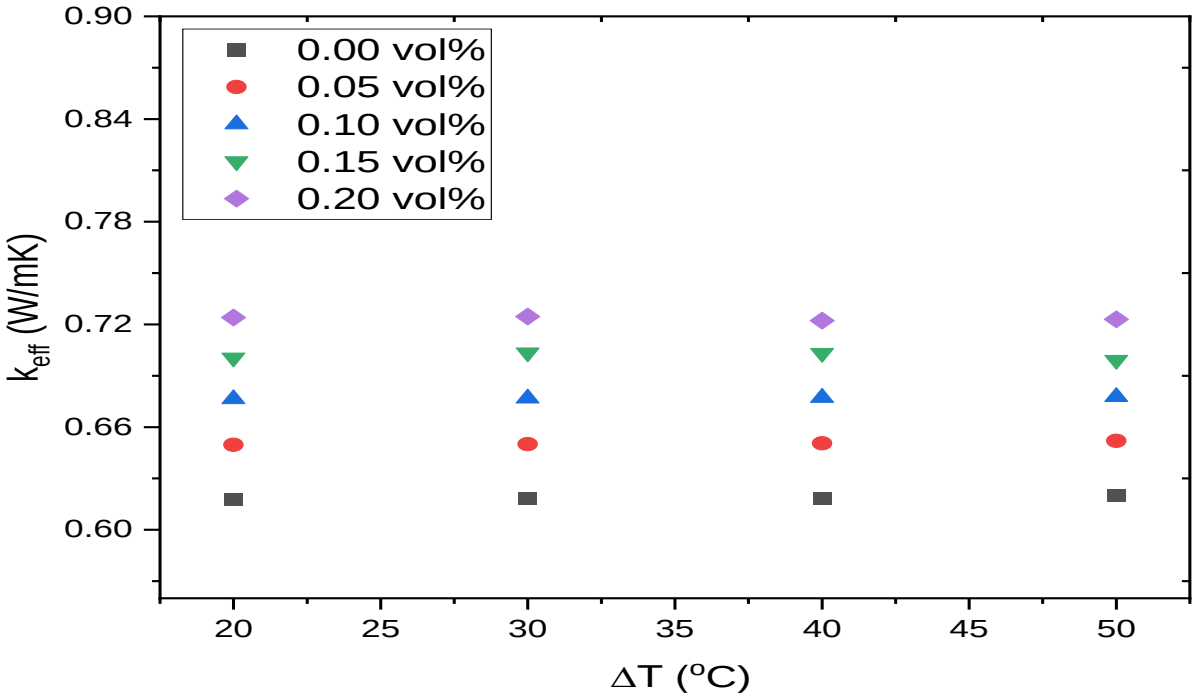

Figure 4.10: Thermal conductivity of Al_2O_3 - MWCNT (10:90) hybrid nanofluids samples

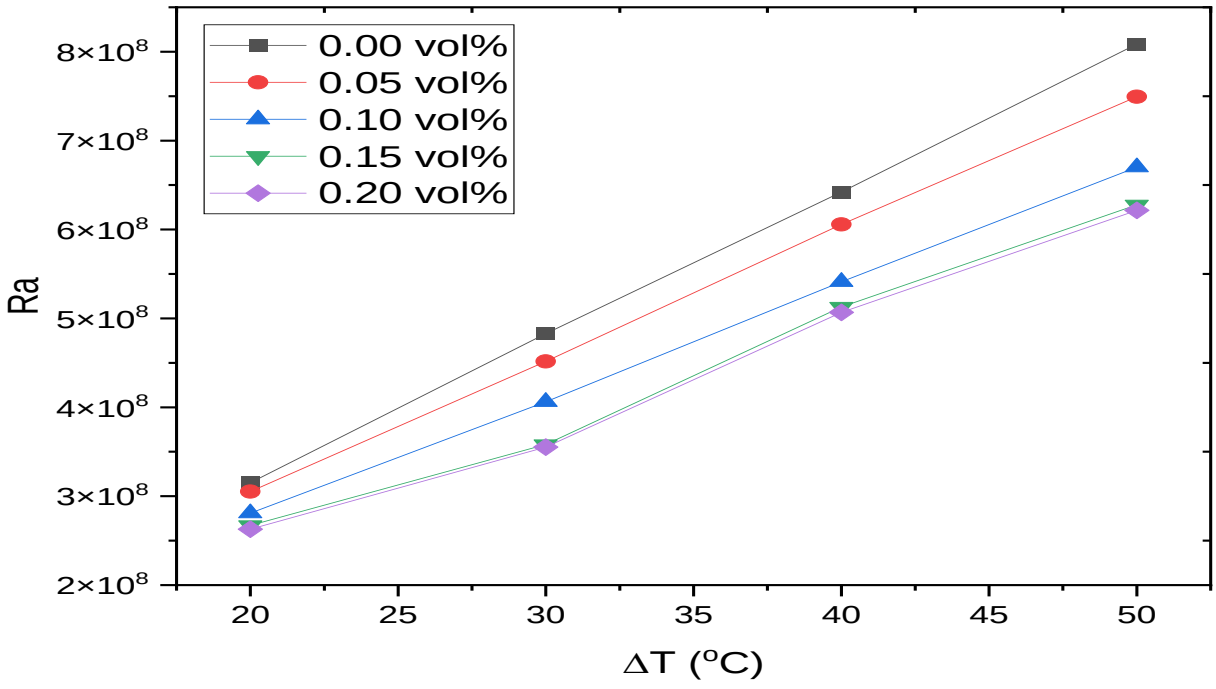

Figure 4.11: Relationship between Ra and ΔT for Al_2O_3 - MWCNT (10:90) hybrid nanofluids samples

4.7. The Effect of Hybrid Nanofluid Volume Concentrations on *Q*

Figure 4.12 demonstrates the Q_{av} of the square cavity as a function of φ at different temperature changes. It is evident from the figure shown that Q_{av} is enhanced at a rise in ΔT from 20 to 50 ºC. In response to an increase in temperature change in the square cavity, the working fluid viscosity decreases, causing more buoyancy and fluid flow, thereby improving the heat transfer capacity.

It was observed that an increment in volume concentration from 0.00 to 0.20 vol% caused both augmentation and reduction of Q_{av}. This is because Q_{av} increased when the volume concentration was lesser than 0.20 vol%, and Q_{av} decreased when the volume concentration was greater than 0.20 vol%. Based on the trends from the data points, it is evident that there is a peak in all temperature differences. Maximum Q_{av} was achieved at φ = 0.10 vol% with ΔT = 50 °C, which agrees with the previous experimental investigation on cavity flows for other nanofluids and hybrid nanofluids [15, 78, 129]. However, different hybrid nanofluids transfer heat to different extents in the same cavity, depending on their concentrations.

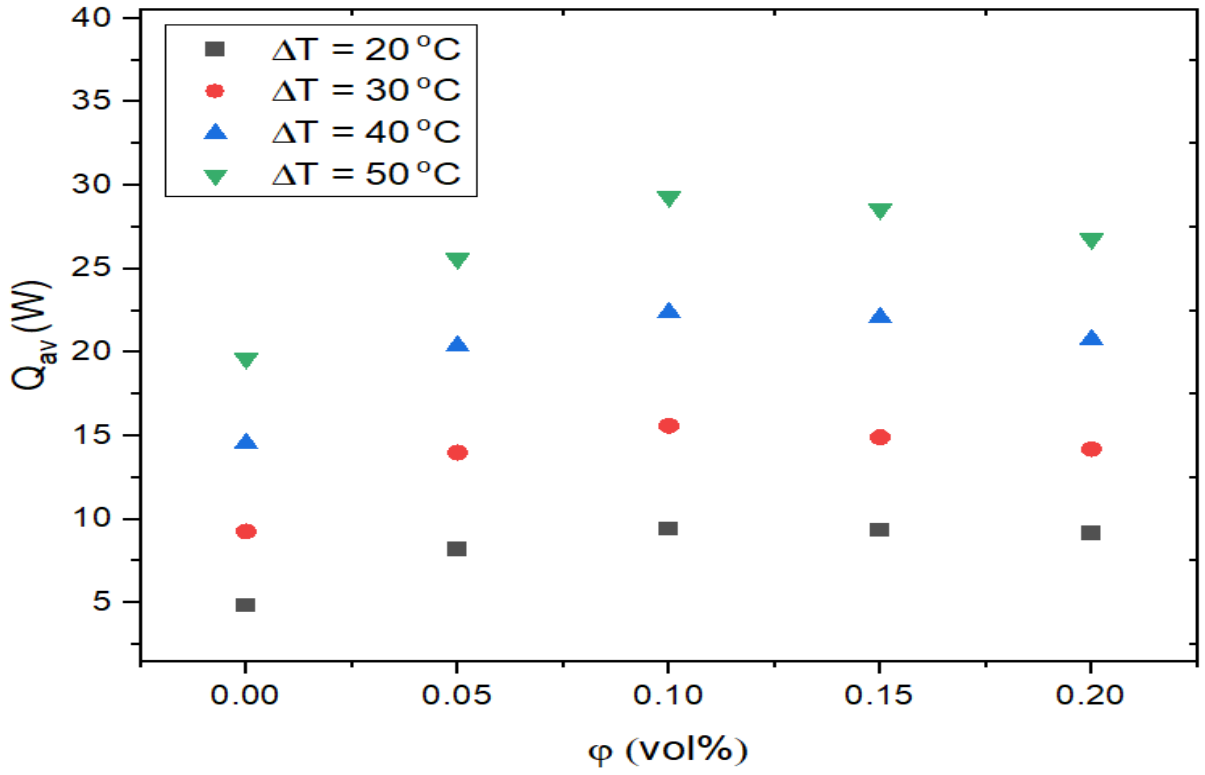

Figure 4.12: Relationship between Q_{av} and φ for Al_2O_3 - MWCNT (10:90) hybrid nanofluids samples at ΔT

The highest enhancements of 30.42%, 49.27%, 45.53% and 36.4% were noted for volume concentrations 0.05, 0.10, 0.15 and 0.20 vol% respectively in comparison with DI water. Figure 4.13 demonstrates the variation in heat transfer with the variations of ΔT.

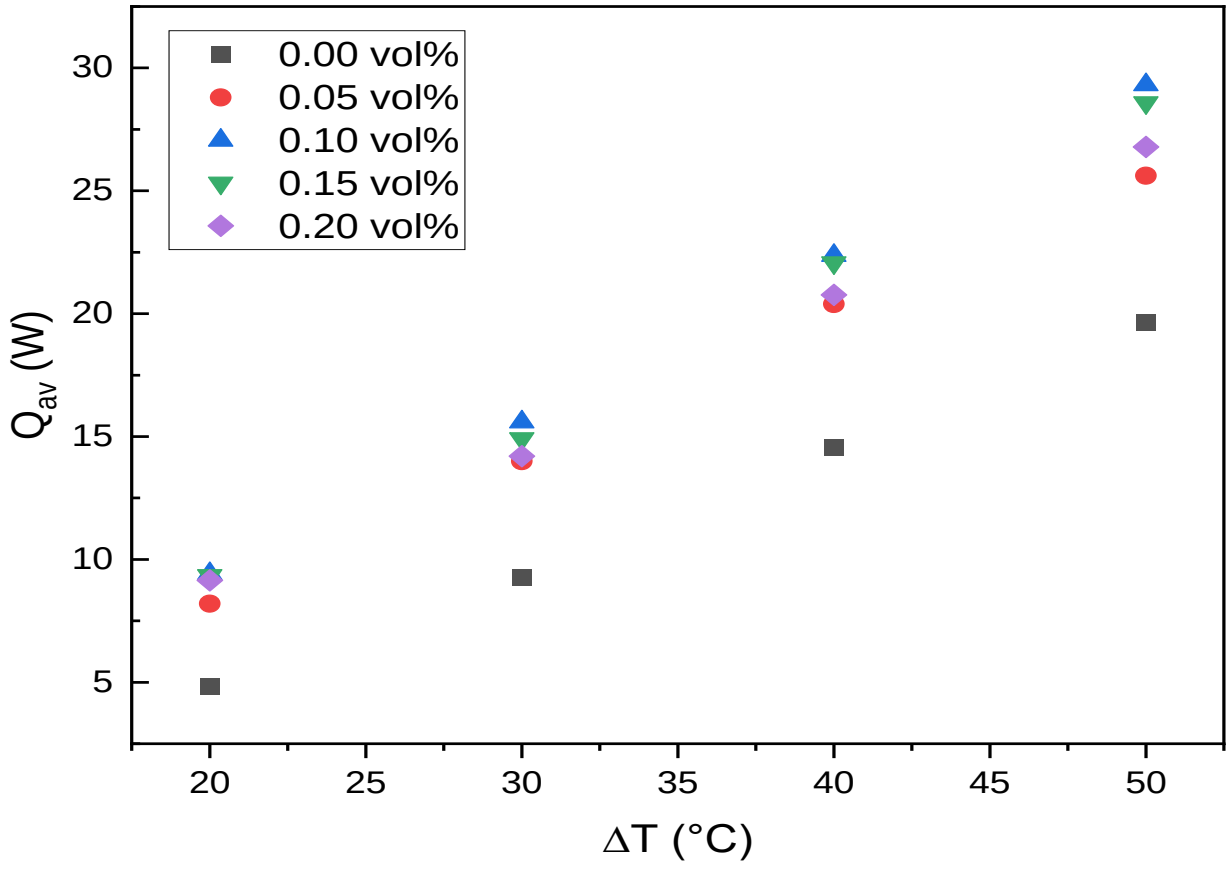

Figure 4.13: Effect of ΔT of the cavity on heat transfer

Figure 4.13 shows that the cavity's heat transfer varies linearly with Δ*T* for all volume concentrations of Al_2O_3–MWCNT (10:90) hybrid nanofluids. Based on the interaction, it appears that the transferred heat in the square cavity could be improved by increasing the change in temperature in the cavity. Additionally, heat transfer is highest for all temperature differences when 0.10 vol% hybrid nanofluid is tested in the cavity.

4.8. Temperature Distribution

The natural convection heat transfer experiments were performed under thermal conditions that were stable. Therefore, thermocouples at different points outside and within the cavity were utilised to measure the temperatures, as shown in Figure 3.4.

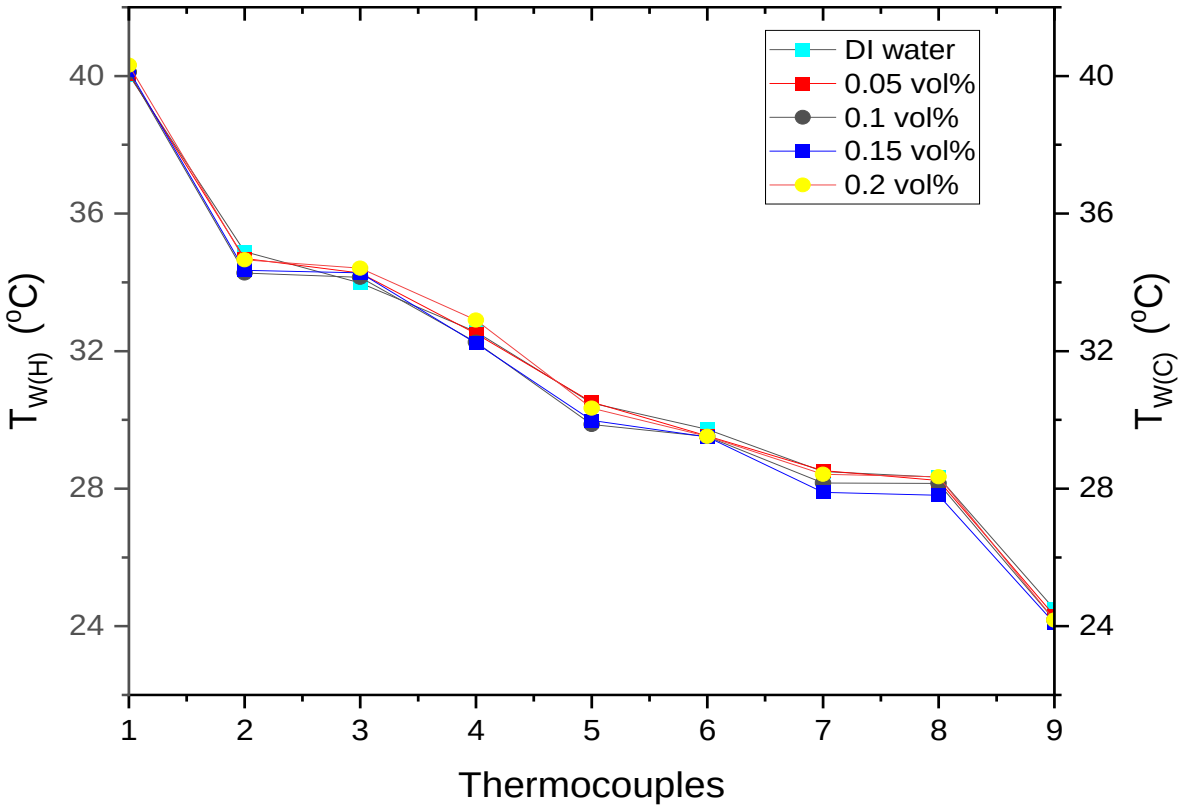

Figure 4.14: Cavity temperature profile for DI water and Al_2O_3 - MWCNT (10:90) /water hybrid nanofluids samples at $\Delta T = 20$ ℃

In addition, the cavity's mid-section temperatures from cold wall to hot wall are displayed in Figure 4.14 to Figure 4.17 for Al_2O_3–MWCNT (10:90) hybrid nanofluids at different φ under different ΔT. In general, it can be noted that the measured temperatures for thermocouples 2 - 7 remained relatively constant for all temperature changes.

The suspension of Al_2O_3–MWCNT (10:90) hybrid nanoparticles into DI water caused a slight temperature reduction. As a result, the temperatures at the hot wall reduced, while the temperatures at the cold wall increased for all temperature changes.

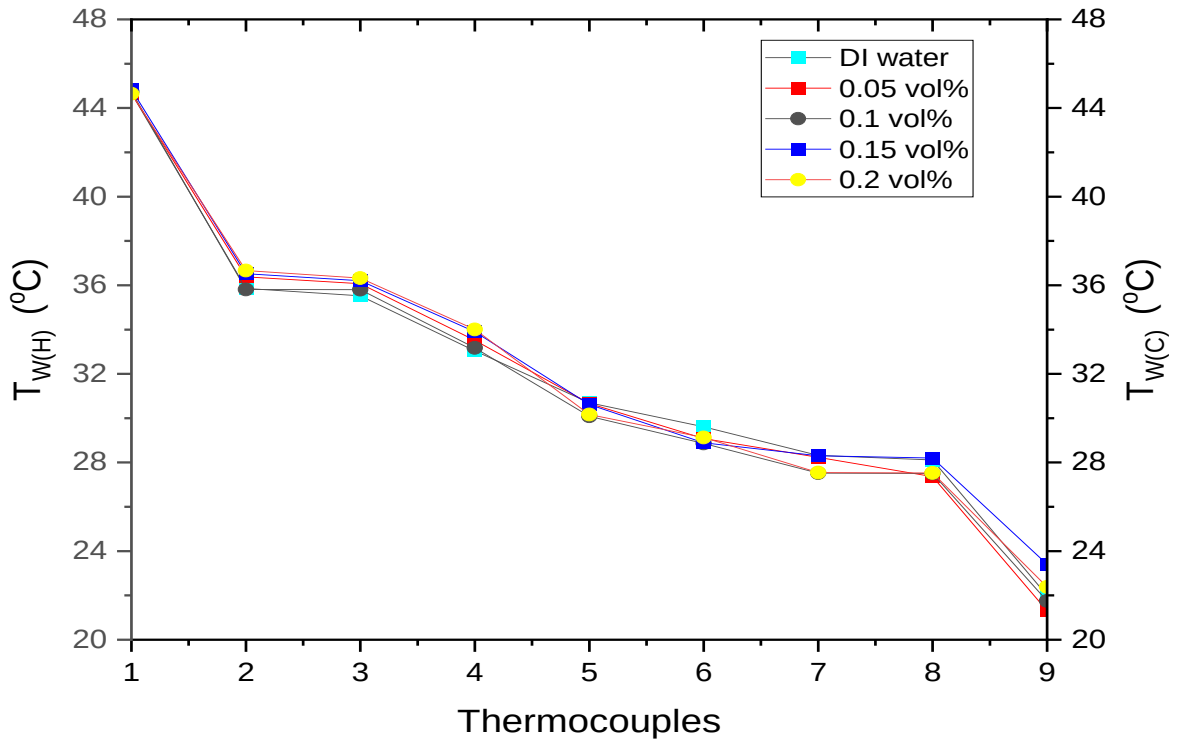

Figure 4.15: Cavity temperature profile for DI water and Al_2O_3 - MWCNT (10:90) /water hybrid nanofluids samples at ΔT = 30 ℃

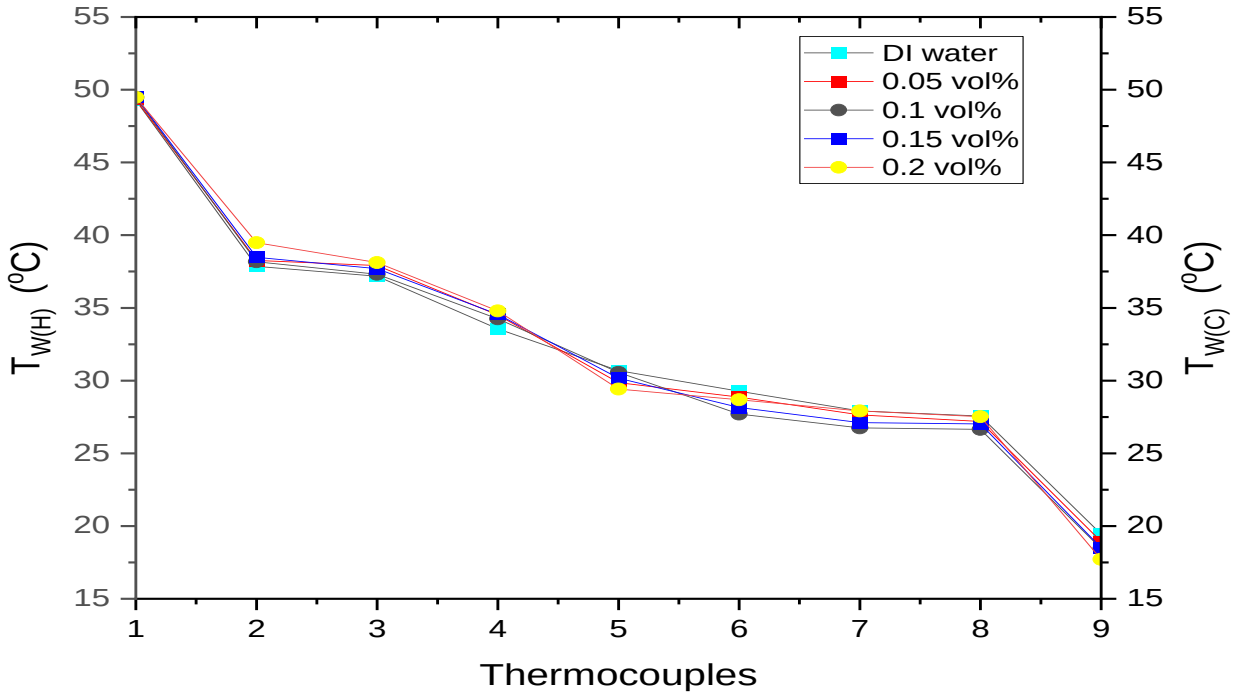

Figure 4.16: Cavity temperature profile for DI water and Al_2O_3 - MWCNT (10:90) /water hybrid nanofluids samples at ΔT = 40 ℃

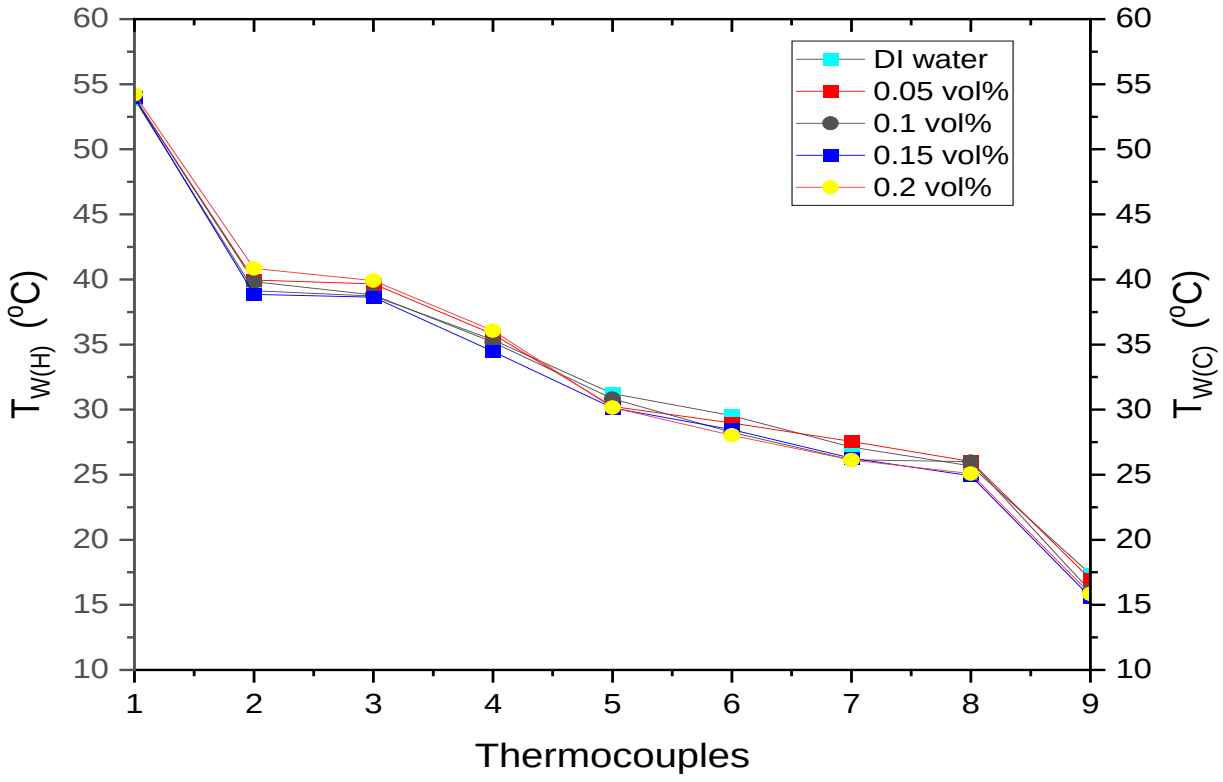

Figure 4.17: Cavity temperature profile for DI water and Al_2O_3 - MWCNT (10:90) /water hybrid nanofluids samples at ΔT = 50 ℃

4.9. Uncertainty Analysis

The uncertainty analysis of the Al_2O_3–MWCNT water hybrid nanofluid's natural convection performance in the cavity was carried out to show the reliability and estimate the error associated with the experimental data. Kline [140] and Moffat [141] methods, commonly reported amongst researchers, were utilised to evaluate the uncertainty of the obtained data. The primary causes of inaccuracies and errors were the measurements of flow rates and temperatures taken and were analysed utilizing Eq (3.14) - (3.16).

Table 4.1 presents the range, accuracy, precision, and bias (the two kinds of errors faced during measurements are precision and bias) of the instruments used in this study. All uncertainties were calculated within 95% confidence. Using Eq (3.14) - (3.16), the maximum uncertainty was determined to be 3.817% for *Q*, 1.826% for *Nu*, and 1.968% for *h*. The complete uncertainty is presented in Appendix C.

Table 4.1: Accuracy of instruments used in this study

Instrument	Range	Accuracy
Weighing balance	10 mg – 220 g	0.001 g
Thermal bath	-30 – 150 ^{o}C	± 0.005 ^{o}C
Vernier calipers	0 – 20 cm	0.02 mm
Thermocouple	< 150 ^{o}C	± 0.1 ^{o}C
Viscometer	0.3 – 10,000 mPa.s	± 3%
Flowmeter	0.0666 – 0.3333 l/s	± 0.01% of full- scale flow rate + 2% (measured flow)

4.10. Conclusion

The natural convection of Al_2O_3–MWCNT (10:90) water-based hybrid nanofluid at various volume concentrations were prepared and experimentally investigated in a square cavity at varied temperatures. The hybrid nanoparticles were characterized using TEM. At 200 nm nanoscale, TEM showed an approximate size of both nanoparticles, which differs from what was specified by the manufacturer. The viscosity stability test indicated that the stability of the formulated hybrid nanofluid is good and remained stable for up to 24 h. The image showed that both nanoparticles were well suspended in DI water. The visual tests also confirmed the stability of all samples after 60 days.

The experimental measurements of DI water viscosity were compared with the theoretical model obtained from the literature. The result showed that both data agreed with one another with a percentage error of 0.415%. It was also noted that as the temperature rose, the viscosity of DI water and Al_2O_3–MWCNT (10:90) hybrid nanofluids reduced. Before the experiments began, the square cavity experimental results were validated as the Nu_{av} data of DI water acquired in this research were compared with the Nu data estimated from the existing empirical model proposed by

Berkovsky and Polevikov [132] and Cioni, et al. [133]. From the analysis, it was noted that the experimental data were significantly higher than the models predicted, illustrating that the models underestimated the experimental data.

The thermo-convection performance of Al_2O_3–MWCNT (10:90)/DI water hybrid nanofluid in the square cavity was evaluated using h_{av}, Nu_{av}, and Q_{av}. The experimental study was conducted for a high *Ra* ranging from 2.81×10^8 to 8.58×10^8. The hybrid nanofluid was prepared using a two-step preparation method with the addition of SDS surfactant and was examined for a volume concentration range of 0 to 0.20%. The suspension of Al_2O_3 and MWCNT nanoparticles into DI water enhanced the natural convection heat transfer coefficient of DI water for some of the Al_2O_3-MWCNT hybrid nanofluid samples. In the search for the optimal heat transfer coefficient at various concentrations of the hybrid nanofluids, results showed that adding Al_2O_3-MWCNT (10:90) hybrid nanoparticles enhanced h_{av} by 43.98% (0.10 vol%) at ΔT of 50 ℃ compared to h_{av} of DI water. It was observed that an additional increase of the hybrid nanoparticles concentration deteriorated *h*.

This study noted that Nu_{av} improved with a rise in *Ra* for Al_2O_3–MWCNT hybrid nanofluids samples at different φ and the base fluid. However, at the same *Ra*, increasing the φ of hybrid nanofluids from 0.05 to 0.20 vol% resulted in a 10.85% reduction of Nu_{av}. In addition, the hybrid nanofluid volume concentration also influences *Ra* such that as the exact temperature that is set for the cooled and heated walls, *Ra* decreased as the hybrid nanofluid concentration increased. It was also noticed that an increment in volume concentration resulted in both attenuation and enhancement of Q_{av}. Maximum Q_{av} was achieved at 0.10 vol% with $\Delta T = 50$ °C, which agrees with previous experimental cavity flow works for other nanofluids and hybrid nanofluids. Finally, the temperature profile of the cavity in this study and the uncertainty analysis for the parameters *Q*, *Nu*, and *h* was presented in this chapter.

CHAPTER 5

CONCLUSION AND RECOMMENDATION

5.1. Summary

Nanofluids are special thermal fluids engineered due to the constraints inflicted by the thresholds of the engineering application of conventional fluids, surface modification, and miniaturization as methods used for the energy system's thermal management. Newly developed nanofluids, called hybrid nanofluids, have been found to improve heat transfer characteristics. They possess better thermal properties in comparison to conventional fluids and mono nanofluids, which improved their convective heat transfer capability.

As a result of the vast engineering applications of thermo-convection, nanofluids are increasingly being used in cavities of various types. A small number of experimental investigations were conducted on the convective heat transfer performance of hybrid nanofluids in cavities compared to numerical techniques. Various techniques have also been used besides hybrid nanofluids to improve the natural convection heat transfer of nanofluids in cavities, including cavity inclination, aspect ratio, magnetic stimuli, and green nanofluid. However, the number of experimental studies involving hybrid nanofluids in enclosures that enhance thermo-convection heating is very limited in the literature. Thus, this study focused primarily on it.

5.2. Conclusion

In conclusion, a square cavity comprising of two opposite vertical walls, with the remaining walls well insulated was utilised to study the natural convection in hybrid nanofluids. The heat transfer performance of Al_2O_3–MWCNT (10:90)/water hybrid nanofluids in an enclosure with an aspect ratio of 1 was studied for various volume concentrations (φ = 0.00, 0.05, 0.10, 0.15, and 0.20%). Two constant temperature baths were used to control or regulate the cavity's constant wall temperature in order for the temperature changes to provide the desired *Ra* of 2.81×10^8 to 8.58×10^8.

According to the study's objectives, Al_2O_3–MWCNT/water hybrid nanofluid was formulated using the two-step preparation technique. The hybrid nanofluid was prepared at a percentage weight ratio of 10:90 (Al_2O_3: MWCNT) for 0.05, 0.10, 0.15, and 0.20 vol% volume concentrations. The

mixture of hybrid nanoparticles, SDS at 0.8 dispersion fraction, and 1.4L of DI water was stirred for 30 minutes using a magnetic stirrer to achieve uniform suspensions. It was then followed by homogenization to achieve good suspension of the hybrid nanoparticles in DI water. The stability of the prepared hybrid nanofluid was verified using the viscosity test and visual inspection technique. Results showed that the formulated hybrid nanofluid appeared stable for 24 h and even after 60 days consecutively. The TEM characterisation of Al_2O_3–MWCNT hybrid nanofluid at 0.10 vol% revealed good suspension into the DI water-base fluid. TEM images showed the shapes of both nanoparticles; Al_2O_3 is spherical-shaped while MWCNT is shaped cylindrically.

Secondly, the effect of hybrid nanofluid volume concentration on *h*, *Nu*, and *Q* was investigated at various temperature changes. For h_{av}, the maximum augmentation of 43.78% occurred at a volume concentration of 0.10 vol% at ΔT of 50 ℃ compared to h_{av} of DI water. It was also noted that an increase in ΔT led to an increase in h_{av} for all the tested samples. Nu_{av} enhanced with a rise in *Ra* for Al_2O_3–MWCNT (10:90) hybrid nanofluids samples at different φ and base fluid. A maximum Q_{av} of 49.27% was accomplished at φ = 0.10 vol% with ΔT = 50 °C compared to DI water. However, different hybrid nanofluids transfer heat to different extents in the same cavity, depending on their concentrations. Garbadeen [149] experimentally examined the natural convection of MWCNT-water nanofluids in a square cavity. The researcher reported a 42% maximum augmentation in heat transfer performance at a volume concentration of 0.10%. In this present study, the mixture of Al_2O_3 and MWCNT (10:90) showed a 7.27% increase compared to the mono nanoparticles (MWCNT) at the same volume concentration (φ = 0.10 vol%) reported by the researcher. It is evident that hybrid nanofluids have an advantage over single nanoparticle nanofluids. The temperature distribution of hybrid nanofluids was presented at several *Ra* and volume concentrations. Furthermore, in order to demonstrate the reliability of the experimental data, uncertainty analysis was conducted. Finally, it can be concluded that hybrid nanofluids as heat transfer fluids have significantly enhanced heat transfer performance compared to DI water.

5.3. Recommendation

The following further research is recommended:

- Since cavity inclination, magnetic stimuli, porosity, and aspect ratio are methods used for improving the natural convection heat transfer in cavities. It is vital to study the effects of the aforementioned methods in cavities utilizing hybrid nanofluids.
- To experimentally examine the influence of hybrid nanoparticle shapes and sizes on the convective heat transfer coefficient.
- In the near future, utilizing green nanofluids and green hybrid nanofluids for thermo-convection is expected due to the limited number of studies conducted with green nanofluids.
- There are relatively few experimental heat transfer studies of natural convection of hybrid nanofluids in several shapes of cavities like triangles and cylinders, and these studies need to be done.

BIBLIOGRAPHY

[1] O. Zeitoun and M. Ali, "Nanofluid impingement jet heat transfer," *Nanoscale research letters,* vol. 7, no. 1, pp. 1-13, 2012.

[2] A. M. Darwish, A.-F. M. R. El-Kersh, M. N. El-Sheikh, and I. M. El-Moghazy, "A review on nanofluid impingement jet heat transfer," *International Journal of Nanotechnology and Allied Sciences,* vol. 1, no. 1, pp. 1-15, 2017.

[3] I. N. Ewis, S. A. Mageed, M. Morsi, and O. Sharaf, "Effect of Nanofluid Jet Impingement on Heat Transfer of Surfaces with Different Shapes," *Int. J. Adv. Sci. Technol,* vol. 5, no. 9, pp. 47-66, 2019.

[4] W. Mutuku, "Ethylene glycol (EG)-based nanofluids as a coolant for automotive radiator, Asia Pac," *J. Chem. Eng,* vol. 3, no. 1, 2016.

[5] H. Ghodsinezhad, M. Sharifpur, and J. Meyer, "Experimental investigation on cavity flow natural convection of Al2O3–water nanofluids," *International Communications in Heat and Mass Transfer,* vol. 76, 06/01 2016, doi: 10.1016/j.icheatmasstransfer.2016.06.005.

[6] F. T. Koabra, "Study of natural convective heat transfer of nanofluids in cubical enclosure," 2016.

[7] A. Moghadassi, E. Ghomi, and F. Parvizian, "A numerical study of water based Al2O3 and Al2O3–Cu hybrid nanofluid effect on forced convective heat transfer," *International Journal of Thermal Sciences,* vol. 92, pp. 50-57, 2015.

[8] H. Ghodsinezhad, "Experimental investigation on natural convection of AI2O3-water nanofluids in cavity flow," University of Pretoria, 2016.

[9] J. Sarkar, P. Ghosh, and A. Adil, "A review on hybrid nanofluids: recent research, development and applications," *Renewable and Sustainable Energy Reviews,* vol. 43, pp. 164-177, 2015.

[10] M. H. Hamzah, N. A. C. Sidik, T. L. Ken, R. Mamat, and G. Najafi, "Factors affecting the performance of hybrid nanofluids: a comprehensive review," *International Journal of Heat and Mass Transfer*, vol. 115, pp. 630-646, 2017.

[11] U. Efemwenkiekie and S. Oyedepo, "Thermal Conductivity of Nanofluids in Heat Transfer Applications–A Review," in *Journal of Physics: Conference Series*, 2019, vol. 1378, no. 3: IOP Publishing, p. 032074.

[12] H. F. Öztop, P. Estellé, W.-M. Yan, K. Al-Salem, J. Orfi, and O. Mahian, "A brief review of natural convection in enclosures under localized heating with and without nanofluids," *International Communications in Heat and Mass Transfer*, vol. 60, pp. 37-44, 2015.

[13] C. Balaji, B. Srinivasan, and S. Gedupudi, "Chapter 6 - Natural convection," in *Heat Transfer Engineering*, C. Balaji, B. Srinivasan, and S. Gedupudi Eds.: Academic Press, 2021, pp. 173-198.

[14] S. U. Ilyas, R. Pendyala, and M. Narahari, "Experimental investigation of natural convection heat transfer characteristics in MWCNT-thermal oil nanofluid," *Journal of Thermal Analysis and Calorimetry*, vol. 135, no. 2, pp. 1197-1209, 2019.

[15] S. O. Giwa, M. Sharifpur, and J. P. Meyer, "Experimental study of thermo-convection performance of hybrid nanofluids of Al2O3-MWCNT/water in a differentially heated square cavity," *International Journal of Heat and Mass Transfer*, vol. 148, p. 119072, 2020/02/01/ 2020, doi: https://doi.org/10.1016/j.ijheatmasstransfer.2019.119072.

[16] M. Torki and N. Etesami, "Experimental investigation of natural convection heat transfer of SiO 2/water nanofluid inside inclined enclosure," *Journal of Thermal Analysis and Calorimetry*, vol. 139, no. 2, pp. 1565-1574, 2020.

[17] S. U. Choi and J. A. Eastman, "Enhancing thermal conductivity of fluids with nanoparticles," Argonne National Lab., IL (United States), 1995.

[18] E. C. Okonkwo, I. Wole-Osho, I. W. Almanassra, Y. M. Abdullatif, and T. Al-Ansari, "An updated review of nanofluids in various heat transfer devices," *Journal of Thermal Analysis and Calorimetry*, pp. 1-56, 2020.

[19] L. S. Sundar, K. Sharma, M. K. Singh, and A. Sousa, "Hybrid nanofluids preparation, thermal properties, heat transfer and friction factor–a review," *Renewable and Sustainable Energy Reviews,* vol. 68, pp. 185-198, 2017.

[20] A. Tiara, S. Chakraborty, I. Sarkar, S. K. Pal, and S. Chakraborty, "Effect of alumina nanofluid jet on the enhancement of heat transfer from a steel plate," *Heat and Mass Transfer,* vol. 53, no. 6, pp. 2187-2197, 2017.

[21] J. Lv, C. Hu, M. Bai, K. Zeng, S. Chang, and D. Gao, "Experimental investigation of free single jet impingement using SiO2-water nanofluid," *Experimental Thermal and Fluid Science,* vol. 84, pp. 39-46, 2017.

[22] D. Dey, P. Kumar, and S. Samantaray, "A review of nanofluid preparation, stability, and thermo-physical properties," *Heat Transfer—Asian Research,* vol. 46, no. 8, pp. 1413-1442, 2017.

[23] L. Kong, J. Sun, and Y. Bao, "Preparation, characterization and tribological mechanism of nanofluids," *Rsc Advances,* vol. 7, no. 21, pp. 12599-12609, 2017.

[24] W. Yu and H. Xie, "A review on nanofluids: preparation, stability mechanisms, and applications," *Journal of nanomaterials,* vol. 2012, 2012.

[25] N. Putra, W. Roetzel, and S. K. Das, "Natural convection of nano-fluids," *Heat and mass transfer,* vol. 39, no. 8, pp. 775-784, 2003.

[26] S. Aminossadati and B. Ghasemi, "Natural convection cooling of a localised heat source at the bottom of a nanofluid-filled enclosure," *European Journal of Mechanics-B/Fluids,* vol. 28, no. 5, pp. 630-640, 2009.

[27] M. M. Maskeen, A. Zeeshan, O. U. Mehmood, and M. Hassan, "Heat transfer enhancement in hydromagnetic alumina–copper/water hybrid nanofluid flow over a stretching cylinder," *Journal of Thermal Analysis and Calorimetry,* vol. 138, no. 2, pp. 1127-1136, 2019.

[28] F. Jamil and H. M. Ali, "Applications of hybrid nanofluids in different fields," in *Hybrid nanofluids for convection heat transfer*: Elsevier, 2020, pp. 215-254.

[29] R. Turcu *et al.*, "New polypyrrole-multiwall carbon nanotubes hybrid materials," *Journal of optoelectronics and advanced materials,* vol. 8, no. 2, pp. 643-647, 2006.

[30] A. J. Chamkha, I. V. Miroshnichenko, and M. A. Sheremet, "Numerical Analysis of Unsteady Conjugate Natural Convection of Hybrid Water-Based Nanofluid in a Semicircular Cavity," *Journal of Thermal Science and Engineering Applications,* vol. 9, no. 4, 2017, doi: 10.1115/1.4036203.

[31] A. Rashad, A. J. Chamkha, M. A. Ismael, and T. Salah, "MHD Natural Convection in a Triangular Cavity filled with a Cu-Al2O3," *Water Hybrid Nanofluid with Localized Heating from Below and Internal Heat Generation,* 2018.

[32] J. R. Babu, K. K. Kumar, and S. S. Rao, "State-of-art review on hybrid nanofluids," *Renewable and Sustainable Energy Reviews,* vol. 77, pp. 551-565, 2017.

[33] L. S. Sundar, M. K. Singh, and A. C. Sousa, "Enhanced heat transfer and friction factor of MWCNT–Fe3O4/water hybrid nanofluids," *International Communications in Heat and Mass Transfer,* vol. 52, pp. 73-83, 2014.

[34] S. Suresh, K. Venkitaraj, P. Selvakumar, and M. Chandrasekar, "Synthesis of Al2O3–Cu/water hybrid nanofluids using two step method and its thermo physical properties," *Colloids and Surfaces A: Physicochemical and Engineering Aspects,* vol. 388, no. 1-3, pp. 41-48, 2011.

[35] D. Toghraie, V. A. Chaharsoghi, and M. Afrand, "Measurement of thermal conductivity of ZnO–TiO 2/EG hybrid nanofluid," *Journal of Thermal Analysis and Calorimetry*, vol. 125, no. 1, pp. 527-535, 2016.

[36] M. Gupta, V. Singh, S. Kumar, and N. Dilbaghi, "Experimental analysis of heat transfer behavior of silver, MWCNT and hybrid (silver+ MWCNT) nanofluids in a laminar tubular flow," *Journal of Thermal Analysis and Calorimetry*, vol. 142, no. 4, pp. 1545-1559, 2020.

[37] M. Sharifpur, S. O. Giwa, K.-Y. Lee, H. Ghodsinezhad, and J. P. Meyer, "Experimental Investigation into Natural Convection of Zinc Oxide/Water Nanofluids in a Square Cavity," *Heat Transfer Engineering*, pp. 1-13, 2020.

[38] K. Farhana *et al.*, "Significance of alumina in nanofluid technology," *Journal of Thermal Analysis and Calorimetry*, vol. 138, no. 2, pp. 1107-1126, 2019.

[39] T. Hayat and S. Nadeem, "Heat transfer enhancement with Ag–CuO/water hybrid nanofluid," *Results in Physics*, vol. 7, pp. 2317-2324, 2017/01/01/ 2017, doi: https://doi.org/10.1016/j.rinp.2017.06.034.

[40] D. Dhinesh Kumar and A. Valan Arasu, "A comprehensive review of preparation, characterization, properties and stability of hybrid nanofluids," *Renewable and Sustainable Energy Reviews*, vol. 81, pp. 1669-1689, 2018/01/01/ 2018, doi: https://doi.org/10.1016/j.rser.2017.05.257.

[41] A. Albert, H. Samuel D.G, and V. Parthasarathy, "Wet Chemical Synthesis of CuO-PVA Hybrid Nanofluid Stabilized by Steric Repulsion," *Asian Journal of Chemistry*, vol. 32, pp. 570-574, 02/10 2020, doi: 10.14233/ajchem.2020.22424.

[42] N. A. Che Sidik, M. Mahmud Jamil, W. M. A. Aziz Japar, and I. Muhammad Adamu, "A review on preparation methods, stability and applications of hybrid nanofluids," *Renewable and Sustainable Energy Reviews*, vol. 80, pp. 1112-1122, 2017/12/01/ 2017, doi: https://doi.org/10.1016/j.rser.2017.05.221.

[43] M. J. Nine, M. Batmunkh, J.-H. Kim, H.-S. Chung, and H.-M. Jeong, "Investigation of Al2O3-MWCNTs hybrid dispersion in water and their thermal characterization," *Journal of nanoscience and nanotechnology*, vol. 12, no. 6, pp. 4553-4559, 2012.

[44] M. Chopkar, P. K. Das, and I. Manna, "Synthesis and characterization of nanofluid for advanced heat transfer applications," *Scripta Materialia*, vol. 55, no. 6, pp. 549-552, 2006/09/01/ 2006, doi: https://doi.org/10.1016/j.scriptamat.2006.05.030.

[45] M. J. Nine, B. Munkhbayar, M. S. Rahman, H. Chung, and H. Jeong, "Highly productive synthesis process of well dispersed Cu2O and Cu/Cu2O nanoparticles and its thermal characterization," *Materials Chemistry and Physics*, vol. 141, no. 2, pp. 636-642, 2013/09/16/ 2013, doi: https://doi.org/10.1016/j.matchemphys.2013.05.032.

[46] M. Gupta, V. Singh, S. Kumar, S. Kumar, N. Dilbaghi, and Z. Said, "Up to date review on the synthesis and thermophysical properties of hybrid nanofluids," *Journal of Cleaner Production*, vol. 190, pp. 169-192, 2018/07/20/ 2018, doi: https://doi.org/10.1016/j.jclepro.2018.04.146.

[47] N. A. C. Sidik, M. M. Jamil, W. M. A. A. Japar, and I. M. Adamu, "A review on preparation methods, stability and applications of hybrid nanofluids," *Renewable and Sustainable Energy Reviews*, vol. 80, pp. 1112-1122, 2017.

[48] P. K. Jena, E. A. Brocchi, and M. S. Motta, "In-situ formation of Cu–Al2O3 nano-scale composites by chemical routes and studies on their microstructures," *Materials Science and Engineering: A*, vol. 313, no. 1, pp. 180-186, 2001/08/31/ 2001, doi: https://doi.org/10.1016/S0921-5093(00)01998-5.

[49] T. Rasheed *et al.*, "Hybrid Nanofluids as Renewable and Sustainable Colloidal Suspensions for Potential Photovoltaic/Thermal and Solar Energy Applications," (in English), *Frontiers in Chemistry*, Review vol. 9, no. 802, 2021-September-27 2021, doi: 10.3389/fchem.2021.737033.

[50] W. T. Urmi, A. Shafiqah, M. M. Rahman, K. Kadirgama, and M. A. Maleque, "Preparation Methods and Challenges of Hybrid Nanofluids: A Review," *Journal of Advanced Research in Fluid Mechanics and Thermal Sciences*, vol. 78, no. 2, pp. 56-66, 2020.

[51] M. Bahrami, M. Akbari, A. Karimipour, and M. Afrand, "An experimental study on rheological behavior of hybrid nanofluids made of iron and copper oxide in a binary mixture of water and ethylene glycol: Non-Newtonian behavior," *Experimental Thermal and Fluid Science*, vol. 79, pp. 231-237, 2016/12/01/ 2016, doi: https://doi.org/10.1016/j.expthermflusci.2016.07.015.

[52] O. Soltani and M. Akbari, "Effects of temperature and particles concentration on the dynamic viscosity of MgO-MWCNT/ethylene glycol hybrid nanofluid: Experimental study," *Physica E: Low-dimensional Systems and Nanostructures*, vol. 84, pp. 564-570, 2016/10/01/ 2016, doi: https://doi.org/10.1016/j.physe.2016.06.015.

[53] S. Suresh, K. P. Venkitaraj, P. Selvakumar, and M. Chandrasekar, "Effect of Al2O3–Cu/water hybrid nanofluid in heat transfer," *Experimental Thermal and Fluid Science*, vol. 38, pp. 54-60, 2012/04/01/ 2012, doi: https://doi.org/10.1016/j.expthermflusci.2011.11.007.

[54] L. F. Chen, M. Cheng, D. J. Yang, and L. Yang, "Enhanced thermal conductivity of nanofluid by synergistic effect of multi-walled carbon nanotubes and Fe2O3 nanoparticles," in *Applied mechanics and materials*, 2014, vol. 548: Trans Tech Publ, pp. 118-123.

[55] S. U. Ilyas, R. Pendyala, and N. Marneni, "Stability of nanofluids," in *Engineering applications of nanotechnology*: Springer, 2017, pp. 1-31.

[56] M. A. Khairul, K. Shah, E. Doroodchi, R. Azizian, and B. Moghtaderi, "Effects of surfactant on stability and thermo-physical properties of metal oxide nanofluids," *International Journal of Heat and Mass Transfer*, vol. 98, pp. 778-787, 2016/07/01/ 2016, doi: https://doi.org/10.1016/j.ijheatmasstransfer.2016.03.079.

[57] S. S. Khaleduzzaman, I. M. Mahbubul, I. M. Shahrul, and R. Saidur, "Effect of particle concentration, temperature and surfactant on surface tension of nanofluids," *International Communications in Heat and Mass Transfer,* vol. 49, pp. 110-114, 2013/12/01/ 2013, doi: https://doi.org/10.1016/j.icheatmasstransfer.2013.10.010.

[58] H. Setia, R. Gupta, and R. Wanchoo, "Stability of nanofluids," in *Materials Science Forum*, 2013, vol. 757: Trans Tech Publ, pp. 139-149.

[59] S. Chakraborty and P. K. Panigrahi, "Stability of nanofluid: A review," *Applied Thermal Engineering,* vol. 174, p. 115259, 2020/06/25/ 2020, doi: https://doi.org/10.1016/j.applthermaleng.2020.115259.

[60] S. Iyahraja and J. S. Rajadurai, "Stability of Aqueous Nanofluids Containing PVP-Coated Silver Nanoparticles," *Arabian Journal for Science and Engineering,* vol. 41, no. 2, pp. 653-660, 2016/02/01 2016, doi: 10.1007/s13369-015-1707-9.

[61] L. Megatif, A. Ghozatloo, A. Arimi, and M. Shariati-Niasar, "Investigation of laminar convective heat transfer of a novel TiO2–carbon nanotube hybrid water-based nanofluid," *Experimental Heat Transfer,* vol. 29, no. 1, pp. 124-138, 2016.

[62] B. Munkhbayar, M. R. Tanshen, J. Jeoun, H. Chung, and H. Jeong, "Surfactant-free dispersion of silver nanoparticles into MWCNT-aqueous nanofluids prepared by one-step technique and their thermal characteristics," *Ceramics International,* vol. 39, no. 6, pp. 6415-6425, 2013.

[63] M. H. Esfe, M. K. Amiri, and A. Alirezaie, "Thermal conductivity of a hybrid nanofluid," *Journal of Thermal Analysis and Calorimetry,* vol. 134, no. 2, pp. 1113-1122, 2018.

[64] M. H. Esfe, P. M. Behbahani, A. A. A. Arani, and M. R. Sarlak, "Thermal conductivity enhancement of SiO 2–MWCNT (85: 15%)–EG hybrid nanofluids," *Journal of Thermal Analysis and Calorimetry,* vol. 128, no. 1, pp. 249-258, 2017.

[65] S. S. Botha, P. Ndungu, and B. J. Bladergroen, "Physicochemical Properties of Oil-Based Nanofluids Containing Hybrid Structures of Silver Nanoparticles Supported on Silica," *Industrial & Engineering Chemistry Research,* vol. 50, no. 6, pp. 3071-3077, 2011/03/16 2011, doi: 10.1021/ie101088x.

[66] M. I. Limited. *Zeta potential- An introduction in 30 minutes,* Malvern, 2015. [Online]. Available: https://www.research.colostate.edu/wp-content/uploads/2018/11/ZetaPotential-Introduction-in-30min-Malvern.pdf.

[67] P. M. V. Raja and A. R. Barron, "Zeta Potential Analysis," ed, 2021.

[68] V. V. Wanatasanappan, M. Z. Abdullah, and P. Gunnasegaran, "Thermophysical properties of Al2O3-CuO hybrid nanofluid at different nanoparticle mixture ratio: An experimental approach," *Journal of Molecular Liquids,* vol. 313, p. 113458, 2020/09/01/ 2020, doi: https://doi.org/10.1016/j.molliq.2020.113458.

[69] Y. Fovet, J.-Y. Gal, and F. Toumelin-Chemla, "Influence of pH and fluoride concentration on titanium passivating layer: stability of titanium dioxide," *Talanta,* vol. 53, no. 5, pp. 1053-1063, 2001/01/26/ 2001, doi: https://doi.org/10.1016/S0039-9140(00)00592-0.

[70] A. Ghadimi, H. Metselaar, and B. LotfizadehDehkordi, "Nanofluid stability optimization based on UV-Vis spectrophotometer measurement," vol. 10, pp. 32-40, 01/01 2015.

[71] K. Pate and P. Safier, "12 - Chemical metrology methods for CMP quality," in *Advances in Chemical Mechanical Planarization (CMP),* S. Babu Ed.: Woodhead Publishing, 2016, pp. 299-325.

[72] N. Gupta, S. M. Gupta, and S. K. Sharma, "Preparation of stable metal/COOH-MWCNT hybrid nanofluid," *Materials Today: Proceedings,* vol. 36, pp. 649-656, 2021/01/01/ 2021, doi: https://doi.org/10.1016/j.matpr.2020.04.492.

[73] D. Cabaleiro, M. J. Pastoriza-Gallego, M. M. Piñeiro, and L. Lugo, "Characterization and measurements of thermal conductivity, density and rheological properties of zinc oxide nanoparticles dispersed in (ethane-1,2-diol+water) mixture," *The Journal of Chemical Thermodynamics*, vol. 58, pp. 405-415, 2013/03/01/ 2013, doi: https://doi.org/10.1016/j.jct.2012.10.014.

[74] H. Wei Xian, N. A. Che Sidik, S. R. Aid, T. L. Ken, and Y. Asako, "Review on Preparation Techniques, Properties and Performance of Hybrid Nanofluid in Recent Engineering Applications," *Journal of Advanced Research in Fluid Mechanics and Thermal Sciences*, vol. 45, no. 1, pp. 1-13, 12/01 2020. [Online]. Available: https://akademiabaru.com/submit/index.php/arfmts/article/view/2176.

[75] A. K. Singh and V. S. Raykar, "Microwave synthesis of silver nanofluids with polyvinylpyrrolidone (PVP) and their transport properties," *Colloid and Polymer Science*, vol. 286, no. 14, pp. 1667-1673, 2008/12/01 2008, doi: 10.1007/s00396-008-1932-9.

[76] B. Sun, Y. Zhang, D. Yang, and H. Li, "Experimental study on heat transfer characteristics of hybrid nanofluid impinging jets," *Applied Thermal Engineering*, vol. 151, pp. 556-566, 2019.

[77] M. F. Nabil, W. H. Azmi, K. A. Hamid, N. N. M. Zawawi, G. Priyandoko, and R. Mamat, "Thermo-physical properties of hybrid nanofluids and hybrid nanolubricants: A comprehensive review on performance," *International Communications in Heat and Mass Transfer*, vol. 83, pp. 30-39, 2017/04/01/ 2017, doi: https://doi.org/10.1016/j.icheatmasstransfer.2017.03.008.

[78] C. Ho, W. Liu, Y. Chang, and C. Lin, "Natural convection heat transfer of alumina-water nanofluid in vertical square enclosures: An experimental study," *International Journal of Thermal Sciences*, vol. 49, no. 8, pp. 1345-1353, 2010.

[79] M. M. Rashidi *et al.*, "Thermophysical Properties of Hybrid Nanofluids and the Proposed Models: An Updated Comprehensive Study," *Nanomaterials*, vol. 11, no. 11, p. 3084, 2021. [Online]. Available: https://www.mdpi.com/2079-4991/11/11/3084.

[80] M. U. Sajid and H. M. Ali, "Thermal conductivity of hybrid nanofluids: A critical review," *International Journal of Heat and Mass Transfer*, vol. 126, pp. 211-234, 2018/11/01/ 2018, doi: https://doi.org/10.1016/j.ijheatmasstransfer.2018.05.021.

[81] N. Ali, J. A. Teixeira, and A. Addali, "A Review on Nanofluids: Fabrication, Stability, and Thermophysical Properties," *Journal of Nanomaterials*, vol. 2018, p. 6978130, 2018/06/04 2018, doi: 10.1155/2018/6978130.

[82] R. Shende and R. Sundara, "Nitrogen doped hybrid carbon based composite dispersed nanofluids as working fluid for low-temperature direct absorption solar collectors," *Solar Energy Materials and Solar Cells*, vol. 140, pp. 9-16, 2015/09/01/ 2015, doi: https://doi.org/10.1016/j.solmat.2015.03.012.

[83] I. Gonçalves *et al.*, "Thermal Conductivity of Nanofluids: A Review on Prediction Models, Controversies and Challenges," *Applied Sciences*, vol. 11, no. 6, p. 2525, 2021. [Online]. Available: https://www.mdpi.com/2076-3417/11/6/2525.

[84] G. Huminic, A. Huminic, F. Dumitrache, C. Fleacă, and I. Morjan, "Study of the thermal conductivity of hybrid nanofluids: Recent research and experimental study," *Powder Technology*, vol. 367, pp. 347-357, 2020.

[85] A. Shahsavar, M. Saghafian, M. R. Salimpour, and M. B. Shafii, "Effect of temperature and concentration on thermal conductivity and viscosity of ferrofluid loaded with carbon nanotubes," *Heat and Mass Transfer*, vol. 52, no. 10, pp. 2293-2301, 2016/10/01 2016, doi: 10.1007/s00231-015-1743-8.

[86] M. H. Ahmadi, A. Mirlohi, M. Alhuyi Nazari, and R. Ghasempour, "A review of thermal conductivity of various nanofluids," *Journal of Molecular Liquids*, vol. 265, pp. 181-188, 2018/09/01/ 2018, doi: https://doi.org/10.1016/j.molliq.2018.05.124.

[87] M. Farbod and A. Ahangarpour, "Improved thermal conductivity of Ag decorated carbon nanotubes water based nanofluids," *Physics Letters A*, vol. 380, no. 48, pp. 4044-4048, 2016/12/16/ 2016, doi: https://doi.org/10.1016/j.physleta.2016.10.014.

[88] G. Paul, J. Philip, B. Raj, P. K. Das, and I. Manna, "Synthesis, characterization, and thermal property measurement of nano-Al95Zn05 dispersed nanofluid prepared by a two-step process," *International Journal of Heat and Mass Transfer*, vol. 54, no. 15, pp. 3783-3788, 2011/07/01/ 2011, doi: https://doi.org/10.1016/j.ijheatmasstransfer.2011.02.044.

[89] T. T. Baby and S. Ramaprabhu, "Synthesis and nanofluid application of silver nanoparticles decorated graphene," *Journal of Materials Chemistry*, 10.1039/C0JM04106H vol. 21, no. 26, pp. 9702-9709, 2011, doi: 10.1039/C0JM04106H.

[90] T. Ambreen and M.-H. Kim, "Influence of particle size on the effective thermal conductivity of nanofluids: A critical review," *Applied Energy*, vol. 264, p. 114684, 2020.

[91] X. Wang, X. Xu, and S. U. Choi, "Thermal conductivity of nanoparticle-fluid mixture," *Journal of thermophysics and heat transfer*, vol. 13, no. 4, pp. 474-480, 1999.

[92] J. Philip and S. P Damodaran, "Thermal properties of nanofluids- A Review," *Advances in Colloid and Interface Science*, vol. 183-184, pp. 30-45, 08/07 2012, doi: 10.1016/j.cis.2012.08.001.

[93] S. M. S. Murshed, K. C. Leong, and C. Yang, "Enhanced thermal conductivity of TiO2—water based nanofluids," *International Journal of Thermal Sciences*, vol. 44, no. 4, pp. 367-373, 2005/04/01/ 2005, doi: https://doi.org/10.1016/j.ijthermalsci.2004.12.005.

[94] J. Glory, M. Bonetti, M. Helezen, M. Mayne-L'Hermite, and C. Reynaud, "Thermal and electrical conductivities of water-based nanofluids prepared with long multiwalled carbon nanotubes," *Journal of applied physics*, vol. 103, no. 9, p. 094309, 2008.

[95] M. H. Esfe, S. Esfandeh, M. Afrand, M. Rejvani, and S. H. Rostamian, "Experimental evaluation, new correlation proposing and ANN modeling of thermal properties of EG based hybrid nanofluid containing ZnO-DWCNT nanoparticles for internal combustion engines applications," *Applied Thermal Engineering*, vol. 133, pp. 452-463, 2018.

[96] I. Wole-Osho, E. C. Okonkwo, H. Adun, D. Kavaz, and S. Abbasoglu, "An intelligent approach to predicting the effect of nanoparticle mixture ratio, concentration and temperature on thermal conductivity of hybrid nanofluids," *Journal of Thermal Analysis and Calorimetry*, vol. 144, no. 3, pp. 671-688, 2021.

[97] P. K. Das, "A review based on the effect and mechanism of thermal conductivity of normal nanofluids and hybrid nanofluids," *Journal of Molecular Liquids*, vol. 240, pp. 420-446, 2017/08/01/ 2017, doi: https://doi.org/10.1016/j.molliq.2017.05.071.

[98] A. Brusly Solomon, J. van Rooyen, M. Rencken, M. Sharifpur, and J. P. Meyer, "Experimental study on the influence of the aspect ratio of square cavity on natural convection heat transfer with Al2O3/Water nanofluids," *International Communications in Heat and Mass Transfer*, vol. 88, pp. 254-261, 2017/11/01/ 2017, doi: https://doi.org/10.1016/j.icheatmasstransfer.2017.09.007.

[99] R. R. Sahoo, "Experimental study on the viscosity of hybrid nanofluid and development of a new correlation," *Heat and Mass Transfer*, vol. 56, no. 11, pp. 3023-3033, 2020.

[100] S. Sharma, A. Tiwari, S. Tiwari, and R. Prakash, "Viscosity of hybrid nanofluids: Measurement and comparison," *Journal of Mechanical Engineering and Sciences*, vol. 12, no. 2, p. 3614, 2018.

[101] M. H. Esfe, A. A. A. Arani, M. Rezaie, W.-M. Yan, and A. Karimipour, "Experimental determination of thermal conductivity and dynamic viscosity of Ag–MgO/water hybrid nanofluid," *International Communications in Heat and Mass Transfer*, vol. 66, pp. 189-195, 2015.

[102] P. S. Joshi and A. Pattamatta, "Enhancement of natural convection heat transfer in a square cavity using MWCNT/Water nanofluid: an experimental study," *Heat and Mass Transfer*, vol. 54, no. 8, pp. 2295-2303, 2018/08/01 2018, doi: 10.1007/s00231-017-2098-0.

[103] Y. Xuan, Q. Li, and W. Hu, "Aggregation structure and thermal conductivity of nanofluids," *AIChE Journal*, vol. 49, no. 4, pp. 1038-1043, 2003.

[104] S. M. Abbasi, A. Rashidi, A. Nemati, and K. Arzani, "The effect of functionalisation method on the stability and the thermal conductivity of nanofluid hybrids of carbon nanotubes/gamma alumina," *Ceramics International*, vol. 39, no. 4, pp. 3885-3891, 2013/05/01/ 2013, doi: https://doi.org/10.1016/j.ceramint.2012.10.232.

[105] A. Asadi, I. M. Alarifi, and L. K. Foong, "An experimental study on characterization, stability and dynamic viscosity of CuO-TiO2/water hybrid nanofluid," *Journal of Molecular Liquids*, vol. 307, p. 112987, 2020/06/01/ 2020, doi: https://doi.org/10.1016/j.molliq.2020.112987.

[106] A. S. Dalkılıç *et al.*, "Experimental investigation on the viscosity characteristics of water based SiO2-graphite hybrid nanofluids," *International Communications in Heat and Mass Transfer*, vol. 97, pp. 30-38, 2018/10/01/ 2018, doi: https://doi.org/10.1016/j.icheatmasstransfer.2018.07.007.

[107] K. S. Suganthi, V. Leela Vinodhan, and K. S. Rajan, "Heat transfer performance and transport properties of ZnO–ethylene glycol and ZnO–ethylene glycol–water nanofluid coolants," *Applied Energy*, vol. 135, pp. 548-559, 2014/12/15/ 2014, doi: https://doi.org/10.1016/j.apenergy.2014.09.023.

[108] A. K. Tiwari, N. S. Pandya, H. Shah, and Z. Said, "Experimental comparison of specific heat capacity of three different metal oxides with MWCNT/water-based hybrid nanofluids: proposing a new correlation," *Applied Nanoscience,* pp. 1-11, 2020.

[109] A. B. Çolak, O. Yildiz, M. Bayrak, A. Celen, and S. Wongwises, "Experimental study on the specific heat capacity measurement of water-based al2o3-cu hybrid nanofluid by using differential thermal analysis method," *Current Nanoscience,* vol. 16, no. 6, pp. 912-928, 2020.

[110] R. S. Vajjha and D. K. Das, "Specific Heat Measurement of Three Nanofluids and Development of New Correlations," *Journal of Heat Transfer,* vol. 131, no. 7, 2009, doi: 10.1115/1.3090813.

[111] G. Huminic and A. Huminic, "Hybrid nanofluids for heat transfer applications–a state-of-the-art review," *International Journal of Heat and Mass Transfer,* vol. 125, pp. 82-103, 2018.

[112] C. J. Ho, J. B. Huang, P. S. Tsai, and Y. M. Yang, "Preparation and properties of hybrid water-based suspension of Al2O3 nanoparticles and MEPCM particles as functional forced convection fluid," *International Communications in Heat and Mass Transfer,* vol. 37, no. 5, pp. 490-494, 2010/05/01/ 2010, doi: https://doi.org/10.1016/j.icheatmasstransfer.2009.12.007.

[113] S. Askari, H. Koolivand, M. Pourkhalil, R. Lotfi, and A. Rashidi, "Investigation of Fe3O4/Graphene nanohybrid heat transfer properties: Experimental approach," *International Communications in Heat and Mass Transfer,* vol. 87, pp. 30-39, 2017/10/01/ 2017, doi: https://doi.org/10.1016/j.icheatmasstransfer.2017.06.012.

[114] E. Ghahremani, R. Ghaffari, H. Ghadjari, and J. Mokhtari, "Effect of Variable Thermal Expansion Coefficient and Nanofluid Properties on Steady Natural Convection in an Enclosure," *Journal of Applied and Computational Mechanics,* vol. 3, 03/24 2017, doi: 10.22055/jacm.2017.21451.1099.

[115] A. Nayak, R. Singh, and P. Kulkarni, "Measurement of volumetric thermal expansion coefficient of various nanofluids," *Technical Physics Letters*, vol. 36, no. 8, pp. 696-698, 2010.

[116] M. S. Sadeghi *et al.*, "On the natural convection of nanofluids in diverse shapes of enclosures: an exhaustive review," *Journal of Thermal Analysis and Calorimetry*, 2020/09/21 2020, doi: 10.1007/s10973-020-10222-y.

[117] W. Yu and S. Choi, "The role of interfacial layers in the enhanced thermal conductivity of nanofluids: a renovated Maxwell model," *Journal of nanoparticle research*, vol. 5, no. 1, pp. 167-171, 2003.

[118] Z. Wu, L. Wang, and B. Sundén, "Pressure drop and convective heat transfer of water and nanofluids in a double-pipe helical heat exchanger," *Applied Thermal Engineering*, vol. 60, no. 1, pp. 266-274, 2013/10/02/ 2013, doi: https://doi.org/10.1016/j.applthermaleng.2013.06.051.

[119] S. O. Giwa, M. Sharifpur, M. H. Ahmadi, S. Sohel Murshed, and J. P. Meyer, "Experimental investigation on stability, viscosity, and electrical conductivity of water-based hybrid nanofluid of MWCNT-Fe2O3," *Nanomaterials*, vol. 11, no. 1, p. 136, 2021.

[120] S. O. Giwa, M. Sharifpur, M. H. Ahmadi, and J. P. Meyer, "A review of magnetic field influence on natural convection heat transfer performance of nanofluids in square cavities," *Journal of Thermal Analysis and Calorimetry*, vol. 145, no. 5, pp. 2581-2623, 2021/09/01 2021, doi: 10.1007/s10973-020-09832-3.

[121] M. Ghalambaz, A. Doostani, E. Izadpanahi, and A. J. Chamkha, "Conjugate natural convection flow of Ag–MgO/water hybrid nanofluid in a square cavity," *Journal of Thermal Analysis and Calorimetry*, vol. 139, no. 3, pp. 2321-2336, 2020.

[122] F. Selimefendigil and A. J. Chamkha, "Natural convection of a hybrid nanofluid-filled triangular annulus with an opening," *Computational Thermal Sciences: An International Journal*, vol. 8, no. 6, 2016.

[123] H. R. Ashorynejad and A. Shahriari, "MHD natural convection of hybrid nanofluid in an open wavy cavity," *Results in Physics*, vol. 9, pp. 440-455, 2018/06/01/ 2018, doi: https://doi.org/10.1016/j.rinp.2018.02.045.

[124] M. Asmadi, R. Md. Kasmani, Z. Siri, and H. Saleh, "Thermal performance analysis for moderate Rayleigh numbers of Newtonian hybrid nanofluid-filled U-shaped cavity with various thermal profiles," *Physics of Fluids*, vol. 33, no. 3, p. 032006, 2021.

[125] M. A. Almeshaal, K. Kalidasan, F. Askri, R. Velkennedy, A. S. Alsagri, and L. Kolsi, "Three-dimensional analysis on natural convection inside a T-shaped cavity with water-based CNT–aluminum oxide hybrid nanofluid," *Journal of Thermal Analysis and Calorimetry*, vol. 139, no. 3, pp. 2089-2098, 2020.

[126] Y. Hu, Y. He, C. Qi, B. Jiang, and H. Inaki Schlaberg, "Experimental and numerical study of natural convection in a square enclosure filled with nanofluid," *International Journal of Heat and Mass Transfer*, vol. 78, pp. 380-392, 2014/11/01/ 2014, doi: https://doi.org/10.1016/j.ijheatmasstransfer.2014.07.001.

[127] M. Sharifpur, A. B. Solomon, T. L. Ottermann, and J. P. Meyer, "Optimum concentration of nanofluids for heat transfer enhancement under cavity flow natural convection with TiO2 – Water," *International Communications in Heat and Mass Transfer*, vol. 98, pp. 297-303, 2018/11/01/ 2018, doi: https://doi.org/10.1016/j.icheatmasstransfer.2018.09.010.

[128] R. Choudhary and S. Subudhi, "Aspect ratio dependence of turbulent natural convection in Al2O3/water nanofluids," *Applied Thermal Engineering*, vol. 108, pp. 1095-1104, 2016.

[129] I. D. Garbadeen, M. Sharifpur, J. M. Slabber, and J. P. Meyer, "Experimental study on natural convection of MWCNT-water nanofluids in a square enclosure," *International*

Communications in Heat and Mass Transfer, vol. 88, pp. 1-8, 2017/11/01/ 2017, doi: https://doi.org/10.1016/j.icheatmasstransfer.2017.07.019.

[130] D. Dey and D. S. Sahu, "Experimental study in a natural convection cavity using nanofluids," *Materials Today: Proceedings*, vol. 41, pp. 403-412, 2021/01/01/ 2021, doi: https://doi.org/10.1016/j.matpr.2020.09.631.

[131] M. R. Kiran and S. R. Babu, "Experimental investigation on natural convection heat transfer enhancement using transformer oil-TiO2 nanofluid," *IRJET*, vol. 5, no. 7, pp. 1412-1418, 2018.

[132] B. Berkovsky and V. Polevikov, "Numerical study of problems on high-intensive free convection," 1977.

[133] S. Cioni, S. Ciliberto, and J. Sommeria, "Experimental study of high-Rayleigh-number convection in mercury and water," *Dynamics of Atmospheres and Oceans*, vol. 24, no. 1-4, pp. 117-127, 1996.

[134] W. Leong, K. Hollands, and A. Brunger, "Experimental Nusselt numbers for a cubical-cavity benchmark problem in natural convection," *International Journal of Heat and Mass Transfer*, vol. 42, no. 11, pp. 1979-1989, 1999.

[135] C. Nwaokocha, M. Momin, S. Giwa, M. Sharifpur, S. Murshed, and J. Meyer, "Experimental investigation of thermo-convection behaviour of aqueous binary nanofluids of MgO-ZnO in a square cavity," *Thermal Science and Engineering Progress*, p. 101057, 2021.

[136] "Nanoparticles safety guide." The University of Texas. https://www.uth.edu/dotAsset/c6d9a7b4-bdc9-424b-b849-bd6cbadcc398.pdf. (accessed 23, 2021).

[137] "Guidelines for Safety during Nanomaterials Research." University of Washington. https://www.ehs.washington.edu/system/files/resources/nanosafeguide.pdf (accessed 23, 2021).

[138] "Working Safely with Engineered Nanoparticles." University of South Australia. https://i.unisa.edu.au/siteassets/human-resources/ptc/files/guidelines/safety-and-wellbeing/nano_particles_working_safely.pdf. (accessed 24, 2021).

[139] A. Rashad, A. J. Chamkha, M. A. Ismael, and T. Salah, "Magnetohydrodynamics natural convection in a triangular cavity filled with a Cu-Al2O3/water hybrid nanofluid with localized heating from below and internal heat generation," *Journal of Heat Transfer*, vol. 140, no. 7, 2018.

[140] S. J. Kline, "Describing uncertainty in single sample experiments," *Mech. Engineering*, vol. 75, pp. 3-8, 1953.

[141] R. J. Moffat, "Describing the uncertainties in experimental results," *Experimental thermal and fluid science*, vol. 1, no. 1, pp. 3-17, 1988.

[142] S. Giwa, M. Sharifpur, J. P. Meyer, S. Wongwises, and O. Mahian, "Experimental measurement of viscosity and electrical conductivity of water-based γ-Al 2 O 3/MWCNT hybrid nanofluids with various particle mass ratios," *Journal of Thermal Analysis and Calorimetry*, vol. 143, no. 2, pp. 1037-1050, 2021.

[143] C. O. Popiel and J. Wojtkowiak, "Simple Formulas for Thermophysical Properties of Liquid Water for Heat Transfer Calculations (from 0°C to 150°C)," *Heat Transfer Engineering*, vol. 19, no. 3, pp. 87-101, 1998/01/01 1998, doi: 10.1080/01457639808939929.

[144] M. Kole and T. K. Dey, "Viscosity of alumina nanoparticles dispersed in car engine coolant," *Experimental Thermal and Fluid Science*, vol. 34, no. 6, pp. 677-683, 2010/09/01/ 2010, doi: https://doi.org/10.1016/j.expthermflusci.2009.12.009.

[145] M. Hemmat Esfe, A. A. Abbasian Arani, M. Rezaie, W.-M. Yan, and A. Karimipour, "Experimental determination of thermal conductivity and dynamic viscosity of Ag–MgO/water hybrid nanofluid," *International Communications in Heat and Mass Transfer*, vol. 66, pp. 189-195, 2015/08/01/ 2015, doi: https://doi.org/10.1016/j.icheatmasstransfer.2015.06.003.

[146] H. Babar, M. U. Sajid, and H. M. Ali, "Viscosity of hybrid nanofluids: a critical review," *Thermal Science*, vol. 23, no. 3 Part B, pp. 1713-1754, 2019.

[147] A. A. Hussien, W. Al-Kouz, N. M. Yusop, M. Z. Abdullah, and A. A. Janvekar, "A Brief Survey of Preparation and Heat Transfer Enhancement of Hybrid Nanofluids," *Strojniski Vestnik/Journal of Mechanical Engineering*, vol. 65, 2019.

[148] L. Ottermann, "Experimental and Numerical investigation into the natural convection of TiO 2-Water nanofluid inside a cavity by Tanja," 2017.

[149] D. Garbadeen, "Natural convection of multi-walled carbon nanotubes with water in a square enclosure," University of Pretoria, 2015.

[150] S. Kline, "The purposes of uncertainty analysis," 1985.

APPENDICES

APPENDIX A: WEIGHTS OF NPS AND SURFACTANTS

A.1 Introduction

This part of the appendix provides the estimation of the amounts of surfactants and nanoparticles utilised for the preparation of Al_2O_3–MWCNT (10:90) hybrid nanofluids.

A.2 Calculation of weights of HNPs and Surfactants

Nanoparticles of Al_2O_3 and MWCNT at percentage weigh of 10% and 90%, respectively, were dispersed in DI water of 1.4L to prepare Al_2O_3–MWCNT/water hybrid nanofluids using 0.8 SDS surfactant dispersion fraction.

In order to calculate the approximate value of the weight of Al_2O_3 and MWCNT nanoparticles as a function of volume concentrations of 0.05 – 0.20 vol%, as presented in Table A.1, Eq (3.1) was used. Additionally, the SDS weights were determined using Eq (3.2) which depended on the volume concentration.

Table A.1: Weights (g) of NPs and surfactant (SDS) engaged in the preparation of Al_2O_3-MWCNT hybrid nanofluids

φ	Al_2O_3	MWCNT	SDS	Total
0.05	0.1608	1.6075	1.4146	3.1829
0.1	0.3199	3.1998	2.8158	6.3355
0.15	0.4876	4.8761	4.2910	9.6547
0.2	0.6493	6.4932	5.7140	12.8565

A.3 Conclusion

In this section, the weights of surfactants and nanoparticles used to formulate this study's Al_2O_3–MWCNT (10:90) hybrid nanofluids were estimated and presented. The weights presented were found to be primarily dependent on the density and percentage weight of the different

nanoparticles. In addition, the overall weights of hybrid nanoparticles and surfactants relied on the volume concentration of Al_2O_3–MWCNT hybrid nanofluids to be formulated.

APPENDIX B: THERMOCOUPLES CALIBRATION

B.1 Introduction

This chapter discusses the thermocouples calibration utilised in the square cavity for the natural convection heat transfer analysis of Al_2O_3–MWCNT (10:90) hybrid nanofluid. This chapter also presents the calibration factors for each thermocouple.

B.2 Thermocouples Calibration

The calibration of the thermocouples was carried out using the thermal bath (PR2OR-30 Polyscience; accuracy = ±0.005 °C). The ranges of temperature from 15 to 65 °C with 5 °C intervals were selected. At first, 400 points of temperature measurements were obtained at the desired temperature set using a data logger at a 2 Hz frequency. This procedure was then repeated up to three times.

The average measured temperature obtained was then plotted against the reference temperatures utilizing PT-100 (the thermal bath internal thermocouple) for all the T-type thermocouples within and outside the cavity and is presented in Figure B.1. Finally, a linear curve was fitted in order to obtain the calibration factors using Eq B.1.

$$T_{cal} = mT_{uncali} + c \tag{B.1}$$

In order to minimise error, the averaged *m* and *c* were used as the calibration factors for the thermocouples. Figure B.1 depicts a linear relationship with R^2 =1 between the measured and reference temperatures. It indicates a great relationship between the two variables demonstrating outstanding behaviour of the thermocouples in the measurement of the reference temperature.

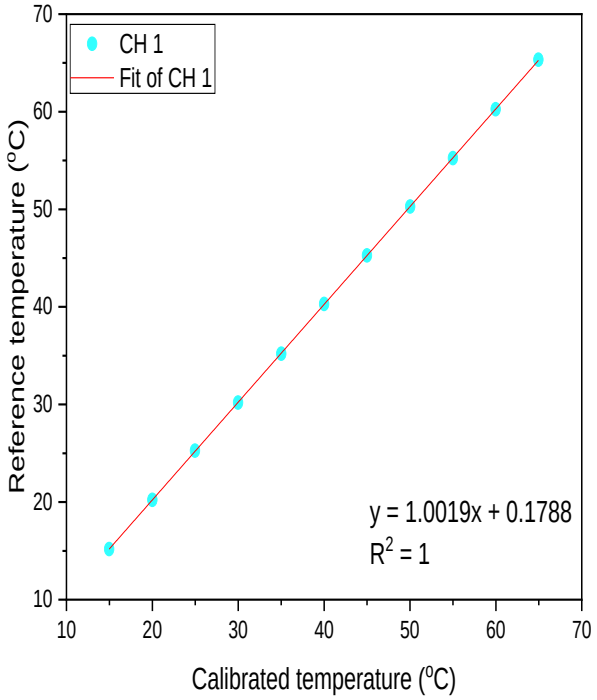
CH 1
Fit of CH 1
y = 1.0019x + 0.1788
R2 = 1
Reference temperature (°C)
Calibrated temperature (°C)

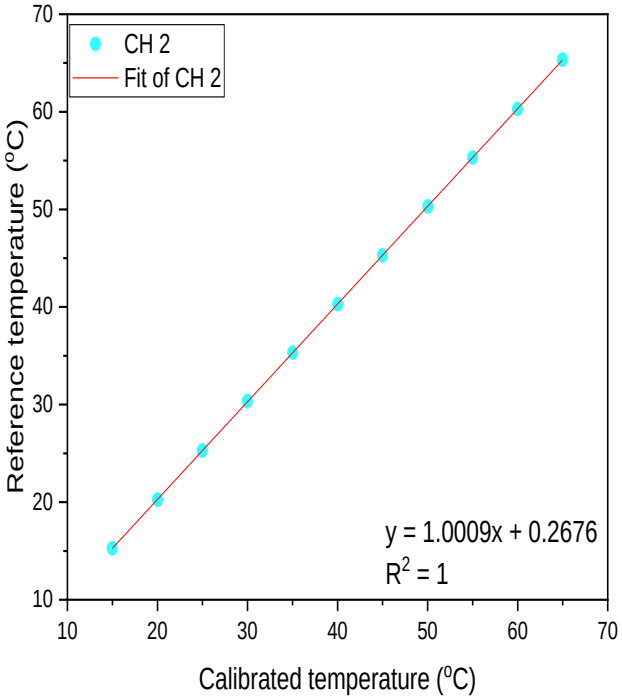
CH 2
Fit of CH 2
y = 1.0009x + 0.2676
R2 = 1
Reference temperature (°C)
Calibrated temperature (°C)

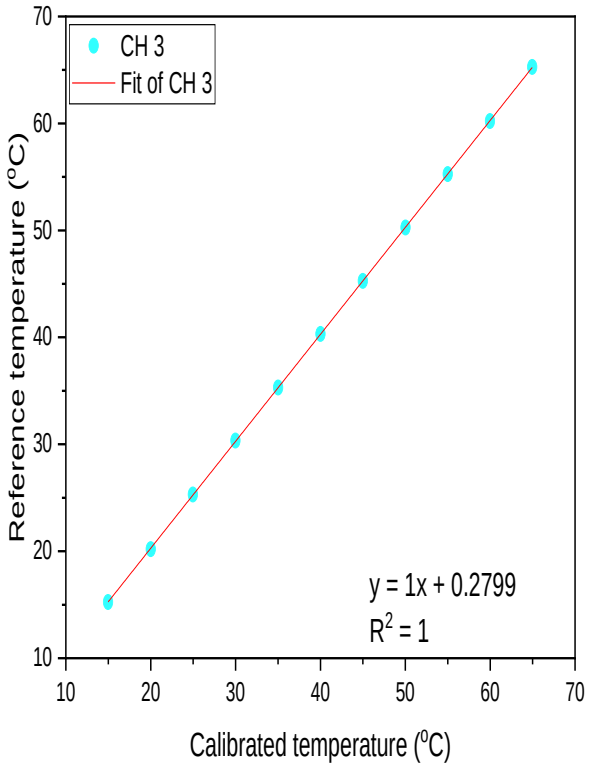
CH 3
Fit of CH 3
y = 1x + 0.2799
R2 = 1
Reference temperature (°C)
Calibrated temperature (°C)

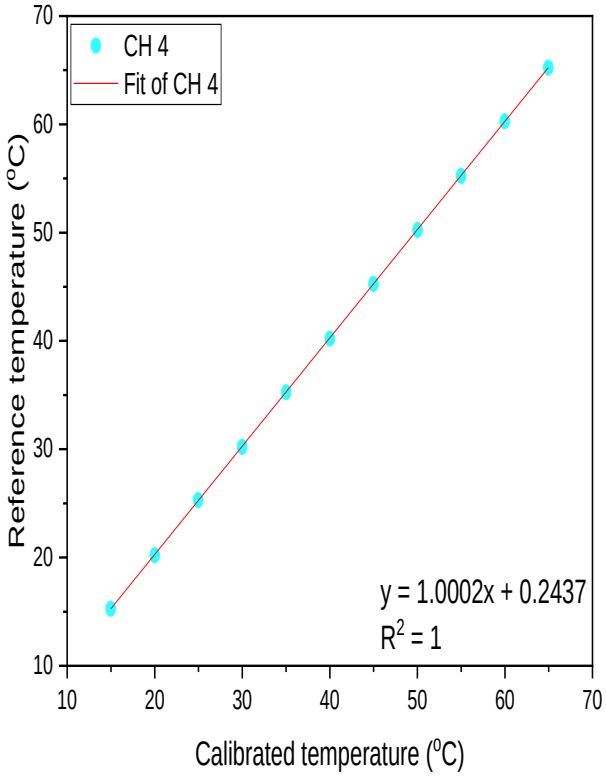
CH 4
Fit of CH 4
y = 1.0002x + 0.2437
R2 = 1
Reference temperature (°C)
Calibrated temperature (°C)

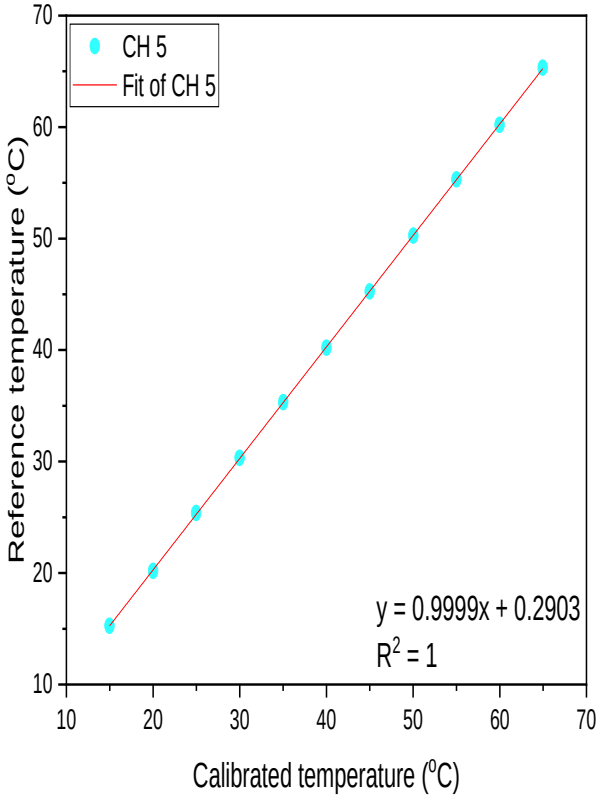
CH 5
Fit of CH 5
y = 0.9999x + 0.2903
R2 = 1
Reference temperature (°C)
Calibrated temperature (°C)

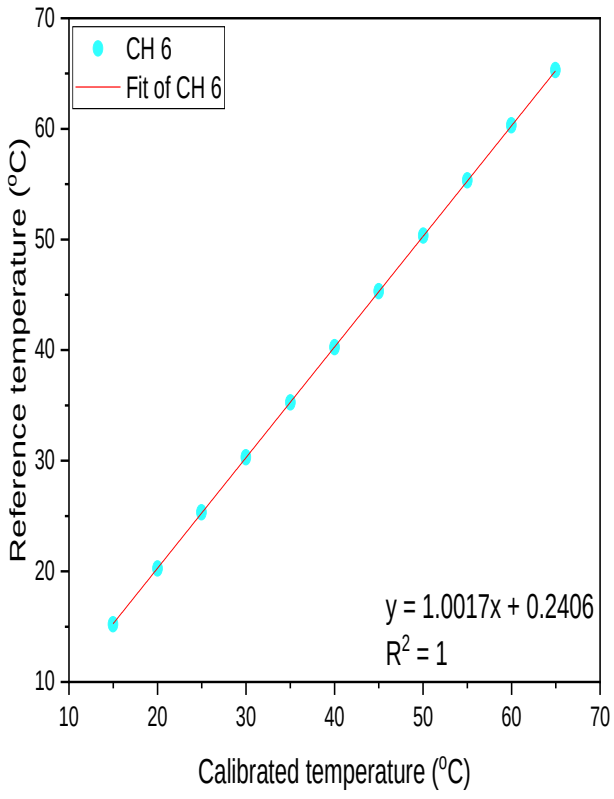
CH 6
Fit of CH 6
y = 1.0017x + 0.2406
R2 = 1
Reference temperature (°C)
Calibrated temperature (°C)

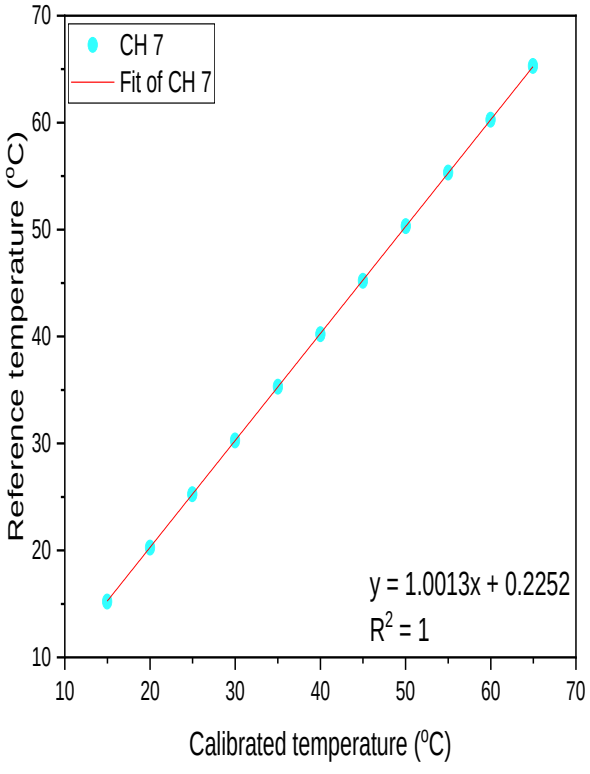
CH 7
Fit of CH 7
y = 1.0013x + 0.2252
R2 = 1
Reference temperature (°C)
Calibrated temperature (°C)

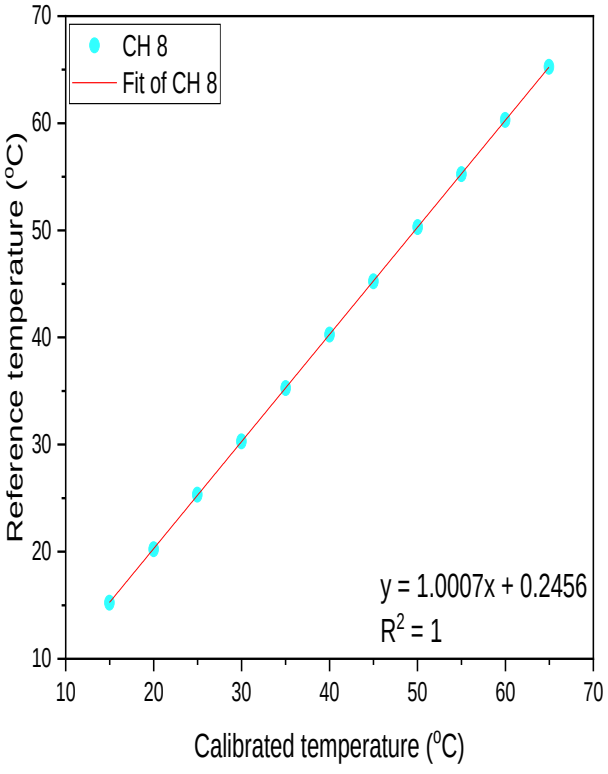
CH 8
Fit of CH 8
y = 1.0007x + 0.2456
R2 = 1
Reference temperature (°C)
Calibrated temperature (°C)

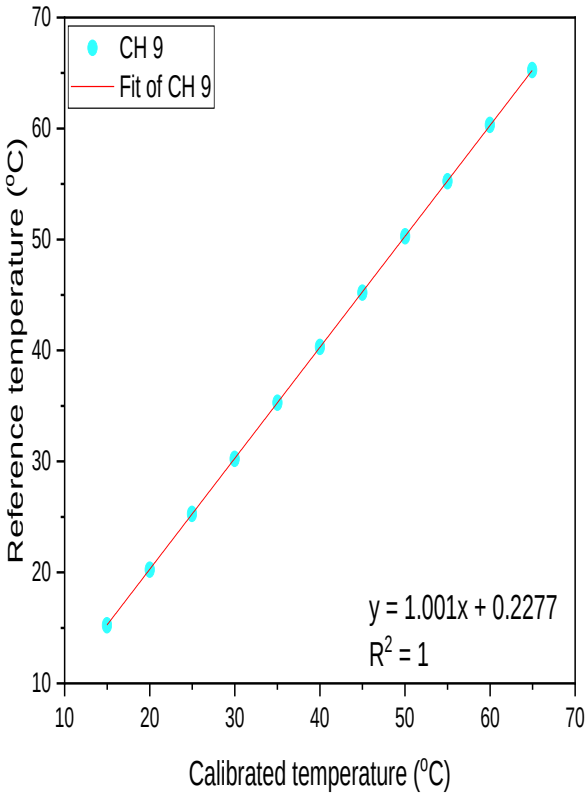
CH 9
Fit of CH 9
y = 1.001x + 0.2277
R2 = 1
Reference temperature (°C)
Calibrated temperature (°C)
10
20
30
40
50
60
70

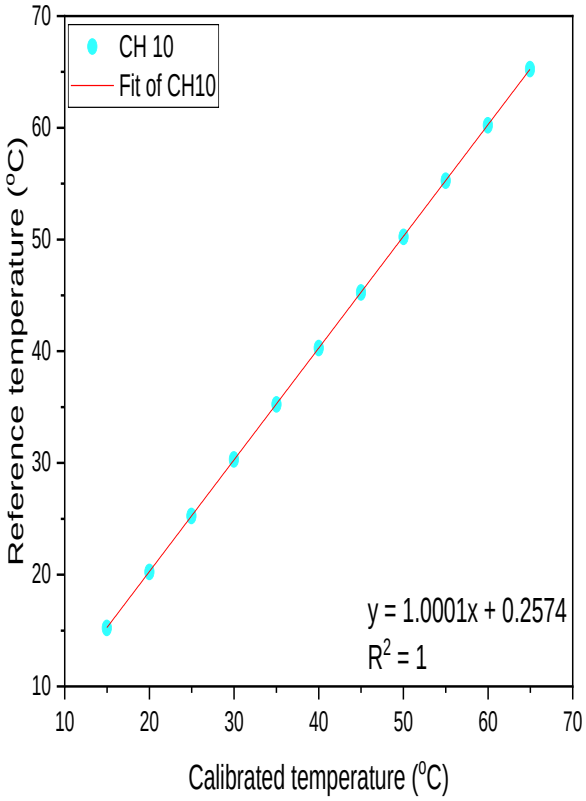
CH 10
Fit of CH10
y = 1.0001x + 0.2574
R2 = 1
Reference temperature (°C)
Calibrated temperature (°C)
10
20
30
40
50
60
70

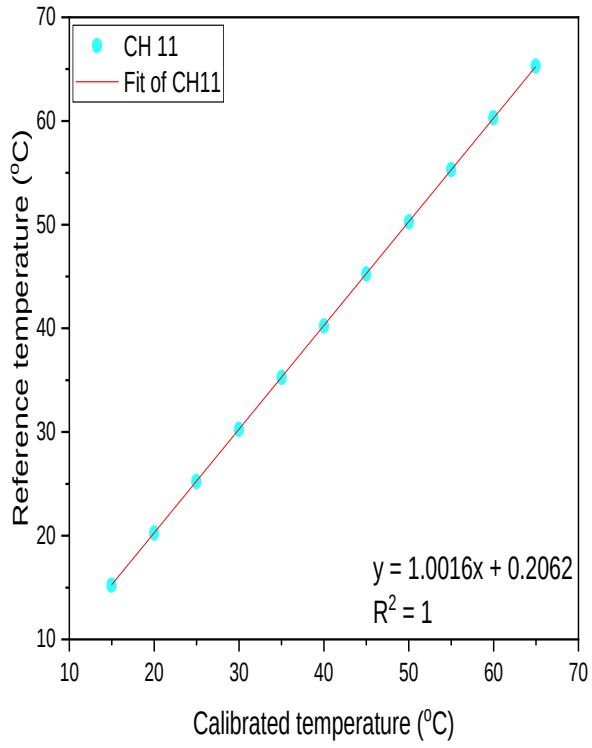
CH 11
Fit of CH11
y = 1.0016x + 0.2062
R2 = 1
Reference temperature (°C)
Calibrated temperature (°C)
10
20
30
40
50
60
70

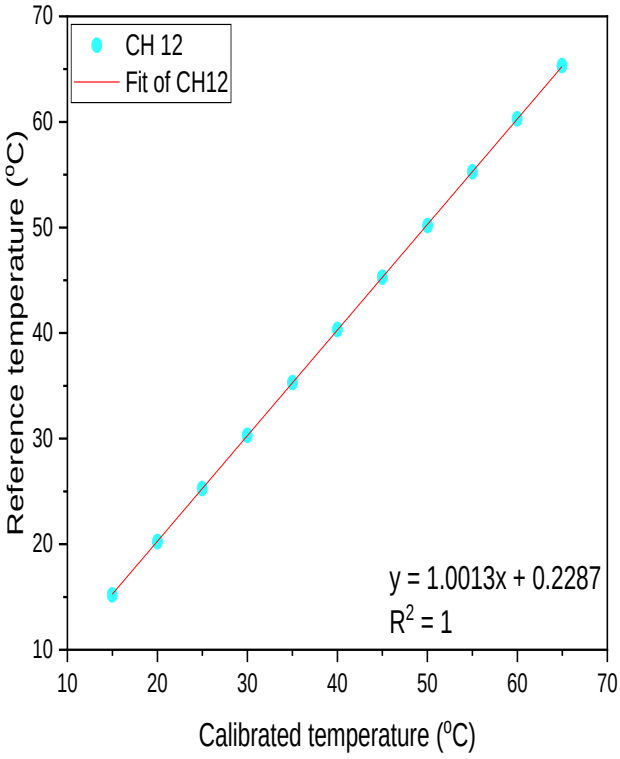
CH 12
Fit of CH12
y = 1.0013x + 0.2287
R2 = 1
Reference temperature (°C)
Calibrated temperature (°C)
10
20
30
40
50
60
70

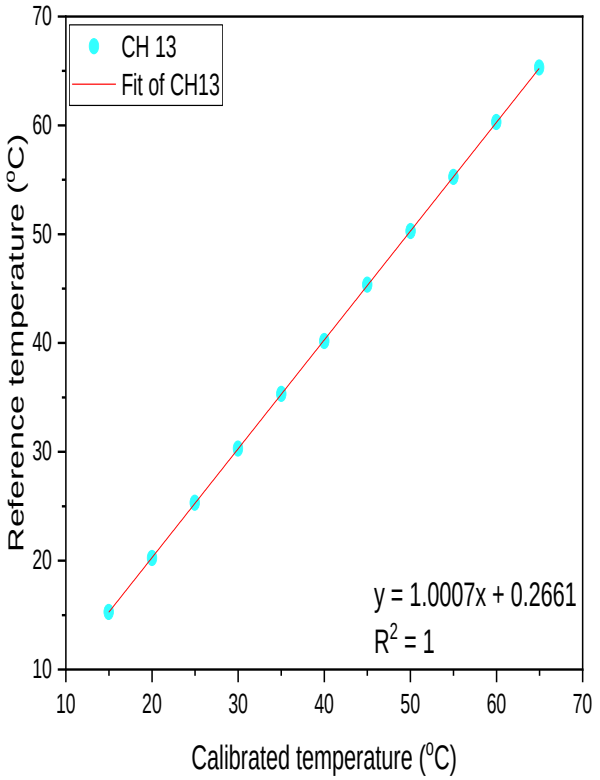
CH 13
Fit of CH13
y = 1.0007x + 0.2661
R2 = 1
Reference temperature (°C)
Calibrated temperature (°C)

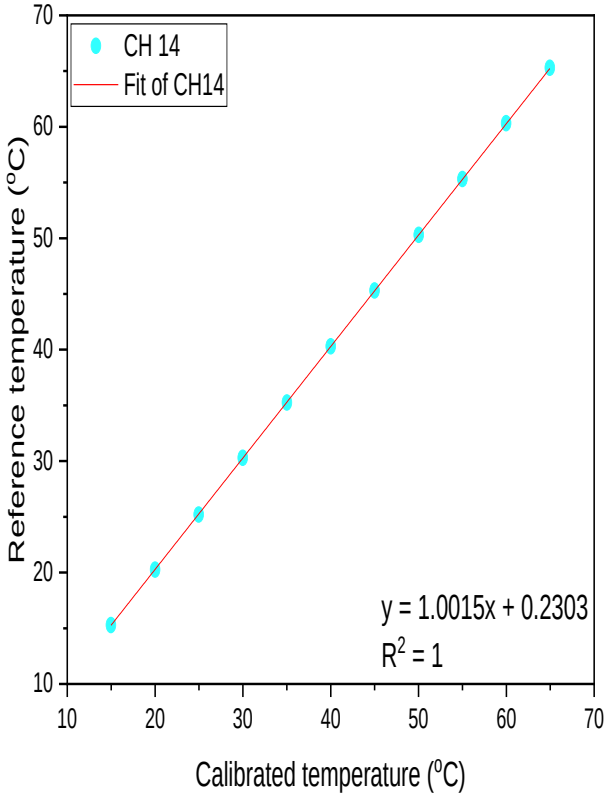
CH 14
Fit of CH14
y = 1.0015x + 0.2303
R2 = 1
Reference temperature (°C)
Calibrated temperature (°C)

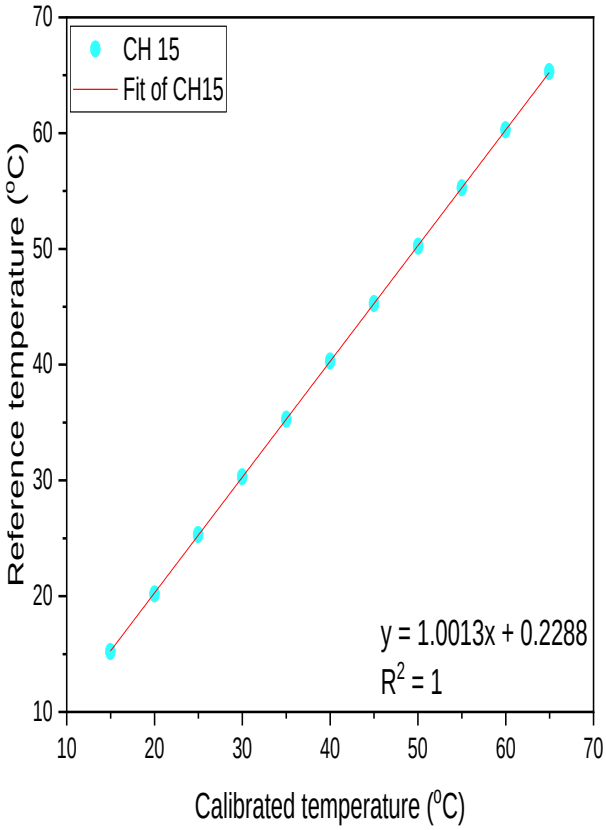
CH 15
Fit of CH15
y = 1.0013x + 0.2288
R2 = 1
Reference temperature (°C)
Calibrated temperature (°C)

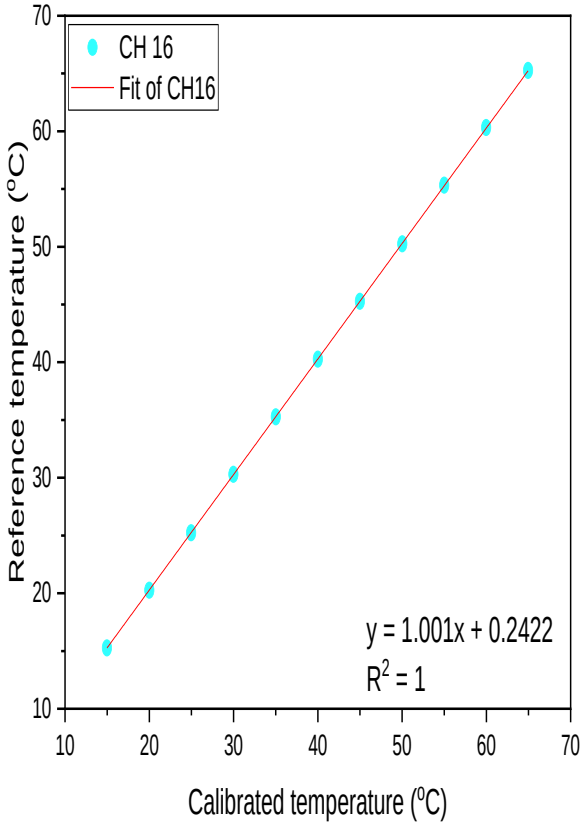
CH 16
Fit of CH16
y = 1.001x + 0.2422
R2 = 1
Reference temperature (°C)
Calibrated temperature (°C)

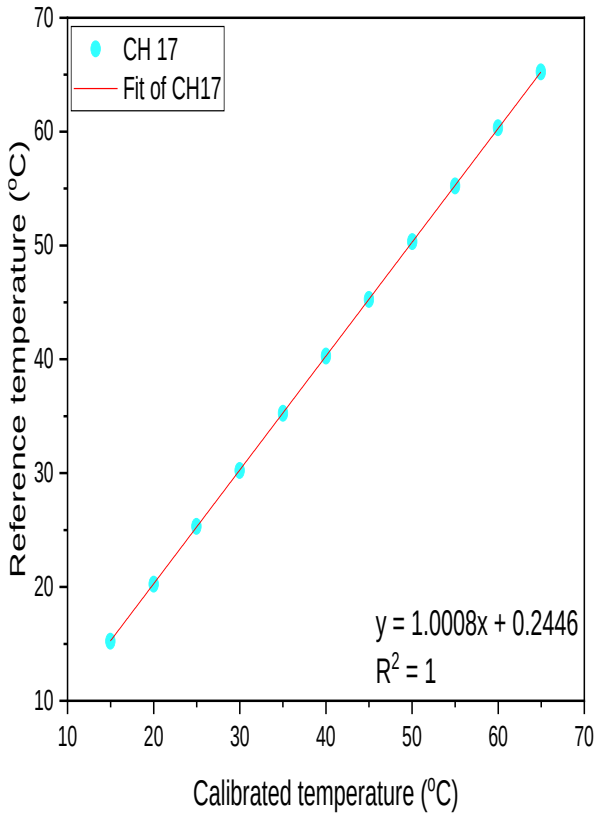
CH 17
Fit of CH17
y = 1.0008x + 0.2446
R2 = 1
Reference temperature (°C)
Calibrated temperature (°C)

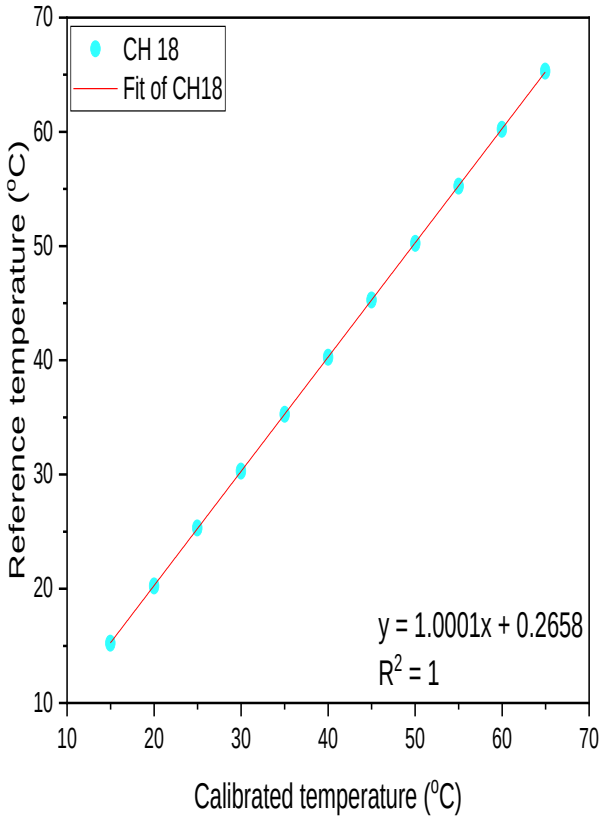
CH 18
Fit of CH18
y = 1.0001x + 0.2658
R2 = 1
Reference temperature (°C)
Calibrated temperature (°C)

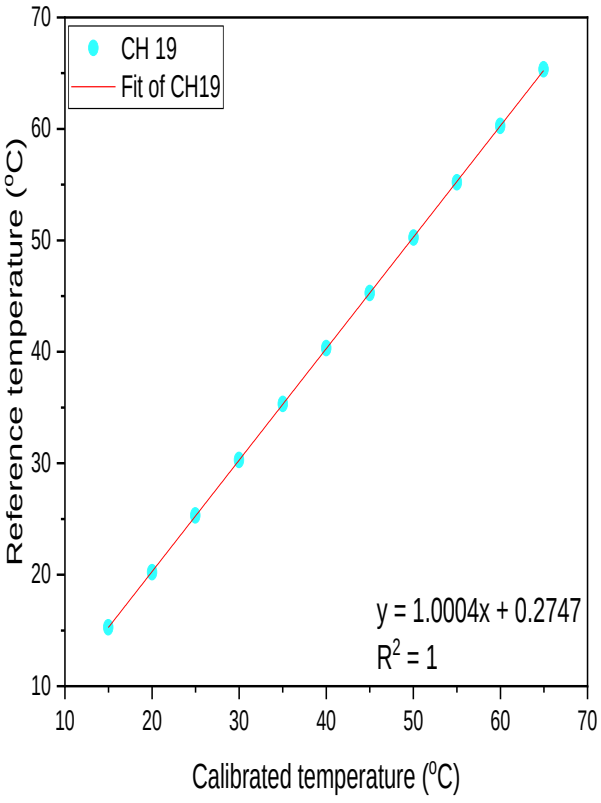
CH 19
Fit of CH19
y = 1.0004x + 0.2747
R2 = 1
Reference temperature (°C)
Calibrated temperature (°C)

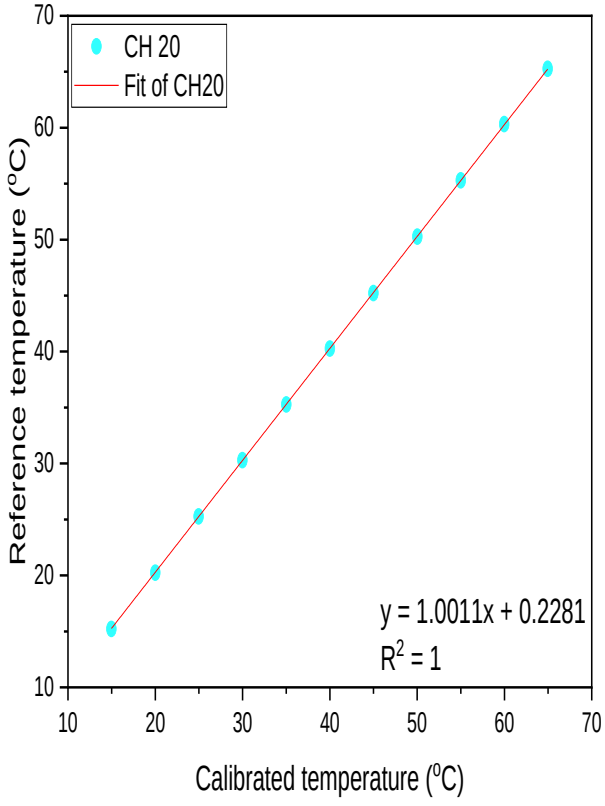
CH 20
Fit of CH20
y = 1.0011x + 0.2281
R2 = 1
Reference temperature (°C)
Calibrated temperature (°C)

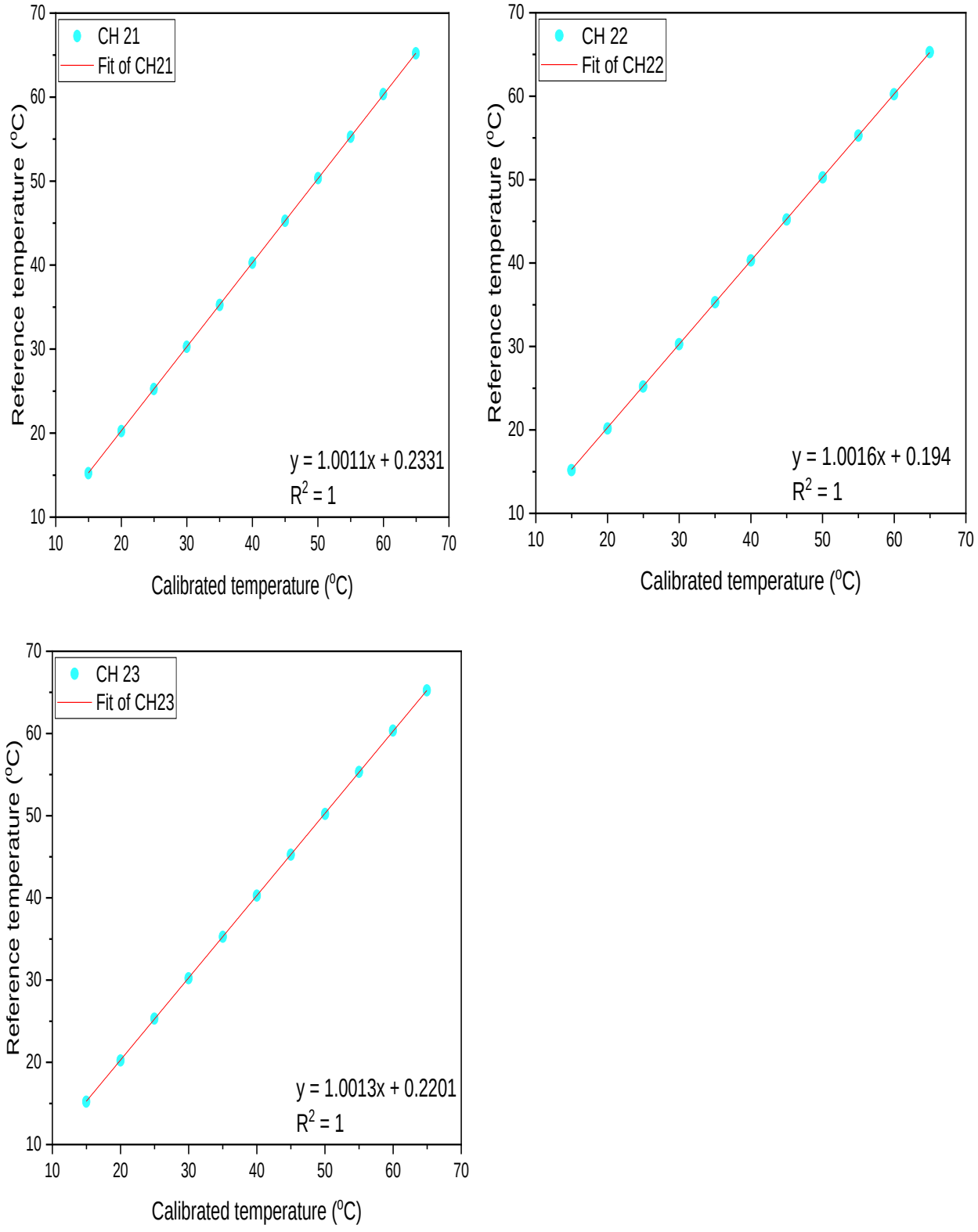

Figure B.1: Averaged measured temperatures of thermocouples against reference temperatures (CH 1- CH 23)

B.3 Conclusion

In conclusion, the thermocouples calibration was carried out and presented in this section. The calibrations on the thermocouples were carried out based on the range of temperatures 15 to 60 °C using a thermal bath with an accuracy of ± 0.005 °C. There were observations of linear relationships between the thermocouple's measured temperature and reference temperature. It was noted that the average standard deviation of the thermocouples was 0.0334 °C.

APPENDIX C: UNCERTAINTY ANALYSIS

C.1 Introduction

It is necessary to describe inaccuracies in measurements since no measurement is perfect [150]. This experimental study involves many measurements. Therefore, there is a need to present the possibility of an error value for the measured value, which diverges from the undetermined true value. This chapter outlines the instruments' accuracy used to study the heat transfer coefficient of hybrid nanofluids in natural convection. An in-depth study was conducted to examine the uncertainty of the measurements obtained from the experiments, which were used for estimating the error of the calculated parameters such as *h*, *Ra*, and *Nu*.

C.2 Theory of Uncertainty Analysis

There are two components to the uncertainty analysis: systematic error, also known as bias, and random error, also known as precision [8]. The error attributed to the accuracy of the measurement is known as bias, and these measurements are usually specified by the instrument manufacturer. Errors such as these are often the result of inaccurate measuring equipment or calibration. Precision errors, on the other hand, occur as a result of random fluctuations when many repetitive measurements of the same physical quantity are made. The cause of this sort of error can be a measurement variation process or electrical noise.

The level of bias and precision errors relates to a probability of 95%, in which the estimated error is smaller than the actual error. The uncertainty has to do with bias and precision for a single measurement. Uncertainty is expressed in Eq (C.1) [8].

$$\delta x_i = \sqrt{\left(b_i^2 + p_i^2\right)} \tag{C.1}$$

Where δx_1 is the standard deviation multiplied by the student's t-variable, and x_i is a single measurement. On the other hand, the measurement of R depends on many parameters and can be estimated using a set of equations, as shown in Eq (C.2) [141].

$$R = R\left(x_1, x_2, x_3, x_4, \ldots, x_n\right) \tag{C.2}$$

The uncertainty of the measurements of R can be evaluated, as expressed in Eq (C.3) since the uncertainties of x_i identified [141].

$$\delta R = \frac{\partial R}{\partial x_i}\delta x_i \tag{C.3}$$

Where the partial differential uncertainty coefficient (δR) is the sensitivity coefficient for estimating the outcome of x_i on the uncertainty in general. By utilizing the root sum square technique, the estimate of the uncertainty of the numerous independent parameters could be archived using Eq (C.4) [141].

$$\delta R = \left(\sum_{i=1}^{n} \left(\frac{\partial R}{\partial x_i}\delta x_i \right)^2 \right)^{\frac{1}{2}} \tag{C.4}$$

C.3 Instruments

Flow meters, fluid volume, the mass of nanoparticles and thermocouples are the primary cause of error in this experiment. For each instrument, a manufacturer's specification for accuracy has been used as a bias. By taking 1000 samples which were acquired through the data logger, the precision of the apparatus was obtained, and the average standard deviation was calculated; this was then multiplied by two to fall into the 95% confidence region. The range and uncertainty of the instruments used in this research are presented in Table C.1.

C.3.1 Thermocouples

The thermocouples calibrations were discussed exhaustively in B.2. The thermocouples and thermal bath accuracy were specified as 0.1 ℃ and ±0.005 ℃, respectively. The calculation of the precision was done by multiplying the student's t-value with the average standard deviation of the temperatures acquired from the data logger. The uncertainty was therefore evaluated using Eq (C.1). The results showed that the average uncertainty of the thermocouples was ± 0.12℃.

C.3.2 Flow meter

The flow meters used in this study had an accuracy of ±0.01% of full-scale flow rate + 2% (measured value), which were used as the bias. The calculation of the precision was done by multiplying the student's t-value with the average standard deviation of the temperatures acquired from the data logger. The uncertainty was then evaluated using Eq (C.1).

C.3.3 Weighing balance

The accuracy of the digital weighing balance provided by the manufacturer was 0.001 g, which was used as the bias. The average standard deviation of the hybrid nanoparticle weights for the prepared hybrid nanofluids was acquired and used as the precision. It was then multiplied by the student's t-value. The uncertainty was then estimated using Eq (C.1).

C.3.4 Viscometer

The provided viscometer accuracy was used as the bias. The average standard deviation of the measured viscosity of the hybrid nanofluid was then multiplied by the student's t-value. The uncertainty was therefore evaluated using Eq (C.1).

Table C.1: Independent reading error in apparatus

Instrument	Symbols	Range	Uncertainty
Thermocouple	δT	< 150 ^{o}C	$\pm$0.12℃
Weighing balance	δm_p	10 mg – 220 g	$\pm$0.0001g
Viscometer	$\delta \mu$	0.3 – 10,000 mPa.s	$\pm$3%
Length	δl	0.02 mm	$\pm$0.02 mm
Flow meter	$\delta \dot{m}$	0.0666 – 0.3333 l/s	$\pm$2.01%

C.4 Parameters

C.4.1 Temperatures

With the uncertainty of the thermocouples known, the uncertainty associated with temperature measurements within and without a cavity was determined. The temperature uncertainty of water flowing in and out of the thermal baths was assumed to be equal for adiabatic conduction with close to absolute insulation. It is expressed by Eq (C.5).

$$\delta T_{in} = \delta T_{o} \tag{C.5}$$

The uncertainties of the temperature of the cold and hot sides of the square cavity were estimated using Eq (C.6) and (C.7). Where *T* is the absolute temperature used in the correlations to determine other properties' uncertainty.

$$\delta T_C = \frac{1}{3}\sqrt{\left(\delta T_{C,1}\right)^2 + \left(\delta T_{C,2}\right)^2 + \left(\delta T_{C,3}\right)^2} \tag{C.6}$$

$$\delta T_H = \frac{1}{3}\sqrt{\left(\delta T_{H,1}\right)^2 + \left(\delta T_{H,2}\right)^2 + \left(\delta T_{H,3}\right)^2} \tag{C.7}$$

C.4.2 Cavity area

The uncertainty of the square cavity area was estimated using Eq (C.8)

$$\delta A = \sqrt{\left(\frac{\partial A}{\partial W}\delta W\right)^2 + \left(\frac{\partial A}{\partial H}\delta H\right)^2} \tag{C.8}$$

$$\partial W = \partial H = \partial L$$

C.4.3 Thermophysical properties

In order to estimate the uncertainty of viscosity and thermal conductivity of the base fluid, Eqs (C.9) – (C.10) representing the correlation used to obtain the experimental data of the base fluid viscosity and thermal conductivity were used.

$$\mu_{bf} = \frac{1}{557.82468 + (19.408782 \times T) + (0.1360459 \times T^2) - (3.1160832 \times 10^{-4} \times T^3)} \tag{C.9}$$

$$k_{bf} = 0.5636 + (0.001946 \times T) - (0.000008151 \times T^2) \tag{C.10}$$

The empirical formula used for the uncertainty of other thermal properties for the base fluid is expressed in Eq (C.11) – (C.13).

$$\rho_{bf} = 999.79684 + (0.068317355 \times T) - (0.010740248 \times T^2) + (0.00082140905 \times T^{2.5}) - (2.3030988 \times 10^{-5} \times T^3) \tag{C.11}$$

$$\beta_{bf} = \frac{(0.000000841 \times T^3) - (0.000155704 \times T^2) + (0.015892349 \times T) - 0.055807193}{1000} \quad \text{(C.12)}$$

$$C_{p-bf} = ((4.214 - (0.002286 \times T) + (0.00004991 \times T^2) - (0.0000004519 \times T^3) + (0.000000001857 \times T^4)) \times 1000 \quad \text{(C.13)}$$

The uncertainties of k, ρ, β, and C_p of the base fluid were estimated using Eq (C.14) – (C.17), respectively.

$$\delta k_{bf} = \sqrt{\left(\frac{\partial k_{bf}}{\partial T}\delta T\right)^2} \quad \text{(C.14)}$$

$$\delta \rho_{bf} = \sqrt{\left(\frac{\partial \rho_{bf}}{\partial T}\delta T\right)^2} \quad \text{(C.15)}$$

$$\delta \beta_{bf} = \sqrt{\left(\frac{\partial \beta_{bf}}{\partial T}\delta T\right)^2} \quad \text{(C.16)}$$

$$\delta C_{p-bf} = \sqrt{\left(\frac{\partial C_{p-bf}}{\partial T}\delta T\right)^2} \quad \text{(C.17)}$$

Using Eq (C.18) for volume concentration, which is a simpler form of Eq (3.1), the uncertainty of the volume concentration was estimated using Eq (C.19)

$$\varphi = \frac{v_{hnp}}{v_{hnp} + v_{bf}} = \frac{\frac{m_{hnp}}{\rho_{hnp}}}{\frac{m_{hnp}}{\rho_{hnp}} + v_{bf}} \quad \text{(C.18)}$$

$$\delta\varphi = \sqrt{\left(\frac{\partial \varphi}{\partial m_{hnp}}\delta m_{hnp}\right)^2 + \left(\frac{\partial \varphi}{\partial v_{bf}}\delta v_{bf}\right)^2} \quad \text{(C.19)}$$

Where $\frac{\partial \varphi}{\partial m_{hnp}} = \frac{\rho_{hnp} v_{bf}}{\left(m_{hnp} + \rho_{hnp} v_{bf}\right)^2}$ *and* $\frac{\partial \varphi}{\partial v_{bf}} = \frac{-\rho_{hnp} m_{hnp}}{\left(m_{hnp} + \rho_{hnp} v_{bf}\right)^2}$

Empirical models for ρ_{hnf}, $C_{p\text{-}hnf}$, and β_{hnf} as expressed using Eqs (C.20) – (C.22), respectively.

$$\rho_{hnf} = (1-\varphi_{hnf})\rho_{bf} + (\varphi\rho)_{MWCNT} + (\varphi\rho)_{Al_2O_3} \tag{C.20}$$

$$C_{p-hnf} = \frac{(1-\varphi_{hnf})(\rho C_p)_{bf} + \varphi_{MWCNT}(\rho C_p)_{MWCNT} + \varphi_{Al_2O_3}(\rho C_p)_{Al_2O_3}}{\rho_{hnf}} \tag{C.21}$$

$$\beta_{hnf} = \frac{(1-\varphi_{hnf})(\rho\beta)_{bf} + \varphi_{MWCNT}(\rho\beta)_{MWCNT} + \varphi_{Al_2O_3}(\rho\beta)_{Al_2O_3}}{\rho_{hnf}} \tag{C.22}$$

The uncertainties of ρ_{hnf}, $C_{p\text{-}hnf}$, and β_{hnf} were estimated using Eq (C.23) – (C.25), respectively.

$$\delta\rho_{hnf} = \sqrt{\left(\frac{\partial\rho_{hnf}}{\partial\varphi}\delta\varphi\right)^2 + \left(\frac{\partial\rho_{hnf}}{\partial\rho_{bf}}\delta\rho_{bf}\right)^2} \tag{C.23}$$

Where $\frac{\partial\rho_{hnf}}{\partial\varphi} = \rho_{hnp} - \rho_{bf}$ *and* $\frac{\partial\rho_{hnf}}{\partial\rho_{bf}} = 1-\varphi$

$$\delta C_{p-hnf} = \sqrt{\left(\frac{\partial C_{p-hnf}}{\partial\varphi}\delta\varphi\right)^2 + \left(\frac{\partial C_{p-hnf}}{\partial\rho_{bf}}\delta\rho_{bf}\right)^2 + \left(\frac{\partial C_{p-hnf}}{\partial C_{p-bf}}\delta C_{p-bf}\right)^2 + \left(\frac{\partial C_{p-hnf}}{\partial\rho_{hnf}}\delta\rho_{hnf}\right)^2} \tag{C.24}$$

Where $\frac{\partial C_{p-hnf}}{\partial\varphi} = \frac{-(\rho C_p)_{bf}}{\rho_{hnf}}$, $\frac{\partial C_{p-hnf}}{\partial\rho_{bf}} = \frac{(1-\varphi)C_{p-bf}}{\rho_{hnf}}$, $\frac{\partial C_{p-hnf}}{\partial C_{p-bf}} = \frac{(1-\varphi)\rho_{bf}}{\rho_{hnf}}$,

and $\frac{\partial C_{p-hnf}}{\partial\rho_{hnf}} = \frac{-\left((1-\varphi)(\rho C_p)_{bf} + (\rho C_p)_{hnp}\right)}{(\rho_{hnf})^2}$

$$\delta\beta_{hnf} = \sqrt{\left(\frac{\partial\beta_{hnf}}{\partial\varphi}\delta\varphi\right)^2 + \left(\frac{\partial\beta_{hnf}}{\partial\rho_{bf}}\delta\rho_{bf}\right)^2 + \left(\frac{\partial\beta_{hnf}}{\partial\beta_{bf}}\delta\beta_{bf}\right)^2 + \left(\frac{\partial\beta_{hnf}}{\partial\rho_{hnf}}\delta\rho_{hnf}\right)^2} \quad \text{(C.25)}$$

Where $\frac{\partial\beta_{hnf}}{\partial\varphi} = \frac{-(\rho\beta)_{bf}}{\rho_{hnf}}$, $\frac{\partial\beta_{hnf}}{\partial\rho_{bf}} = \frac{(1-\varphi)\beta_{bf}}{\rho_{hnf}}$, $\frac{\partial\beta_{hnf}}{\partial\beta_{bf}} = \frac{(1-\varphi)\rho_{bf}}{\rho_{hnf}}$,

$$and \quad \frac{\partial\beta_{hnf}}{\partial\rho_{hnf}} = \frac{-\left((1-\varphi)(\rho\beta)_{bf} + (\rho\beta)_{hnp}\right)}{(\rho_{hnf})^2}$$

C.4.4 Heat transfer

The estimation of the uncertainty of *Q* is described in Eq (C.26).

$$\delta Q = \left(\left(\frac{\partial Q}{\partial\dot{m}}\delta\dot{m}\right)^2 + \left(\frac{\partial Q}{\partial C_{p-bf}}\delta C_{p-bf}\right)^2 + \left(\frac{\partial Q}{\partial T_H}\delta T_H\right)^2 + \left(\frac{\partial Q}{\partial T_C}\delta T_C\right)^2\right)^{\frac{1}{2}} \quad \text{(C.26)}$$

Where $\frac{\partial Q}{\partial\dot{m}} = C_{p-bf}\Delta T$, $\frac{\partial Q}{\partial C_{p-bf}} = \dot{m}\Delta T$, *and* $\frac{\partial Q}{\partial\Delta T} = \dot{m}C_{p-bf}$

C.4.5 Nusselt number

The estimation of the uncertainty of *Nu* is described in Eq (C.27).

$$\delta Nu = \left(\left(\frac{\partial Nu}{\partial h}\delta h\right)^2 + \left(\frac{\partial Nu}{\partial L_c}\delta L_c\right)^2 + \left(\frac{\partial Nu}{\partial k_{eff}}\delta k_{eff}\right)^2\right)^{\frac{1}{2}} \quad \text{(C.27)}$$

Where $\frac{\partial Nu}{\partial h} = \frac{L_c}{k}$, $\frac{\partial Nu}{\partial L_c} = \frac{h}{k}$, *and* $\frac{\partial Nu}{\partial k} = \frac{-hL_c}{k^2}$

C.4.6 Heat transfer coefficient

The estimation of the uncertainty of h is described in Eq (C.28).

$$\delta h = \left(\left(\frac{\partial h}{\partial Q} \delta Q \right)^2 + \left(\frac{\partial h}{\partial A} \delta A \right)^2 + \left(\frac{\partial h}{\partial T_H} \delta T_H \right)^2 + \left(\frac{\partial h}{\partial T_C} \delta T_C \right)^2 \right)^{\frac{1}{2}} \quad \text{(C.28)}$$

Where

$$\frac{\partial h}{\partial Q} = \frac{1}{(T_h - T_c)A}, \quad \frac{\partial h}{\partial A} = \frac{-Q}{(T_h - T_c)A^2}, \quad \frac{\partial h}{\partial T_h} = \frac{-Q}{(T_h - T_c)^2 A}, \text{ and } \frac{\partial h}{\partial T_c} = \frac{Q}{(T_h - T_c)^2 A}$$

The uncertainties of thermophysical properties and parameters evaluated in this research are provided in

Table C.2.

Table C.2: Uncertainties of the experiment due to propagated errors

Uncertainty	Value
δT_{H-W}	5.774×10^{-2}
δT_{C-W}	3.464×10^{-2}
δA	2.715×10^{-6}
δk_{bf}	1.72×10^{-4}
$\delta \rho_{bf}$	3.781
$\delta \beta_{bf}$	1.028×10^{-3}
δC_{p-bf}	2.82×10^{-2}
$\delta \mu_{bf}$	2.50×10^{-3}

Uncertainty	Value
$\delta\varphi$	7.99×10^{-2}
$\delta\rho_{hnf}$	1.020
δC_{p-hnf}	3.332
$\delta\beta_{hnf}$	8.20×10^{-4}
δQ	1.365
δNu	2.004
δh	10.375

C.5 Conclusion

This section highlighted the theory and method of uncertainty. The instruments' accuracy and precision were used for the uncertainty estimation, which is related to the parameters involved in this investigation.